UC Irvine
UC Irvine Previously Published Works

Title

Search for electroweak ttWj production in multileptonic final states at (Formula presented) = 13 TeV with the ATLAS detector and bounds on effective field theory operators

Permalink

https://escholarship.org/uc/item/3d6426k8

Journal

Physical Review D, 114(1)

ISSN

2470-0010

Authors

Aad, G

Aakvaag, E

Abbott, B

et al.

Publication Date

2026

DOI

10.1103/P5NZ-95M3

Copyright Information

This work is made available under the terms of a Creative Commons Attribution-NonCommercial License, available at https://creativecommons.org/licenses/by-nc/4.0/

Peer reviewed

eScholarship.org Powered by the California Digital Library
University of California

Search for electroweak $t\bar{t}Wj$ production in multileptonic final states at $\sqrt{s} = 13$ TeV with the ATLAS detector and bounds on effective field theory operators

G. Aad *et al.*[*]
(ATLAS Collaboration)

(Received 24 September 2025; accepted 6 April 2026; published 1 July 2026)

A search is presented for the electroweak production of a top-quark pair in association with a W boson and at least one additional jet known as the $t\bar{t}Wj_{\mathrm{EW}}$ process. This process has embedded within it a tW-scattering vertex, which is probed directly for the first time. The collision data were collected with the ATLAS detector during Run 2 of the LHC and correspond to an integrated luminosity of 140 fb^{-1} at $\sqrt{s} = 13$ TeV. The search uses same-charge pairs of electrons and muons together with jets, of which at least one is b-tagged. The properties of the most forward jet relative to the rest of the event are used to discriminate the electroweak $t\bar{t}Wj_{\mathrm{EW}}$ production process from its strong $t\bar{t}W$ production counterpart. A measured (expected) 95% CL upper limit on the cross section is set at $\sigma_{t\bar{t}Wj_{\mathrm{EW}}} < 251$ fb (230 fb), to be compared with the expected Standard Model (SM) cross section of 47.7 fb. Limits are set on the SM effective field theory (EFT) operators O_{Ht} and $O_{HQ}^{(1)}$, which modify the electroweak couplings of the top quark through contributions to the tW-scattering vertex. The interpretation acts as a case study to emphasize the importance of energy-dependent sensitivity, multiprocess, and multioperator EFT contributions.

DOI: 10.1103/p5nz-95m3

I. INTRODUCTION

One of the key physics goals of the Large Hadron Collider (LHC) physics program is to probe the nature of electroweak (EW) symmetry breaking (EWSB), both in the Standard Model (SM) and beyond (BSM). The production of top quarks in association with EW bosons offers a unique testing ground to contribute to these goals. In particular, $t\bar{t}W$ production, which superficially appears to be a simple process composed of well-known SM couplings, proves to have a rich phenomenology. The EW production of $t\bar{t}W$ in association with an additional jet, $t\bar{t}Wj_{\mathrm{EW}}$, is especially interesting because it probes new dynamics at the LHC, the tW-scattering vertex. The dominant contributing Feynman diagrams for the $t\bar{t}W$ process, including additional quantum chromodynamics (QCD) and EW corrections, are presented in Fig. 1, where Fig. 1(d) shows an example of one $t\bar{t}Wj_{\mathrm{EW}}$ contribution. The $t\bar{t}Wj_{\mathrm{EW}}$ process produces a "forward" jet with greater pseudorapidity than the QCD $t\bar{t}W$ production process. This forward jet can be used to separate the processes experimentally. The tW-scattering vertex provides strong energy-enhanced sensitivity potential to BSM effects not present in the SM EWSB. These EWSB-specific BSM signatures can be investigated through effective field theory (EFT) approaches. A deviation of the top EW couplings from the SM with a signature of energy growth that diverges quadratically with momentum would be a signal of BSM physics. This would indicate that the top quark is strongly coupled to the sector responsible for EWSB [1,2].

The $t\bar{t}Wj_{\mathrm{EW}}$ process can be understood in the wider context of next-to-leading-order (NLO) QCD and EW corrections to $t\bar{t}W$ production. The traditionally "leading" NLO EW corrections (of order $\alpha^2\alpha_s^2$, where α and α_s refer to the electroweak and strong coupling constants, respectively) cause few-percent negative changes to the inclusive $t\bar{t}W$ cross section; however, even larger positive contributions from traditionally "subleading" NLO EW corrections (of order $\alpha^3\alpha_s$) were pointed out in Refs. [1,4,5]. It is this subleading contribution, of order $\alpha^3\alpha_s$, which corresponds to the $t\bar{t}Wj_{\mathrm{EW}}$ signal considered here.

Measurements of $t\bar{t}Wj_{\mathrm{EW}}$ production also provide a better understanding of $t\bar{t}W$ production. The $t\bar{t}W$ process is an important background in LHC searches and precision measurements, as one of the few SM processes that provides an irreducible source of same-charge dilepton and trilepton events. This is especially important given

[*]Full author list given at the end of the article.

Published by the American Physical Society under the terms of the Creative Commons Attribution 4.0 International license. Further distribution of this work must maintain attribution to the author(s) and the published article's title, journal citation, and DOI. Funded by SCOAP[3].

 © 2026 CERN, for the ATLAS Collaboration

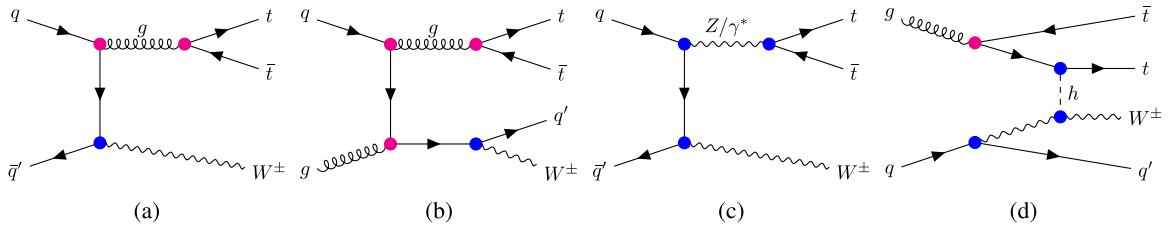


FIG. 1. Illustrative Feynman diagrams for the dominant production modes of $t\bar{t}W$ [3]: (a) the leading-order (LO) contribution ($\alpha\alpha_s^2$), (b) a real emission diagram from the NLO QCD contribution ($\alpha\alpha_s^3$), (c) the tree-level EW contribution (α^3), and (d) a representative diagram of the combined NLO QCD and EW contributions ($\alpha^3\alpha_s$). The pink circles correspond to QCD couplings and the blue circles correspond to EW couplings.

existing observations of tension with the SM predictions in direct measurements of $t\bar{t}W$ production. Measurements of $t\bar{t}W$ production by the ATLAS and CMS Collaborations at $\sqrt{s} = 8$ TeV [6,7] were in agreement with the SM. However, at $\sqrt{s} = 13$ TeV higher precision measurements [3,8–11] observe tensions with the SM predictions. These tensions are somewhat alleviated by the inclusion of higher-order effects [4,12,13]. Therefore, tests of the modeling of higher-order effects, i.e., $t\bar{t}W$ with additional jets, are especially important for measurements where this is the dominant background, such as $t\bar{t}H$ [14,15] and $t\bar{t}t\bar{t}$ [16,17].

A. EFT sensitivity

As shown in Fig. 2, the $t\bar{t}Wj_{\mathrm{EW}}$ process can be considered to contain an effective vertex probing various SM couplings such as the top-quark Z boson (t–Z) and top Yukawa (y_t) couplings. The sensitivity of this vertex to new physics has a significant quadratic energy dependence due to the scattering topology, contrasting with at most linear energy dependence in $t\bar{t}Z$ and $t\bar{t}H$ processes. This enhanced energy dependence is also true of BSM EWSB EFT operators that can contribute to $t\bar{t}Wj_{\mathrm{EW}}$ production.

This unique sensitivity to the t–Z coupling, which is complementary to dedicated measurements, serves as an additional handle on deviations from the SM that could be a sign of new physics effects in the EWSB mechanism [18–25]. The different structure of $t\bar{t}Wj_{\mathrm{EW}}$ production, compared with $t\bar{t}Z$ production, lifts degeneracies when considering multiple EFT operators, such as O_{Ht} and $O_{HQ}^{(1)}$.

The tW-scattering vertex shown in Fig. 2 is also sensitive to EFT operators affecting the top-quark Higgs boson coupling, such as O_{tH}. However, the sensitivity is less than in dedicated measurements [26] and therefore these are not considered in this analysis.

EFT frameworks are a self-consistent way to search for new physics at high energies. A general SM EFT (SMEFT) Lagrangian considering operators up to mass-dimension-six takes the form

$$\mathcal{L}_{\mathrm{EFT}} = \mathcal{L}_{\mathrm{SM}} + \sum_i \frac{c_i}{\Lambda^2}\mathcal{O}_i,$$

where $\mathcal{L}_{\mathrm{SM}}$ is the SM Lagrangian, the $\mathcal{O}_i$ are the operators of mass-dimension-six, and the c_i are the associated Wilson coefficients for a given general cutoff scale Λ. In a measurement only the ratio c_i/Λ^2 is relevant, and here $\Lambda = 1$ TeV is used to set the counting scale of c_i. The cutoff scale for the EFT corresponds to the energy scale where new physics would arise. Using the notation defined in Ref. [27], the two operators of relevance for this analysis are

$$\frac{c_{Ht}}{\Lambda^2}O_{Ht} = \frac{c_{Ht}}{\Lambda^2}(H^\dagger i\overleftrightarrow{D}_\mu H)(\bar{t}_R\gamma^\mu t_R)$$

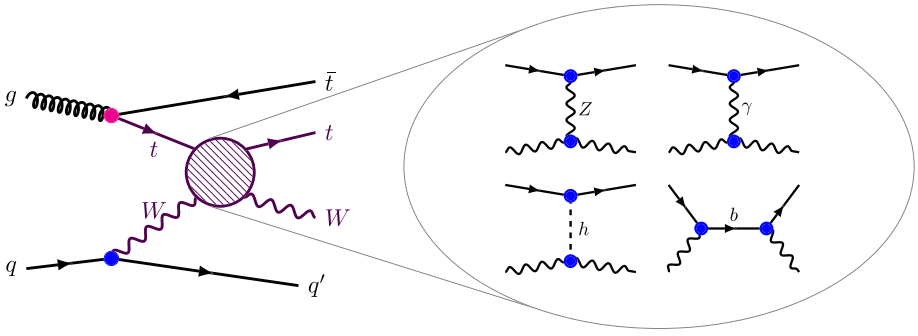


FIG. 2. A schematic representation of the tW-scattering vertex in the Feynman diagram of the $t\bar{t}Wj_{\mathrm{EW}}$ process, showing different contributing subprocesses, modified from Ref. [1].

and

$$\frac{c_{HQ}^{(1)}}{\Lambda^2} O_{HQ}^{(1)} = \frac{c_{HQ}^{(1)}}{\Lambda^2} (H^\dagger \overleftrightarrow{D}_\mu H)(\bar{Q}_L \gamma^\mu Q_L).$$

These operators have a strong effect on the $t\bar{t}Wj_{\mathrm{EW}}$ process at current experimental constraints. In $t\bar{t}Z$ production EFT effects for these operators manifest mainly through corrections that are linear in c_i/Λ^2, whereas in $t\bar{t}Wj_{\mathrm{EW}}$ the energy growth leads to a significant quadratic dependence in c_i/Λ^2 where the linear interference term is strongly suppressed due to symmetries in the SM amplitude [2]. This phenomenology arises because of the presence of two longitudinally polarized gauge bosons in the tW-scattering topology but not in $t\bar{t}Z$ production [1,2]. The EFT can still be valid in the perturbative expansion in this case even when the linear term is very small compared with the quadratic term [28]. Several EFT interpretation configurations are considered in this measurement and it is shown that additional constraints from $t\bar{t}Wj_{\mathrm{EW}}$ production can provide separation between the O_{Ht} and $O_{HQ}^{(1)}$ operators, which can otherwise suffer from degenerate directions in the measurement.

B. Analysis strategy

A signal-enriched region (SR) is defined to target the signal $t\bar{t}Wj_{\mathrm{EW}}$ production process by selecting events that contain two same-charge leptons (electrons or muons) and at least four jets. At least one jet is required to be identified as containing a b-hadron (b-tagged). In addition, control regions (CRs) are defined that are enriched in and used to normalize background processes.

The signal contribution in the SR is then measured with a simultaneous binned profile-likelihood fit exploiting the difference in kinematics between the signal and the dominant QCD-induced $t\bar{t}Wj$ background.

Finally, an EFT interpretation is performed, using Monte Carlo (MC) samples to model the contributions of the O_{Ht} and $O_{HQ}^{(1)}$ operators on both the $t\bar{t}Wj_{\mathrm{EW}}$ and $t\bar{t}Z$ processes. Sensitivity to $t\bar{t}Z$ comes primarily from the CR enriched in this process. The EFT operators are considered both independently and simultaneously and 95% confidence intervals are determined.

The paper is structured as follows: Section II briefly describes the ATLAS detector, Section III provides an overview of the data and MC samples used in the measurements, and Sec. IV details the object reconstruction and selection. Section V describes the event selection criteria, and data-driven background estimates are described in Sec. VI. An overview of the systematic uncertainties is given in Sec. VII, the results of the SM measurement are presented in Sec. VIII, and the EFT interpretation is detailed in Sec. IX. Finally, conclusions are given in Sec. X.

II. ATLAS DETECTOR

The ATLAS detector [29] at the LHC covers nearly the entire solid angle around the collision point.[1] It consists of an inner tracking detector surrounded by a thin superconducting solenoid, electromagnetic and hadronic calorimeters, and a muon spectrometer incorporating three large superconducting air-core toroidal magnets.

The inner-detector system (ID) is immersed in a 2 T axial magnetic field and provides charged-particle tracking in the range of $|\eta| < 2.5$. The high-granularity silicon pixel detector covers the vertex region and typically provides four measurements per track, the first hit generally being in the insertable B-layer installed before Run 2 [30,31]. It is followed by the SemiConductor Tracker, which usually provides eight measurements per track. These silicon detectors are complemented by the Transition Radiation Tracker (TRT), which enables radially extended track reconstruction up to $|\eta| = 2.0$. The TRT also provides electron identification information based on the fraction of hits (typically 30 in total) above a higher energy-deposit threshold corresponding to transition radiation.

The calorimeter system covers the pseudorapidity range $|\eta| < 4.9$. Within the region $|\eta| < 3.2$, electromagnetic calorimetry is provided by barrel and end cap high-granularity lead/liquid-argon (LAr) calorimeters, with an additional thin LAr presampler covering $|\eta| < 1.8$ to correct for energy loss in material upstream of the calorimeters. Hadronic calorimetry is provided by the steel/scintillator-tile calorimeter, segmented into three barrel structures within $|\eta| < 1.7$, and two copper/LAr hadronic end cap calorimeters. The solid angle coverage is completed with forward copper/LAr and tungsten/LAr calorimeter modules optimized for electromagnetic and hadronic energy measurements, respectively.

The muon spectrometer (MS) comprises separate trigger and high-precision tracking chambers measuring the deflection of muons in a magnetic field generated by the superconducting air-core toroidal magnets. The field integral of the toroids ranges between 2.0 and 6.0 Tm across most of the detector. Three layers of precision chambers, each consisting of layers of monitored drift tubes, cover the region $|\eta| < 2.7$, complemented by cathode-strip chambers in the forward region, where the background is highest. The muon trigger system covers the range $|\eta| < 2.4$ with

[1]ATLAS uses a right-handed coordinate system with its origin at the nominal interaction point (IP) in the center of the detector and the z-axis along the beam pipe. The x-axis points from the IP to the center of the LHC ring, and the y-axis points upward. Polar coordinates (r, ϕ) are used in the transverse plane, ϕ being the azimuthal angle around the z-axis. The pseudorapidity is defined in terms of the polar angle θ as $\eta = -\ln\tan(\theta/2)$ and is equal to the rapidity $y = \frac{1}{2}\ln(\frac{E+p_z}{E-p_z})$ in the relativistic limit. Angular distance is measured in units of $\Delta R \equiv \sqrt{(\Delta y)^2 + (\Delta\phi)^2}$.

resistive-plate chambers in the barrel, and thin-gap chambers in the end cap regions.

The luminosity is measured mainly by the LUCID–2 [32] detector that records Cherenkov light produced in the quartz windows of photomultipliers located close to the beampipe.

Events were selected by the first-level trigger system implemented in custom hardware, followed by selections made by algorithms implemented in software in the high-level trigger [33]. The first-level trigger accepted events from the 40 MHz bunch crossings at a rate close to 100 kHz, which the high-level trigger further reduced to record complete events to disk at about 1.25 kHz.

A software suite [34] is used in data simulation, in the reconstruction and analysis of real and simulated data, in detector operations, and in the trigger and data acquisition systems of the experiment.

III. DATA AND SIMULATED EVENT SAMPLES

The data used are the full LHC Run 2 (2015–2018) recorded by the ATLAS detector at $\sqrt{s} = 13$ TeV, which corresponds to an integrated luminosity of 140 fb^{-1}. Only events from time periods in which LHC beams were stable and all ATLAS detectors were operational are selected [35]. The data are collected using a combination of single-electron and single-muon triggers, with requirements on the identification, isolation, and transverse momentum (p_{T}) of the leptons to maintain high efficiency across the full momentum range while controlling the trigger rates [33,36,37]. For electrons the trigger thresholds for 2016–2018 (2015) data are $p_{\mathrm{T}} = 26$, 60, and 140 GeV ($p_{\mathrm{T}} = 24$, 60, and 120 GeV), whereas for muons the thresholds are $p_{\mathrm{T}} = 26$ and 50 GeV ($p_{\mathrm{T}} = 20$ and 50 GeV). Isolation requirements are applied to the triggers with the lowest p_{T} threshold for both electrons and muons [38–41].

Samples of simulated events are used to model the signal and the prompt SM background. The samples are processed to include the effects of the ATLAS detector with a simulation in Geant4 [42]. All simulated events are processed with the same reconstruction software as the data and corrected so that the object reconstruction, identification and trigger efficiencies, energy scales, and energy resolutions match the data. The effect of multiple interactions in the same and neighboring bunch crossings (pileup) is modeled by overlaying each simulated hard-scattering event with inelastic pp events generated with Pythia 8.1 [43] using the NNPDF2.3LO [44] set of parton distribution functions (PDFs) and the A3 set of tuned parameters. Separate MC production campaigns are used to model the different pileup distributions observed in the 2015–2016, 2017, and 2018 data. The samples of simulated events are reweighted to reproduce the observed distribution of the average number of collisions per bunch crossing in each data-taking period.

In all cases, the top-quark mass is set to 172.5 GeV. Unless specified below, samples interfaced to Pythia 8.2 [45] use NNPDF3.0NLO [46] and NNPDF2.3LO PDF sets for the matrix element (ME) and the parton showering respectively, and the A14 tune. The decays of bottom and charm hadrons are simulated using the EvtGen 1.2-1.6 program [47] for all generators except Sherpa.

The $t\bar{t}Wj_{\mathrm{EW}}$ signal sample is generated with Sherpa 2.2.10 [48,49] at LO, namely $\mathcal{O}(\alpha_s\alpha^3)$, for the ME and showered with the default Sherpa 2.2.10 settings and NNPDF3.0NNLO [50]. The renormalization and factorization scales, μ_{R} and μ_{F}, are set to $H_{\mathrm{T}}/2 = \frac{1}{2}\sum_i \sqrt{m_i^2 + p_{\mathrm{T},i}^2}$ where i runs over all outgoing partons from the ME calculation. The cross section from the generator is $\sigma_{t\bar{t}Wj_{\mathrm{EW}}} = 42.1^{+1.7}_{-1.3}$ fb. This is scaled (by a factor of 1.13) to match the theoretical cross section predicted at NLO in QCD from Ref. [12], $\sigma_{t\bar{t}Wj_{\mathrm{EW}}} = 47.7^{+1.9}_{-1.4}$ fb.

The $t\bar{t}W$ QCD sample is generated with Sherpa 2.2.10 at NLO accuracy in QCD with $\mu_R = \mu_F = H_{\mathrm{T}}/2$. The ME was calculated for up to one additional parton at NLO and up to two partons at LO using COMIX [51] and OpenLoops [52–54], and merged with the Sherpa parton shower [55] using the MEPS@NLO prescription [56,56–59] with a merging scale of 30 GeV. The sample is normalized to the next-to-next-to-leading-order (NNLO) cross section of $710.7^{+37.4}_{-48.1}$ fb quoted in Ref. [13].

The $t\bar{t}Z/\gamma^*$, $t\bar{t}H$, tqZ/γ^*, tqH, tWZ, and tWH samples are generated at NLO with MadGraph5_aMC@NLO and showered with Pythia 8.2. These samples are normalized to the best theoretical predictions at NLO using k-factors [60]. Other minor backgrounds with top quarks ($t\bar{t}t$, $t\bar{t}t\bar{t}$, $t\bar{t}W^+W^-$) are generated at LO with MadGraph5_aMC@NLO and showered with Pythia 8.2.

Diboson (VV) processes with four charged leptons, three charged leptons, and a neutrino, or two charged leptons and two neutrinos (all with or without extra partons) are simulated with Sherpa 2.2.2 with the PDF set NNPDF3.0NNLO. The processes are generated with up to one extra parton at NLO and up to three extra partons at LO using the same formalism as in $t\bar{t}W$.

Nonprompt and fake leptons can be generated from many different sources. Nonprompt leptons originate mainly from semileptonic hadron decays, while fake leptons are mostly due to misidentified jets. These two categories are jointly hereafter referred to as "fake leptons." The fake-lepton background, primarily arising from $t\bar{t}$ production, is derived from a data-driven approach. The MC production of $t\bar{t}$ events is modeled using the Powheg Box2 generator [61] at NLO with the NNPDF3.0NLO PDF set and the damping factor h_{damp} set to 1.5 times the top-quark mass. The events are interfaced with Pythia 8.2. Single top-quark production in the s- and t-channels, and tW production, is simulated similarly.

The production of W and Z bosons with multiple jets (V + jets) is simulated with the Sherpa 2.2.1 generator using

NLO-accurate MEs for up to two jets and LO-accurate MEs for up to four jets, calculated with the COMIX [51] and OpenLoops libraries. They are matched with the Sherpa parton shower using the MEPS@NLO prescription. The NNPDF3.0NNLO set of PDFs is used and the samples are normalized to NNLO predictions.

Processes with three heavy gauge bosons (WWW, WWZ, WZZ, and ZZZ) with up to six leptons in the final state are simulated with Sherpa 2.2.2 and the NNPDF3.0NLO PDF set. Final states with no additional partons are calculated at NLO, whereas final states with one, two, or three additional partons are calculated at LO.

For the dominant prompt processes, alternative MC samples are used to estimate modeling uncertainties. These are described in more detail in Sec. VII.

Additional MC samples for EFT contributions are produced at LO in QCD for the $t\bar{t}Wj_{\mathrm{EW}}$ and $t\bar{t}Z$ processes, using the MadGraph v2.9.3 generator and Pythia 8.2 parton shower. The SMEFTsim 3.0 model [62] is used as the Universal FeynRules Output [63], in the M_W electroweak input scheme [64] with the top flavor restrictions. The nominal events are generated according to the SM, and the MadGraph reweighting module is used to compute alternative event weights corresponding to the inclusion of dimension-six EFT vertices and linearized propagator corrections in the production Feynman diagrams. The event weights are used to extract the dependence of various observables, including the cross section, on different EFT operators. The EFT samples are processed to include the effects of the ATLAS detector with a fast simulation in AtlFast II [65] and are reconstructed to perform the EFT interpretation in Sec. IX.

IV. OBJECT RECONSTRUCTION

Interaction vertices from the pp collisions are reconstructed from at least two tracks with p_{T} larger than 500 MeV that are consistent with originating from the beam collision region in the x–y plane. If more than one primary vertex candidate is found in the event, the candidate for which the associated tracks from the largest sum of squared p_{T} is selected as the hard-scatter primary vertex [66].

Electron candidates are reconstructed from energy clusters in the electromagnetic calorimeter matched to a track in the ID [67]. They are required to satisfy $p_{\mathrm{T}} > 7$ GeV and $|\eta| < 2.47$, excluding the transition region between the end cap and barrel calorimeters ($1.37 < |\eta| < 1.52$). "Loose" and "tight" electron identification working points are used, which are based on a likelihood discriminant employing calorimeter, tracking, and combined variables that provide separation between electrons and jets. Electrons are further required to satisfy a boosted decision tree (BDT) discriminant threshold designed to reject charge misidentification.

Muon candidates are reconstructed by performing a combined fit to the track information from the ID and MS [68]. The resulting muon candidates are refitted using the complete track information from both detector systems. They are required to satisfy $p_{\mathrm{T}} > 7$ GeV and $|\eta| < 2.5$. The "medium" muon identification working point is used.

Electron (muon) candidates are matched to the primary vertex by requiring that the significance of their transverse impact parameter, d_0,[2] satisfies $|d_0/\sigma(d_0)| < 5(3)$, where $\sigma(d_0)$ is the measured uncertainty in d_0, and by requiring that their longitudinal impact parameter, z_0,[3] satisfies $|z_0 \sin\theta| < 0.5$ mm.

Leptons from heavy-flavor hadron decays, misidentified jets, or photon conversions are suppressed using a BDT discriminant referred to as the nonprompt lepton BDT [68]. This BDT uses isolation and lifetime information associated with a track jet that matches the electron or muon candidate. A "tight" working point is defined with a prompt electron (muon) efficiency of 65% (80%) for a candidate lepton $p_{\mathrm{T}} = 20$ GeV, increasing to 90% (95%) at $p_{\mathrm{T}} = 45$ GeV. The rejection factors for nonprompt electrons (muons) from heavy-flavor decays range from 60 (30) at low p_{T} to 30 (20) at high p_{T}. The rejection factor for electrons from photon conversions is 5 at low p_{T} and 1.5 at high p_{T}.

The constituents for jet reconstruction are identified by combining measurements from both the ID and the calorimeter using a particle flow (PFlow) algorithm [69]. Jet candidates are reconstructed from "PFlow objects" using the anti-k_t algorithm [70,71] with a radius parameter of $R = 0.4$. They are calibrated using simulation with corrections obtained by using *in situ* techniques in data [72]. Only jet candidates with $p_{\mathrm{T}} > 25$ GeV and within $|\eta| < 4.5$ are selected. To reduce the effect of pileup, each jet with $p_{\mathrm{T}} < 60$ GeV and $|\eta| < 2.4$ must satisfy the tight working point of the jet vertex tagger (JVT) [73] used to identify jets that originate from the primary vertex. A set of quality criteria is also applied to reject events containing at least one jet arising from noncollision sources or detector noise [74].

Jets containing b-hadrons are identified (b-tagged) with an algorithm [75] that uses a deep-learning neural network based on the distinctive features of b-hadron decays, primarily the impact parameters of tracks and the displaced vertices reconstructed in the ID. Additional input to this network is provided by discriminating variables constructed by recurrent neutral networks [76], which exploit the spatial and kinematic correlations between tracks originating from the same b-hadron. A multivariate b-tagging discriminant value is calculated for each jet. A jet is considered b-tagged if it satisfies $|\eta| < 2.4$ and passes the working point corresponding to 77% average expected efficiency to tag a b-quark jet, with rejection factors of 5.6 and 192 for c-jets and

[2]The transverse impact parameter, d_0, is defined in the x–y plane as the distance of closest approach of the track to the beamline.

[3]The longitudinal impact parameter, z_0, is defined as the distance in z between the primary vertex and the point on the track used to evaluate d_0.

light-flavor jets,[4] respectively. Correction factors derived from dedicated calibration samples enriched in b-jets, c-tagged jets, or light-tagged jets are applied to the simulated event samples [77–79].

To avoid double counting of detector signatures, objects are removed using the angular distance $\Delta R \equiv \sqrt{(\Delta y)^2 + (\Delta\phi)^2}$, where y is the rapidity. The overlap removal is performed in the following order: electrons sharing a track with a muon; jets within $\Delta R = 0.2$ of an electron; electrons within $\Delta R = 0.4$ of a jet; jets within $\Delta R = 0.4$ of a muon if they have at most two associated tracks; muons within $\Delta R = 0.4$ of a jet.

The missing transverse momentum $\vec{p}_{\mathrm{T}}^{\,\mathrm{miss}}$ (with magnitude $E_{\mathrm{T}}^{\mathrm{miss}}$) is defined as the negative vector sum of the $\vec{p_{\mathrm{T}}}$ of all selected and calibrated objects in the event, including a term to account for the momenta of soft particles that are not associated with any of the selected objects [80]. This soft term is calculated from ID tracks matched to the primary vertex, which makes it more resilient to contamination from pileup interactions.

Scale factors are used to correct the efficiencies in simulation to match the efficiencies measured in data for the electron [67,81] and muon [68,82] trigger, reconstruction, and identification and isolation criteria. Additional scale factors are also applied for the JVT requirement [73], for pileup, and for the b-tagging efficiencies for jets that originate from the hadronization of b-quarks [77], c-quarks [78], and light quarks or gluons [79].

V. EVENT SELECTION

The analysis primarily targets $t\bar{t}Wj_{\mathrm{EW}}$ events in which the W boson decays leptonically, the same-charge top-quark decays via a W boson to $\ell\nu b$, and the other top-quark decays hadronically, giving rise to a dilepton signature including same-charge leptons, which can be exploited to suppress other dilepton backgrounds. Signal events are expected to present five jets: two b-tagged jets originating from the two top quarks, two light jets originating from the hadronic top-quark decay, and an additional spectator jet.

A preselection, defined to loosely match the expected signal topology, requires that the events contain exactly two same-charge leptons (electrons or muons). At least one lepton is required to be above $p_{\mathrm{T}}(l_0) > 28$ GeV and to be trigger matched, while $p_{\mathrm{T}}(l_1) > 20$ GeV is required for the subleading lepton to reduce the fake-lepton background. The pseudorapidity of the muons must fulfill $|\eta| < 2.5$, while $|\eta| < 2.0$ is required for the electrons. Electrons are required to satisfy the tight identification working point. The event is required to contain at least three jets, with the leading jet having a transverse momentum $p_{\mathrm{T}}(j_0) > 60$ GeV. A requirement of the dilepton invariant mass, m_{ll}, to be greater than 30 GeV is imposed to remove fake-lepton events. At least one of the jets must be b-tagged. These requirements are summarized in Table I.

TABLE I. Summary of the definition of the preselection and signal regions. The m_{ee} selection is used to exclude events with an electron-pair invariant mass compatible with that of the Z boson mass (81.1 GeV $< m_{ee} <$ 101.1 GeV).

	Preselection	Signal region
Leptons	2 same-charge leptons	2 same-charge leptons
$p_{\mathrm{T}}(l_0)$	>28 GeV	>80 GeV
$p_{\mathrm{T}}(l_1)$	>20 GeV	>40 GeV
$\lvert\eta(e)\rvert$	<2.0	<2.0
$\lvert\eta(\mu)\rvert$	<2.5	<2.5
N (jets)	≥3	≥4
N (b-jets)	≥1	≥1
$p_{\mathrm{T}}(j_0)$	···	>60 GeV
m_{ll}	>30 GeV	>125 GeV
m_{ee}	···	∉ [81.1, 101.1] GeV
$\lvert\Delta\eta_j\rvert$	···	>2.0
$\sum p_{\mathrm{T}}(j)$	···	>250 GeV
Conversion radius (e)	···	≥50 mm

The signal is characterized by a topology with a forward jet and a high energy scale. The selection for the signal region requires at least four jets and the expected high energy scale is reflected in the requirements for a high $m_{ll} > 125$ GeV and lepton $p_{\mathrm{T}}(l_{0(1)}) > 80$ GeV (40 GeV) for the leading (subleading) lepton. The presence of a forward jet in the signal is exploited in the signal region definition, using the distribution of $\Delta\eta_j$: the difference in pseudorapidity between the most forward non-b-tagged jet and the jet with which it produces the highest invariant mass. These variables all help to provide separation between the $t\bar{t}Wj_{\mathrm{EW}}$ process and $t\bar{t}W$ QCD. In the case of dielectron events, events with invariant masses compatible with the Z boson mass (81.1 GeV $< m_{ee} <$ 101.1 GeV) are removed to reduce the contribution from electrons with misidentified charge. Events with fake leptons are reduced by a requirement on the scalar p_{T} sum of all selected jets ($\sum p_{\mathrm{T}}(j) > 250$ GeV). The fake leptons are primarily from the $t\bar{t}$ process that has few jets from the harder scatter process and subsequently on average a lower $\sum p_{\mathrm{T}}(j)$. Photon conversions are reduced by removing events with displaced vertices with a conversion radius (the radial distance from the collision point to conversion location) smaller than 50 mm associated with the electron track, if the conversion vertex is reconstructed. These requirements are also summarized in Table I.

An important background to $t\bar{t}Wj_{\mathrm{EW}}$ but also crucial for the EFT interpretation in Sec. IX, where it is considered a signal, is $t\bar{t}Z$ production. A region created to isolate $t\bar{t}Z$ production [3L-CR (ttZ)] is defined by requiring at least one same-flavor opposite-charge (SFOC) lepton pair with m_{ll} in a range compatible with the Z boson mass and greater than four jets, of which at least two must be b-tagged.

[4]"Light jet" refers to a jet originating from the hadronization of a light quark (u, d, s) or a gluon.

TABLE II. Summary of the definition of the control regions. The "SR Veto" condition requires that an event does not satisfy the Signal Region requirements. The 3L-CR ($t\bar{t}Z$) m_{ll} requirement applies to SFOC leptons.

Control regions	3J -CR	4J-lo$\Delta\eta$ -CR	4J-hi$\Delta\eta$ -CR	Conv-CR	CF-CR	3L-CR ($t\bar{t}Z$)	3L-CR
Leptons	2 same charge	2 same charge	2 same charge	2 same charge (ee or $e\mu$)	2 same-charge ee	3 leptons	3 leptons
$p_{\mathrm{T}}(l_0)$	>28 GeV	>28 GeV	>80 GeV	>28 GeV	>50 GeV	>28 GeV	>28 GeV
$p_{\mathrm{T}}(l_1)$	>20 GeV	>20 GeV	>20 GeV	>20 GeV	>30 GeV	>20 GeV	>20 GeV
$p_{\mathrm{T}}(l_2)$	…	…	…	…	…	>20 GeV	>20 GeV
N(jets)	= 3	≥4	≥4	≥4	≥3	≥4	= 3
N(b-jets)	≥1	≥1	≥1	≥1	≥1	≥2	= 1
$p_{\mathrm{T}}(j_0)$	…	>60 GeV	>60 GeV	>60 GeV	>60 GeV	>60 GeV	…
m_{ll}	>160 GeV	>30 GeV	>30 GeV	>30 GeV	…	SFOC, $\in$ [81.1, 101.1] GeV	…
m_{ee}	$\notin$ [81.1, 101.1] GeV	$\notin$ [81.1, 101.1] GeV	$\notin$ [81.1, 101.1] GeV	$\notin$ [81.1, 101.1] GeV	$\in$ [81.1, 101.1] GeV	…	…
$\lvert\Delta\eta_{jj}\rvert$	…	<2.0	>2.0	(<2.0 OR	…	…	…
$\sum p_{\mathrm{T}}(j)$	…	…	…	<250 GeV)	…	…	…
Conversion radius (e)	…	≥50 mm	≥50 mm	<50 mm	≥50 mm	…	…
$E_{\mathrm{T}}^{\mathrm{miss}}$	…	…	…	…	<100 GeV	…	…
Veto condition	…	…	SR Veto	…	…	…	…

Dedicated control regions enriched in the dominant backgrounds are included in the fit to constrain these backgrounds from data. Table II summarizes the definitions of the control regions used. There are seven control regions in total. Two single-bin regions target the normalizations of backgrounds from photon conversions (Conv-CR) and misidentified electron charge ("charge flips," CF-CR). In CF-CR, a veto on events with $E_{\mathrm{T}}^{\mathrm{miss}} > 100$ GeV is needed to reject contributions from the $t\bar{t}W$ process, featuring neutrinos and genuine $E_{\mathrm{T}}^{\mathrm{miss}}$. The region targeting diboson events (3L-CR) has the same selection except with lower multiplicity jet requirements of exactly three jets, of which exactly one must be b-tagged. To increase the separation between the diboson and $t\bar{t}Z$ processes, the two regions targeting them are binned in H_{T} (the scalar sum of transverse energy in the event excluding the $E_{\mathrm{T}}^{\mathrm{miss}}$). The other three regions (4J-lo$\Delta\eta$, 4J-hi$\Delta\eta$, and 3J CRs) are binned according to the channel (ee, $e\mu$, and $\mu\mu$), the lepton charge, and the number of b-jets, for a total of 12 bins per region. The 4J-lo$\Delta\eta$ region targets the normalization of the $t\bar{t}W$ QCD background at low $\Delta\eta$. The 4J-hi$\Delta\eta$ region targets the normalization of the $t\bar{t}W$ QCD and the fake-lepton background at high $\Delta\eta$ with the same $\Delta\eta$ requirement as in the signal region, but with orthogonal H_{T}, $p_{\mathrm{T}}(l_0)$, $p_{\mathrm{T}}(l_1)$, and m_{ll} requirements to the signal region. The 3J CR constrains the overall non-$t\bar{t}W$ QCD backgrounds at high m_{ll}, in a phase space close to the SR.

VI. BACKGROUND ESTIMATES

Backgrounds consisting of prompt leptons are estimated with the Monte Carlo templates described in Sec. III. The normalizations of the $t\bar{t}Z$, VV, and $t\bar{t}W$ QCD processes are adjusted using unconstrained normalization factors that are determined by performing a likelihood fit to data across the CRs simultaneously with the SR.

Events containing CF electrons or fake leptons are significant backgrounds to the $t\bar{t}Wj_{\mathrm{EW}}$ process. These two categories are difficult to accurately model in simulations and are estimated from data.

The CF background is estimated by extracting charge-flip efficiency in dielectron events close to the Z boson invariant mass peak. The selected events have at most one jet and no b-tagged jets. The corresponding efficiencies are binned in electron p_{T} and η and then applied to opposite-charge events that have otherwise the same event selection applied as in the signal region.

The fake-lepton event yield is estimated from data events using the matrix method (MM) [83], where contributions from "real leptons" (prompt leptons with correctly assigned charge), charge flip, and photon conversion sources are subtracted using simulation.

The MM requires a sample of events with relaxed lepton criteria, which is achieved by removing the isolation requirements for both muons and electrons, and using the loose electron identification selection. The MM model input parameters are the real and fake electron

and muon selection efficiencies for both the nominal and the relaxed criteria, which are extracted from a global simultaneous fit of the MM model. The output of the MM model is a solution in terms of prompt and fake leptons, the latter of which are then used for the estimation of this background in the analysis. The efficiencies are parametrized in lepton flavor, lepton charge, lepton transverse momentum, and number of b-tagged jets. In the following, the fake background estimate is therefore provided grouped into four different templates corresponding to one or two b-jets and positive or negative lepton charges: fakes $1b++/1b--/2b++/2b--$. The fake efficiency extraction regions are similar to the preselection but with inverted requirements on the invariant mass of the two leptons in three-jet events, and inverted maximum jet p_{T} in four-jet events to ensure orthogonality to the other control and signal selections. A validation of the fake-lepton source composition is performed by confirming that agreement with data is observed in validation regions, defined by changing the three-jet selection to a four-jet selection.

The MM control regions have a relatively high predicted contamination of $t\bar{t}W$ events, ranging from 17% in one-b-tagged events to 31% in two-b-tagged events. To reduce the modeling dependence on this process, the MM parameters are determined as a function of the $t\bar{t}W$ cross section. The actual $t\bar{t}W$ cross section is later measured *in situ* and the fake-lepton background is automatically adjusted during the minimization of the likelihood used for the $t\bar{t}Wj_{\mathrm{EW}}$ measurement. This procedure properly accounts for the additional uncertainty induced by the $t\bar{t}W$ dependence of the fake-lepton estimate.

The background of leptons arising from photon conversions is estimated from simulated samples, isolating this contribution using generator-level information, and are normalized with a dedicated control region described in Sec. V.

VII. SYSTEMATIC UNCERTAINTIES

Systematic uncertainties from experimental sources and theoretical predictions can affect both the overall yield and the shape of the observables used in the fit for the statistical analysis.

The MC event yields are normalized to the data using the total integrated luminosity. The uncertainty in the combined 2015–2018 integrated luminosity is 0.83% [84], obtained using the LUCID-2 detector [32] for the primary luminosity measurements, complemented by measurements using the ID and calorimeters. The uncertainty in the reweighting of the MC pileup distribution to match the distribution in data is evaluated by varying the visible inelastic cross section.

For electrons and muons, the reconstruction, identification, isolation, and trigger efficiency scale factors have associated uncertainties [82,85]. The impact of the lepton energy scale and resolution uncertainty is evaluated by scaling or smearing the p_{T} of all leptons accordingly and reapplying the event selection [67,68].

Uncertainties are assigned to the scale and resolution of the soft track component of the $E_{\mathrm{T}}^{\mathrm{miss}}$. They are derived from differences between data and MC simulation in the measurement of the p_{T} balance between the hard and soft $E_{\mathrm{T}}^{\mathrm{miss}}$ components [80].

The jet energy scale (JES) is calibrated using MC simulations, data taken during LHC runs, and test beams as well as *in situ* information [86]. The uncertainty in the JES consists of many correlated components. To achieve a simplified setup with a minimum loss of correlation information, an eigenvector decomposition is used. A similar approach is used for the jet energy resolution uncertainty. The uncertainty associated with the JVT discriminant for pileup jet rejection is obtained by varying the efficiency correction factors [73]. Uncertainties are also considered in the b-tagging algorithm correction factors to the efficiencies measured from data which depend on the jet flavor and kinematic quantities of the jets. Additionally, flavor tagging extrapolation uncertainties for jets with p_{T} above the calibration range are considered.

Alongside detector-related sources of systematic uncertainties, there are also uncertainties associated with the modeling of the MC predictions including their migrations between analysis regions. For prompt backgrounds that do not have free-floating normalizations in the fit, uncertainties in the predicted cross section are included as nuisance parameters: 20% for $t\bar{t}H$ [87], 17% for tZq [88], 20% for other top-quark processes, and 30% for "other" minor processes. These values are chosen as constraints based on previous measurements of the relevant processes.

For the $t\bar{t}Wj_{\mathrm{EW}}$ process the uncertainty due to the ME calculation and the parton shower choices is estimated by comparing the nominal Sherpa sample with the alternative MadGraph5_aMC@NLO+Pythia8 sample also at LO accuracy. The uncertainty due to the choice of parton shower, hadronization, and underlying event model is estimated by comparing the difference between Powheg + Pythia 8 and Powheg + Herwig 7 alternative samples and applying that difference to the nominal Sherpa sample. To estimate the effect of missing higher-order corrections, variations of μ_{R} and μ_{F} simultaneously up or down by a factor of 2 are applied. Uncertainties in the PDFs are evaluated by following the recommended PDF4LHC prescription [89] and include variations of the α_s scale and uncertainties related to the PDF choice. An uncertainty in the JES related to the fractions of quark- and gluon-initiated jets is included through variations relative to the nominal $t\bar{t}Wj_{\mathrm{EW}}$ sample, parametrized in jet η and p_T.

For the $t\bar{t}W$ QCD process, the uncertainty due to the generation of the hard-scattering process and the parton shower choices is estimated by comparing the nominal Sherpa sample with an alternative MadGraph5_aMC@NLO+Pythia 8 sample generated with up to one additional parton at NLO with FxFx merging [12]. The uncertainty due to the choice of parton shower, hadronization, and underlying event model is estimated by computing the difference between

the Powheg + Pythia 8 and Powheg + Herwig 7 alternative samples and applying that difference to the nominal Sherpa sample. The estimation of the effect of missing higher-order corrections via variations of μ_R and μ_F, the PDF uncertainties, and the jet flavor uncertainties are evaluated in the same way as in the $t\bar{t}W j_{EW}$ process.

For the $t\bar{t}Z$ and tZq processes, the uncertainty due to the simulation of the initial-state radiation is taken into account by varying the Var3c parameter of the PYTHIA A14 tune. The uncertainty due to the parton shower choice is estimated by comparing the nominal MadGraph5_aMC@NLO +Pythia 8.2 sample with an alternative MadGraph5_aMC@NLO sample interfaced with Herwig. The PDF uncertainties and the jet flavor uncertainties are evaluated in the same way as in the $t\bar{t}W j_{EW}$ process.

As described in Sec. VI, several sources of uncertainties affecting the estimate of the fake rates are considered. These include the correlation of the lepton fakes with the $t\bar{t}W$ QCD process, the number of events in each p_T bin, and the uncertainties in the background processes that enter into the likelihood fit to estimate the fake-lepton efficiency.

VIII. MEASUREMENT UNDER SM HYPOTHESIS AND CROSS SECTION UPPER LIMIT EXTRACTION

The $t\bar{t}W j_{EW}$ production cross section, $\sigma_{t\bar{t}W j_{EW}}$, is obtained using a profile-likelihood fit [90] to a SR binned in $|\Delta\eta_j|$ and multiple CRs. The fit is performed simultaneously to 46 CR and three SR bins using the TRExFitter [91] framework. The expected signal and background distributions are modeled using template histograms from the MC simulated samples and the data-driven estimates as described in Sec. VI. The sum of signal and background contributions is fitted to the data. The likelihood function is constructed as a product of Poisson terms for the event yields and Gaussian functions to constrain nuisance parameters, which represent systematic uncertainties, across all bins included in the search. For uncertainties related to the finite number of simulated MC events, the Gaussian terms are replaced by Poisson terms, following the Beeston-Barlow "lite" method [92]. The signal strength, which is the ratio of the observed $t\bar{t}W j_{EW}$ production cross section (σ_{obs}) to the theoretical $t\bar{t}W j_{EW}$ cross section (σ_{SM}) and denoted by $\mu_{t\bar{t}W j_{EW}} = \sigma_{obs}/\sigma_{SM}$, is a free parameter in the profile-likelihood fit. The normalizations of the $t\bar{t}Z$, $t\bar{t}W$ QCD, VV, photon conversion, and electron charge misidentification processes are also free parameters in the profile-likelihood fit.

Table III shows the yields in the SR and CRs following a representative fit to data with the $t\bar{t}W j_{EW}$ signal normalization fixed to the SM expectation ($\mu_{t\bar{t}W j_{EW}} = 1$). The quadrature sum of uncertainties is not equal to the total uncertainty because of correlations introduced by the fit. There is significant correlation between some of the fitted parameters, including an approximately 70% anticorrelation between the $t\bar{t}W$ QCD normalization and $\mu_{t\bar{t}W j_{EW}}$, as well as approximately 30% anticorrelations between some of the nuisance parameters relating to the fake-lepton estimates and the $t\bar{t}W$ QCD normalization. Most relevant

TABLE III. Observed and expected event yields in the signal and control regions obtained for an integrated luminosity of 140 fb^{-1} after performing a fit to the data with the $t\bar{t}W j_{EW}$ normalization fixed to the SM expectation ($\mu_{t\bar{t}W j_{EW}} = 1$) but with theory uncertainties implemented as nuisance parameters. The indicated errors include the Monte Carlo statistical uncertainties and all other systematic uncertainties. The quadrature sum of uncertainties is not equal to the total uncertainty because of correlations introduced by the fit. A dash (—) indicates event yields smaller than 0.1 events.

	SR	4J-lo$\Delta\eta$-CR	4J-hi$\Delta\eta$-CR	3J-CR	3L-CR (ttZ)	3L-CR	Conv-CR	CF-CR
$t\bar{t}W_{QCD}$	121 ± 26	250 ± 40	106 ± 22	67 ± 13	2.6 ± 0.6	24 ± 5	0.93 ± 0.25	7.6 ± 1.4
tZq	7.6 ± 1.4	2.20 ± 0.35	9.2 ± 2.2	7.5 ± 1.2	23 ± 4	68 ± 11	—	0.88 ± 0.22
$t\bar{t}Z$	31 ± 4	43 ± 8	30 ± 4	7.2 ± 1.7	133 ± 15	66 ± 14	0.26 ± 0.15	2.2 ± 0.4
VV	30 ± 6	26 ± 5	34 ± 7	34 ± 6	14.1 ± 2.7	152 ± 27	0.23 ± 0.04	3.8 ± 0.7
$t\bar{t}H$	21 ± 4	59 ± 12	29 ± 6	3.9 ± 0.9	3.7 ± 0.8	9.3 ± 1.9	0.27 ± 0.06	2.3 ± 0.5
Other top bkg.	30 ± 6	30 ± 6	27 ± 6	12.8 ± 3.0	13.2 ± 2.7	25 ± 5	14.1 ± 3.2	2.4 ± 0.6
Other	0.25 ± 0.07	1.6 ± 0.5	1.04 ± 0.30	0.20 ± 0.06	—	—	0.34 ± 0.10	6.6 ± 1.9
Conversions	20 ± 7	28 ± 10	24 ± 8	17 ± 6	1.5 ± 0.5	9 ± 4	27 ± 8	13 ± 5
Charge flips	62 ± 9	29 ± 4	55 ± 8	80 ± 12	—	—	0.68 ± 0.11	68 ± 10
Fakes 1b++	11 ± 5	30 ± 10	25 ± 8	15 ± 7	—	16 ± 5	0.8 ± 0.6	1.6 ± 1.4
Fakes 1b−−	3.5 ± 1.6	30 ± 7	27 ± 5	10.0 ± 3.1	—	15.0 ± 3.4	0.9 ± 0.4	3.2 ± 1.4
Fakes 2b++	16 ± 6	22 ± 10	13 ± 6	8.0 ± 3.1	0.9 ± 0.7	—	0.71 ± 0.31	0.65 ± 0.30
Fakes 2b−−	7.1 ± 2.9	22 ± 8	14 ± 5	4.1 ± 2.0	0.66 ± 0.10	—	1.9 ± 0.5	1.8 ± 0.6
$t\bar{t}W j_{EW}$ ($\mu_{t\bar{t}W j_{EW}} = 1$)	15.7 ± 2.6	7.3 ± 2.6	11.5 ± 1.9	1.31 ± 0.26	—	0.124 ± 0.028	—	0.53 ± 0.13
Total	376 ± 20	584 ± 23	405 ± 16	268 ± 12	192 ± 14	384 ± 19	48 ± 7	114 ± 8
Data	379	586	393	267	193	387	49	119

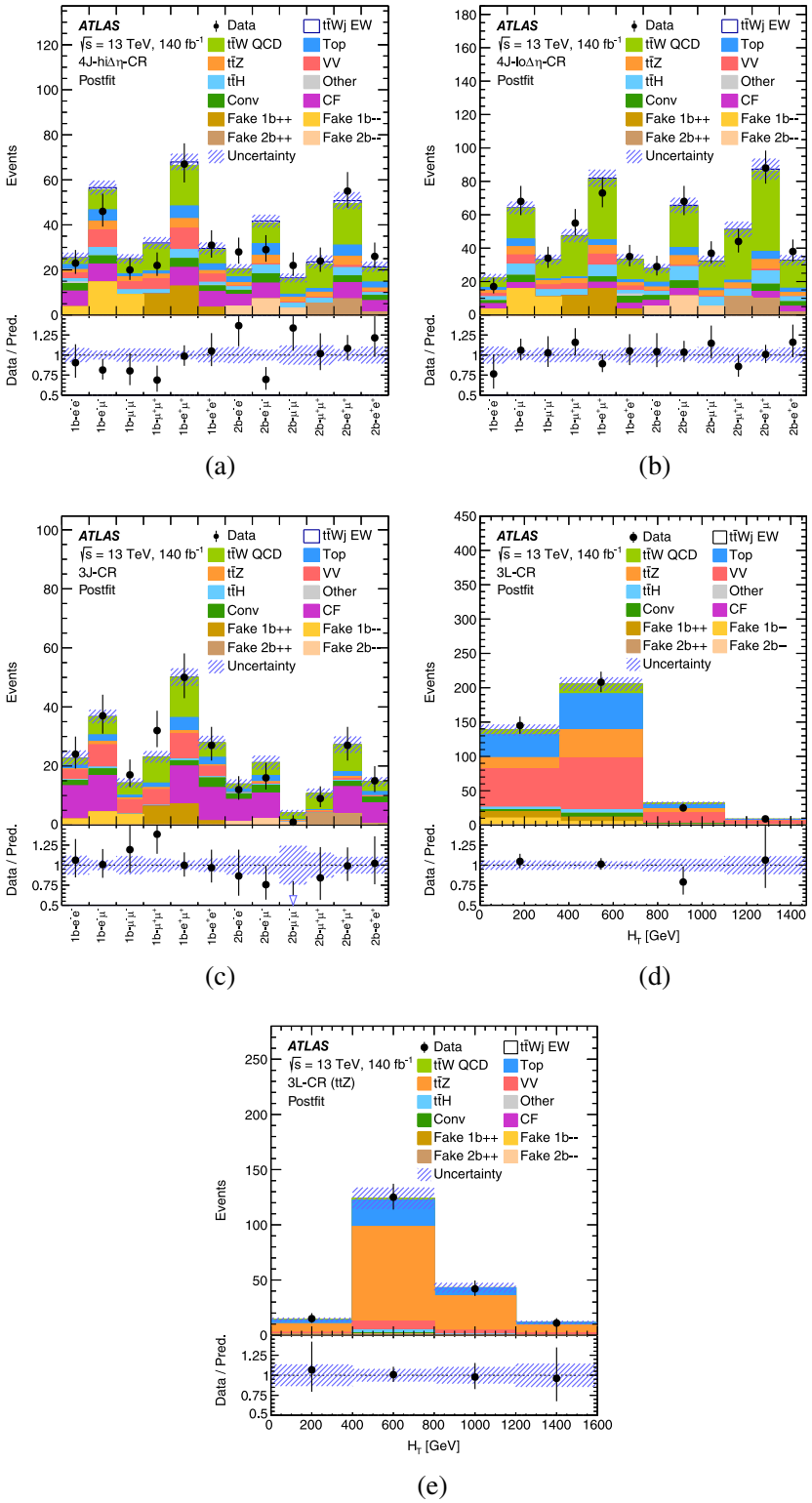


FIG. 3. Postfit distributions in each of the analysis regions: (a) 4J-hi$\Delta\eta$-CR, (b) 4J-lo$\Delta\eta$-CR, (c) 3J-CR, (d) 3L-CR, and (e) 3L-CR (ttZ). The shaded uncertainty bands include all statistical and systematic uncertainties. For the 3L-CR and 3L-CR ($t\bar{t}Z$) distributions, the last bin includes overflow events. For comparison with Table III, "Top" refers to "tZq" and "Other top backgrounds," "CF" refers to "charge-flip" events, and "Conv" refers to "Conversions".

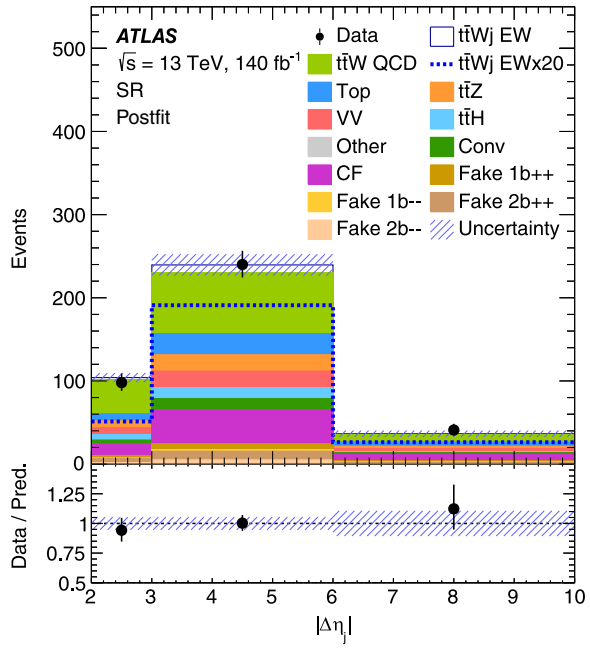


FIG. 4. Postfit distribution of the $|\Delta\eta_j|$ observable in the signal region after the signal-plus-background fit to data. The shaded uncertainty band includes all statistical and systematic uncertainties. The binning starts from 2, following the signal region definition in Table I. For comparison with Table III, "Top" refers to "tZq" and "Other top backgrounds," "CF" refers to "charge-flip" events, and "Conv" refers to "conversions." In addition to the stacked histogram, the signal process is also shown as a dashed line overlaid, multiplied by a factor of 20.

for the processes targeted by the 3L CRs are the approximately 25% anticorrelations between the VV normalization and $t\bar{t}Z$ and tZq normalizations.

Figures 3 and 4 show the postfit distributions in the CRs and the SR, for a fit to data also including a free-floating normalization factor for the $t\bar{t}W j_{\mathrm{EW}}$ signal. The fitted normalization factors for the free-floating processes in this fit are listed in Table IV.

Within the experimental sensitivity, good agreement is found between the data and the SM prediction, resulting in an observed (expected) measurement of $\mu_{t\bar{t}Wj_{\mathrm{EW}}} = 0.9^{+2.4}_{-3.0}$ $(1.0^{+2.4}_{-2.5})$. After applying the CL_s method [93] the observed (expected) 95% CL_s upper limit on the normalization factor is $\mu_{t\bar{t}Wj_{\mathrm{EW}}} < 5.3$ (4.8), which translates to an observed (expected) upper limit on the cross section of $\sigma_{t\bar{t}Wj_{\mathrm{EW}}} < 251$ fb (230 fb), to be compared with the expected SM cross section of $47.7^{+1.9}_{-1.4}$ fb [12]. The measurement is overall dominated by systematic uncertainties detailed in Table V. The leading sources of uncertainty in the fitted value of $\mu_{t\bar{t}Wj_{\mathrm{EW}}}$ are the normalization and modeling of the $t\bar{t}W$ QCD process, uncertainties related to the jet modeling, and the estimate of the fake-lepton contributions. None of the nuisance parameters with significant impact on the signal strength are constrained to less than 70% of their original values. Of those most relevant, the nuisance parameters relating to the statistical uncertainty in fake-lepton estimate ($t\bar{t}W$ QCD parton shower modeling) are constrained to 70% (80%) of their original values.

TABLE IV. Signal and background normalization factors measured in the profile-likelihood signal-plus-background fit to the data. All sources of statistical and systematic uncertainties are included.

Process	Normalization factor (μ)
$t\bar{t}Wj_{\mathrm{EW}}$	$0.9^{+2.4}_{-3.0}$
$t\bar{t}Z$	$0.94^{+0.14}_{-0.13}$
$t\bar{t}W_{\mathrm{QCD}}$	$1.06^{+0.28}_{-0.26}$
VV	$1.11^{+0.20}_{-0.20}$
Conversions	$1.12^{+0.37}_{-0.34}$
Charge flips	$0.92^{+0.14}_{-0.14}$

TABLE V. Grouped impact of systematic uncertainties in the $t\bar{t}Wj_{\mathrm{EW}}$ signal strength, $\mu_{t\bar{t}Wj_{\mathrm{EW}}}$, after the profile-likelihood signal-plus-background fit to the data. The impact of each uncertainty is assessed by fixing the relevant fit parameters for a given uncertainty and refitting to data. The reduction in the total uncertainty in this modified fit gives the quoted impact. The quadrature sum of individual groups of uncertainties is not equal to the total uncertainty because of correlations introduced by the fit.

Uncertainty source	$\Delta\mu_{t\bar{t}Wj_{\mathrm{EW}}}$
Total statistical and systematic	$+2.4/-3.0$
Total systematic	$+2.2/-2.8$
Total statistical	$+0.9/-0.9$
$t\bar{t}W_{\mathrm{QCD}}$ normalization	$+1.6/-2.2$
Jets and $E_{\mathrm{T}}^{\mathrm{miss}}$	$+1.6/-2.2$
$t\bar{t}Wj_{\mathrm{EW}}$ modeling	$+0.4/-1.5$
$t\bar{t}W_{\mathrm{QCD}}$ modeling	$+0.6/-1.2$
MC statistical	$+0.7/-0.9$
Fake leptons	$+0.5/-0.7$
Pileup	$+0.2/-0.5$
$t\bar{t}Z$ normalization	$+0.3/-0.4$
$t\bar{t}Z$ modeling	$+0.23/-0.27$
Background cross sections	$+0.18/-0.31$
Electron ID and isolation	$+0.09/-0.09$
b-tagging	$+0.09/-0.09$
Muons	$+0.07/-0.07$
tZq modeling	$+0.07/-0.07$
Luminosity	$+0.034/-0.034$
Electron energy scale and resolution	$+0.024/-0.024$
JVT	<0.01

IX. EFFECTIVE FIELD THEORY INTERPRETATION

New physics could affect the $t\bar{t}Wj_{\mathrm{EW}}$ process at high energy scales and can be parametrized in the context of an

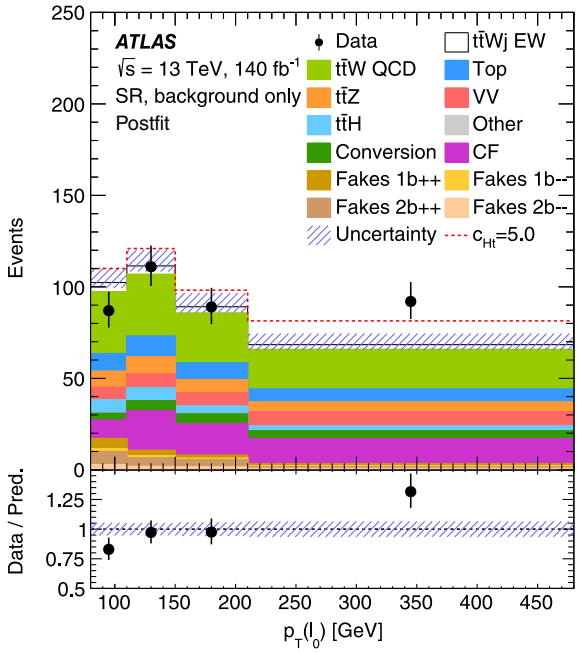
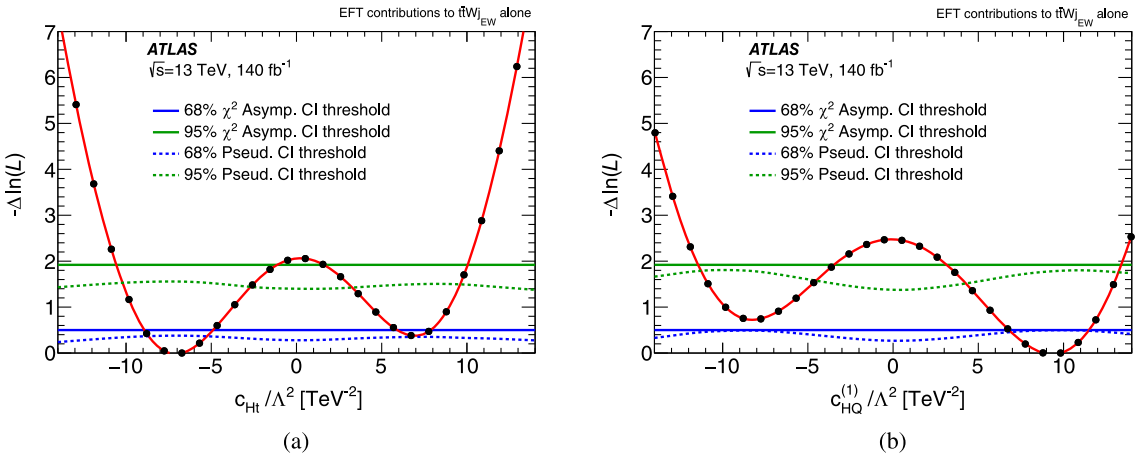


FIG. 5. Distribution of the EFT-sensitive observable $p_{\mathrm{T}}(l_0)$ in the signal region, after a fit to data of the SM processes in the control regions only. The dashed line represents the expected total distribution of an EFT signal stacked on top of the SM processes, with $c_{Ht} = 5$ for illustration purposes. The shaded uncertainty band includes all statistical and systematic uncertainties. The highest bin is inclusive and includes all events above the upper bin edge.

EFT. The $t\bar{t}Wj_{\mathrm{EW}}$ cross section is increased by nonzero Wilson coefficients for operators such as O_{Ht} and $O_{HQ}^{(1)}$ [1]. These operators also contribute to modifications of the $t\bar{t}Z$ process [94]. Therefore, along with an assessment of the effect of O_{Ht} and $O_{HQ}^{(1)}$ on $t\bar{t}Wj_{\mathrm{EW}}$ production, the complementarity with $t\bar{t}Z$ is exploited in a fit assessing contributions from the two EFT operators to both physics processes.

As the effects of O_{Ht} and $O_{HQ}^{(1)}$ grow with the energy scale of the scattering process, the signal region is rebinned in four bins of $p_{\mathrm{T}}(l_0)$ to maximize the sensitivity to the EFT operators. Figure 5 shows the $p_{\mathrm{T}}(l_0)$ distribution in the signal region, comparing observed events to the SM prediction normalized in a fit to the control regions only. The subsequent EFT fits are otherwise performed identically to the SM measurement, with the exception that when an EFT operator is considered to affect the $t\bar{t}Wj_{\mathrm{EW}}$ ($t\bar{t}Z$) process, the floating normalization factor for that process is replaced with a dedicated cross section uncertainty nuisance parameter of size $^{+4\%}_{-3\%}$ [4,12] ($\pm 9.5\%$ [95]). Additionally, a new free-floating parameter is introduced to parametrize the effect of the EFT operator on the $t\bar{t}Wj_{\mathrm{EW}}$ ($t\bar{t}Z$) normalization in each bin of the analysis. The assumed energy scale is set to $\Lambda = 1$ TeV. Several fit configurations are considered for the EFT interpretations. One configuration allows EFT variations only on $t\bar{t}Wj_{\mathrm{EW}}$ production and not $t\bar{t}Z$, and another configuration allows EFT variations on both $t\bar{t}Wj_{\mathrm{EW}}$ and $t\bar{t}Z$. For both these configurations, interpretations are made considering each EFT operator alone, and both operators simultaneously. This combination of interpretations is designed to disentangle the sensitivity from each process to each operator and probes the nature of their complementarity. For these configurations the EFT effects are applied to the relevant processes in the rebinned SR and all CRs.

The asymptotic likelihood approach relies on Wilks's theorem [96] for the extraction of the confidence intervals using the properties of a χ^2 distribution [90]. However, in the EFT fits the $t\bar{t}Wj_{\mathrm{EW}}$ process has non-negligible



(a) (b)

FIG. 6. Difference in the log-likelihood as a function of (a) c_{Ht} and (b) $c_{HQ}^{(1)}$ Wilson coefficients, as determined in the EFT fit to data, considering the impact of each coefficient independently on the $t\bar{t}Wj_{\mathrm{EW}}$ process. The solid lines show the asymptotic χ^2 68% and 95% thresholds (Asymp.) for calculating confidence intervals. The dashed lines show alternative estimations of the 68% and 95% confidence interval thresholds using pseudodatasets (Pseud.), as described in the text.

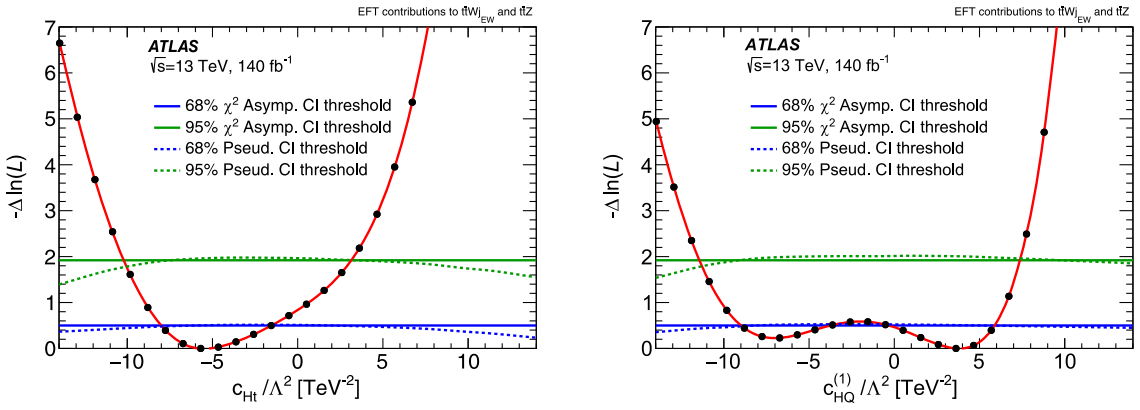


FIG. 7. Difference in the log-likelihood as a function of (a) c_{Ht} and (b) $c_{HQ}^{(1)}$ Wilson coefficients, as determined in the EFT fit to data, considering the corresponding EFT contributions from one coefficient at a time but simultaneously on both the $t\bar{t}Wj_{\mathrm{EW}}$ and $t\bar{t}Z$ processes. The solid lines show the asymptotic χ^2 68% and 95% thresholds (Asymp.) for calculating confidence intervals. The dashed lines show alternative estimations of the 68% and 95% confidence interval thresholds using pseudodatasets (Pseud.), as described in the text.

quadratic dependencies on Wilson coefficients, which lead to violations of Wilks's theorem [97] and over- or under-coverage of the true intervals. An alternative method for extracting confidence intervals is employed in which pseudodatasets are generated at different values of a Wilson coefficient and fitted individually. From these fits, test-statistic distributions are constructed to derive the final confidence intervals.

Figure 6 shows likelihood scans considering the impact of O_{Ht} and $O_{HQ}^{(1)}$ independently on the $t\bar{t}Wj_{\mathrm{EW}}$ process alone. The one-dimensional χ^2 threshold at $-\Delta\ln(L) = 0.5$, which relies on Wilks's theorem, results in compatible but looser confidence intervals than determined from the alternative threshold using pseudodatasets.

Figure 7 shows likelihood scans considering the impact of O_{Ht} and $O_{HQ}^{(1)}$ independently on both the $t\bar{t}Wj_{\mathrm{EW}}$ and $t\bar{t}Z$ processes. The larger linear contributions of the EFT operators to the $t\bar{t}Z$ process mitigate coverage changes due to the violation of Wilks's theorem.

Figure 8 shows the full two-dimensional 95% confidence intervals determined using pseudodatasets when fitting both c_{Ht} and $c_{HQ}^{(1)}$ simultaneously $(O_{Ht} + O_{HQ}^{(1)})$. The numerical results of all fits are summarized in Figs. 9 and 10 and are detailed in Table VI. The EFT fits use both linear and quadratic terms and consider either both EFT operators simultaneously, $c_{Ht} + c_{HQ}^{(1)}$ (profiled), or only individual EFT Wilson coefficients (independent). The fits

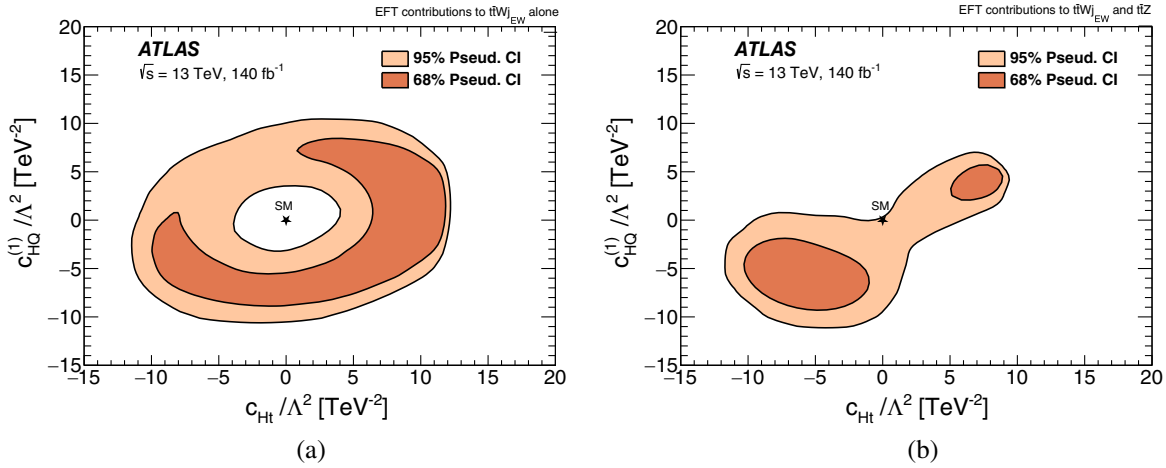


FIG. 8. Two-dimensional 68% and 95% confidence intervals for the simultaneous EFT fit to data of the Wilson coefficients c_{Ht} and $c_{HQ}^{(1)}$, considering their impact on (a) the $t\bar{t}Wj_{\mathrm{EW}}$ process alone or (b) on both the $t\bar{t}Wj_{\mathrm{EW}}$ and $t\bar{t}Z$ processes. The confidence intervals are determined using pseudodatasets (Pseud.).

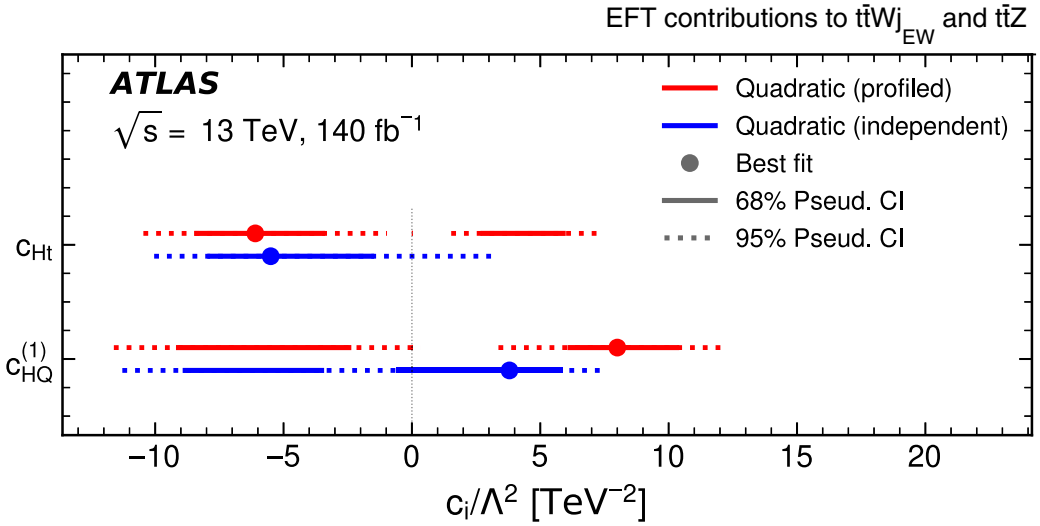


FIG. 9. 95% confidence intervals determined using pseudodatasets (Pseud.) for the c_{Ht} and $c_{HQ}^{(1)}$ Wilson coefficients from fits to both $t\bar{t}Wj_{\mathrm{EW}}$ and $t\bar{t}Z$. The intervals are obtained from both fits to each EFT operator independently (independent), and from two-dimensional fits to both operators simultaneously (profiled).

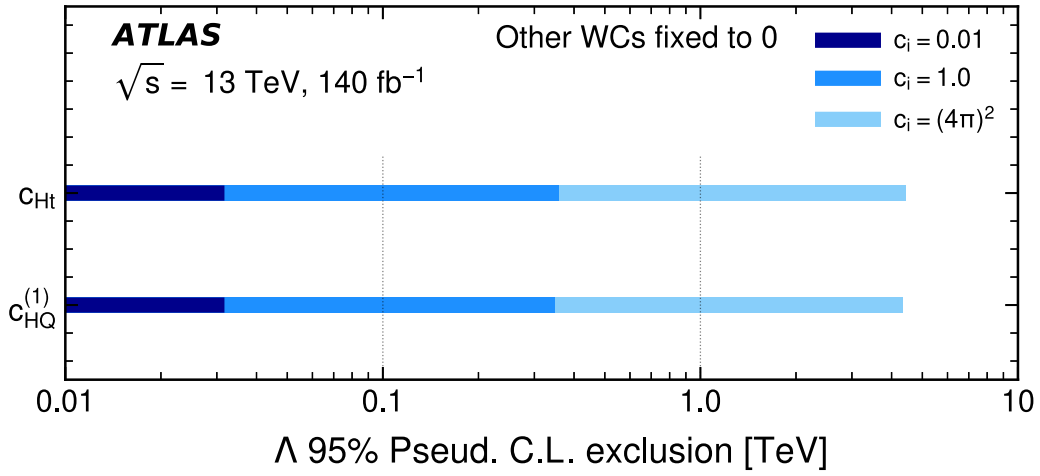


FIG. 10. 95% confidence level exclusion limits on the new physics scale Λ for different assumptions on the value of the (dimensionless) Wilson coefficients c_{Ht} and $c_{HQ}^{(1)}$. The limits are determined for each EFT operator independently by converting the average magnitude of the up and down uncertainties from the pseudodatasets (Pseud.) fits to both $t\bar{t}Wj_{\mathrm{EW}}$ and $t\bar{t}Z$.

TABLE VI. Observed one-dimensional and marginalized 95% confidence intervals on the c_{Ht} and $c_{HQ}^{(1)}$ Wilson coefficients for different fit configurations using pseudodatasets.

		95% CI (observed) (TeV^{-2})	
Operators	Processes	c_{Ht}	$c_{HQ}^{(1)}$
O_{Ht}	$t\bar{t}Wj_{\mathrm{EW}}$	$[-10,-2.7]\cup[3.3,9.6]$	⋯
$O_{HQ}^{(1)}$	$t\bar{t}Wj_{\mathrm{EW}}$	⋯	$[-11,-4.5]\cup[4.3,13]$
$O_{Ht}+O_{HQ}^{(1)}$	$t\bar{t}Wj_{\mathrm{EW}}$	$[-9.9,9.3]$	$[-12,14]$
O_{Ht}	$t\bar{t}Wj_{\mathrm{EW}}+t\bar{t}Z$	$[-10,3.2]$	⋯
$O_{HQ}^{(1)}$	$t\bar{t}Wj_{\mathrm{EW}}+t\bar{t}Z$	⋯	$[-11,7.4]$
$O_{Ht}+O_{HQ}^{(1)}$	$t\bar{t}Wj_{\mathrm{EW}}+t\bar{t}Z$	$[-10,-0.96]\cup[1.5,7.3]$	$[-12,0.33]\cup[3.4,12]$

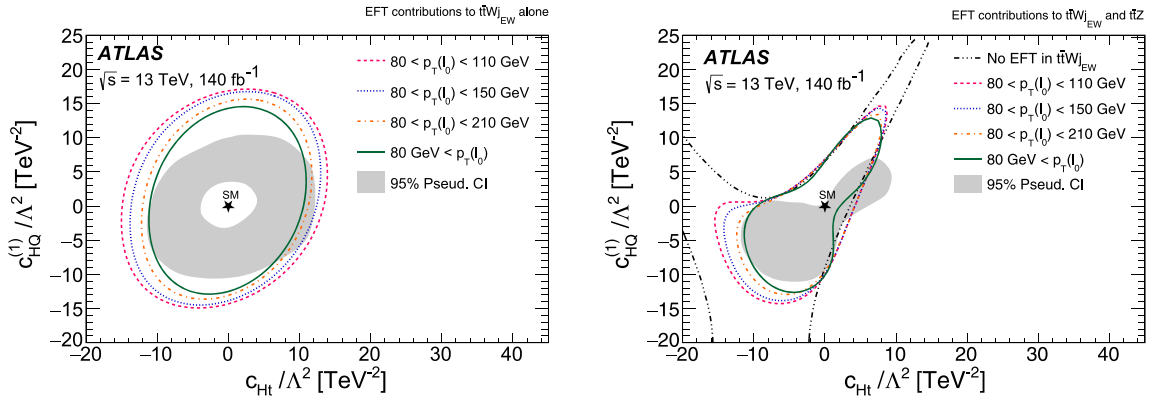


FIG. 11. Two-dimensional 68% and 95% confidence intervals for the simultaneous EFT fit to data of the Wilson coefficients c_{Ht} and $c_{HQ}^{(1)}$, considering their impact on (a) the $t\bar{t}Wj_{\mathrm{EW}}$ process alone or (b) on both the $t\bar{t}Wj_{\mathrm{EW}}$ and $t\bar{t}Z$ processes. The dashed, dotted, and solid line contours use the asymptotic likelihood approach, and highlight the energy-growth behavior of the EFT operators. On (b), the outermost open contour shows the confidence interval when considering the EFT operators on $t\bar{t}Z$ only. Subsequently, on both (a) and (b) the closed contours consider the EFT operators also on $t\bar{t}Wj_{\mathrm{EW}}$ in the four p_{T} bins in the signal region. The outer closed contour uses only the first p_{T} bin and moving inward the contours include higher energy information for the two-bin, three-bin, and four-bin confidence intervals. The solid filled region is the 95% confidence interval determined using pseudodatasets (Pseud.) and the full signal region.

consistently prefer a nonzero value for the EFT Wilson coefficients, due to the difference between data and MC observed in the highest p_{T} bin of Fig. 5, which can be accommodated by the impacts of O_{Ht} and $O_{HQ}^{(1)}$. In the most complex fit, considering the impact of both O_{Ht} or $O_{HQ}^{(1)}$ on the $t\bar{t}Wj_{\mathrm{EW}}$ and $t\bar{t}Z$ processes, the 95% confidence interval contains the SM expectation.

It is informative to visualize the benefits of exploiting the energy-growth dependency of the EFT operators using the $p_{\mathrm{T}}(l_0)$ observable. Figure 11 shows the observed two-dimensional 95% confidence interval contours, using the asymptotic likelihood approach, as a function of the energy-growth dependency of the EFT operators. Fitting from only the first bin of the signal region, with the lowest p_{T}, to all of the signal region up to the highest p_{T} bin, the improvement in the limits is clear from the decreasing size of the contours. Figure 11 also shows the complementarity from considering both the $t\bar{t}Wj_{\mathrm{EW}}$ and $t\bar{t}Z$ processes together. The limits from the $t\bar{t}Z$ process alone, which has larger linear contributions and greater degeneracies between the two EFT operators, is shown by the outermost dotted contour. The degeneracies are reduced by the inclusion of the $t\bar{t}Wj_{\mathrm{EW}}$ process in the fit.

X. CONCLUSIONS

A search is presented for $t\bar{t}Wj_{\mathrm{EW}}$ production in proton-proton collisions using data collected with the ATLAS detector corresponding to an integrated luminosity of 140 fb^{-1} at $\sqrt{s} = 13$ TeV. From the search, limits are set on the Standard Model $t\bar{t}Wj_{\mathrm{EW}}$ process and on effective field theory operators modifying the couplings of the top quark to the Z boson. The search uses same-charge pairs of electrons and muons together with jets, out of which at least one is b-tagged, and uses the properties of the most forward jet to discriminate $t\bar{t}Wj_{\mathrm{EW}}$ production from $t\bar{t}W$ QCD background.

The search is affected by the $t\bar{t}W$ and fake-lepton backgrounds. State-of-the-art modeling is used for $t\bar{t}W$ and data-driven techniques are used for the fake-lepton yield estimate, with special attention paid to the interplay between the two.

The observed (expected) normalization factor is $\mu_{t\bar{t}Wj_{\mathrm{EW}}} = 0.9^{+2.4}_{-3.0}$ $(1.0^{+2.4}_{-2.5})$, resulting in an observed 95% CL$_s$ upper limit of $\mu_{t\bar{t}Wj_{\mathrm{EW}}} < 5.3$. The corresponding 95% CL$_s$ upper limit on the observed cross section is $\sigma_{t\bar{t}Wj_{\mathrm{EW}}} < 251$ fb, to be compared with the Standard Model cross section of $47.7^{+1.9}_{-1.4}$ fb [12]. The results from the measurements are consistent with the Standard Model expectations, and are limited by systematic uncertainties.

The unique tW-scattering vertex embedded within the $t\bar{t}Wj_{\mathrm{EW}}$ process is exploited to gain new sensitivity to EFT operators. The interplay between different processes ($t\bar{t}Wj_{\mathrm{EW}}$ and $t\bar{t}Z$) and different operators (O_{Ht} and $O_{HQ}^{(1)}$) is investigated, demonstrating the benefits of a combined analysis of this type with a detailed case study. Considering both processes when looking at O_{Ht} and $O_{HQ}^{(1)}$ simultaneously closes a degenerate direction present when considering the effects of these operators on $t\bar{t}Z$ production alone. The EFT sensitivity is dominated by uncertainties due to the limited number of events in data, especially at high p_{T}. Increased sensitivity is expected with the LHC

Run 3 data where the interplay between processes with and without sensitivity from significant high energy growth will be even more interesting.

ACKNOWLEDGMENTS

We thank CERN for the very successful operation of the LHC and its injectors, as well as the support staff at CERN and at our institutions worldwide without whom ATLAS could not be operated efficiently. The crucial computing support from all WLCG partners is acknowledged gratefully, in particular from CERN, the ATLAS Tier-1 facilities at TRIUMF/SFU (Canada), NDGF (Denmark, Norway, Sweden), CC-IN2P3 (France), KIT/GridKA (Germany), INFN-CNAF (Italy), NL-T1 (Netherlands), PIC (Spain), RAL (UK), and BNL (USA), the Tier-2 facilities worldwide and large non-WLCG resource providers. Major contributors of computing resources are listed in Ref. [98]. We gratefully acknowledge the support of ANPCyT, Argentina; YerPhI, Armenia; ARC, Australia; BMWFW and FWF, Austria; ANAS, Azerbaijan; CNPq and FAPESP, Brazil; NSERC, NRC, and CFI, Canada; CERN; ANID, Chile; CAS, MOST, and NSFC, China; Minciencias, Colombia; MEYS CR, Czech Republic; DNRF and DNSRC, Denmark; IN2P3-CNRS and CEA-DRF/IRFU, France; SRNSFG, Georgia; BMFTR, HGF, and MPG, Germany; GSRI, Greece; RGC and Hong Kong SAR, China; ICHEP and Academy of Sciences and Humanities, Israel; INFN, Italy; MEXT and JSPS, Japan; CNRST, Morocco; NWO, Netherlands; RCN, Norway; MNiSW, Poland; FCT, Portugal; MNE/IFA, Romania; MSTDI, Serbia; MSSR, Slovakia; ARIS and MVZI, Slovenia; DSI/NRF, South Africa; MICIU/AEI, Spain; SRC and Wallenberg Foundation, Sweden; SERI, SNSF, and Cantons of Bern and Geneva, Switzerland; NSTC, Taipei; TENMAK, Türkiye; STFC/UKRI, United Kingdom; DOE and NSF, USA. Individual groups and members have received support from BCKDF, CANARIE, CRC, and DRAC, Canada; CERN-CZ, FORTE, and PRIMUS, Czech Republic; COST, ERC, ERDF, Horizon 2020, ICSC-NextGenerationEU, and Marie Skłodowska-Curie Actions, European Union; Investissements d'Avenir Labex, Investissements d'Avenir Idex, and ANR, France; DFG and AvH Foundation, Germany; Herakleitos, Thales, and Aristeia programs cofinanced by EU-ESF and the Greek NSRF, Greece; BSF-NSF and MINERVA, Israel; NCN and NAWA, Poland; La Caixa Banking Foundation, CERCA Programme Generalitat de Catalunya and PROMETEO, and GenT Programmes Generalitat Valenciana, Spain; Göran Gustafssons Stiftelse, Sweden; The Royal Society and Leverhulme Trust, United Kingdom; USA. In addition, individual members wish to acknowledge support from CERN: European Organization for Nuclear Research (CERN DOCT); Chile: Agencia Nacional de Investigación y Desarrollo (ANID FONDECYT Regs. No. 1230987, No. FONDECYT 1230812, No. FONDECYT 1240864, No. Fondecyt 3240661, and No. Fondecyt Regular 1240721); China: Chinese Ministry of Science and Technology (Grants No. MOST-2023YFA1605700 and No. MOST-2023YFA1609300), National Natural Science Foundation of China (Grants No. NSFC 12175119 and No. NSFC 12275265); Czech Republic: Czech Science Foundation (Grant No. GACR—24-11373S), Ministry of Education Youth and Sports (Grants No. ERC-CZ-LL2327 and No. FORTE CZ.02.01.01/00/22_008/0004632), PRIMUS Research Programme (Grant No. PRIMUS/21/SCI/017); EU: H2020 European Research Council (Grant No. ERC—101002463); European Union: European Research Council (BARD Grants No. 101116429, No. ERC—948254, and No. ERC 101089007), European Regional Development Fund (HE COFUND GA Grant No. 101081355, ERDF), European Union, Future Artificial Intelligence Research (FAIR-NextGenerationEU Grant No. PE00000013), Italian Center for High Performance Computing, Big Data and Quantum Computing (ICSC, NextGenerationEU), Marie Sklodowska-Curie Actions (Grant No. GAP-101168829); France: Agence Nationale de la Recherche (Grants No. ANR-21-CE31-0013, No. ANR-21-CE31-0022, No. ANR-22-EDIR-0002, and No. ANR-24-CE31-0504-01); Germany: Deutsche Forschungsgemeinschaft (Grants No. DFG—469666862 and No. DFG—CR 312/5-2); China: Research Grants Council (GRF); Italy: Istituto Nazionale di Fisica Nucleare (ICSC, NextGenerationEU), Ministero dell'Università e della Ricerca (Grants No. NextGenEU 153D23001490006 M4C2.1.1, No. NextGenEU I53D23000820006 M4C2.1.1, No. NextGenEU I53D23001490006 M4C2.1.1, and No. SOE2024_0000023); Japan: Japan Society for the Promotion of Science (Grants No. JSPS KAKENHI JP22H01227, No. JSPS KAKENHI JP22H04944, No. JSPS KAKENHI JP22KK0227, No. JSPS KAKENHI JP24K23939, No. JSPS KAKENHI JP24KK0251, No. JSPS KAKENHI JP25H00650, No. JSPS KAKENHI JP25H01291, and No. JSPS KAKENHI JP25K01023); Norway: Research Council of Norway (Grant No. RCN-314472); Poland: Ministry of Science and Higher Education (IDUB AGH, POB8, D4 No. 9722), Polish National Science Centre (Grants No. NCN 2021/42/E/ST2/00350, No. NCN OPUS 2023/51/B/ST2/02507, No. NCN OPUS nr 2022/47/B/ST2/03059, No. NCN UMO-2019/34/E/ST2/00393, No. UMO-2022/47/O/ST2/00148, No. UMO-2023/49/B/ST2/04085, No. UMO-2023/51/B/ST2/00920, and No. UMO-2024/53/N/ST2/00869); Portugal: Foundation for Science and Technology (FCT); Spain: Agencia de Gestión de Ayudas Universitarias y de Investigación (Grant No. AGAUR—2023 BP 00141), Generalitat Valenciana (Grant No. ASFAE/2022/008), Ministry of Science and Innovation (MCIN and NextGenEU Grant No. PCI2022-135018-2, MICIN and FEDER Grants No. PID2021-125273NB, No. RYC2019-028510-I, No. RYC2020-030254-I, No. RYC2021-031273-I, and No. RYC2022-038164-I), Ministerio de Ciencia,

Innovación y Universidades/Agencia Estatal de Investigación (Grant No. PID2022-142604OB-C22); Sweden: Carl Trygger Foundation (Carl Trygger Foundation Grant No. CTS 22:2312), Swedish Research Council (Swedish Research Council Grants No. 2023-04654, No. VR 2021-03651, No. VR 2022-03845, No. VR 2022-04683, No. VR 2023-03403, and No. VR 2024-05451), Knut and Alice Wallenberg Foundation (Grants No. KAW 2018.0458, No. KAW 2022.0358, and No. KAW 2023.0366); Switzerland: Swiss National Science Foundation (Grant No. SNSF—PCEFP2_194658); United Kingdom: Royal Society (Grant No. NIF-R1-231091); USA: U.S. Department of Energy (Grant No. ECA DE-AC02-76SF00515), and Neubauer Family Foundation.

DATA AVAILABILITY

The data that support the findings of this article are not publicly available. The data are available from the authors upon reasonable request.

[1] J. A. Dror, M. Farina, E. Salvioni, and J. Serra, Strong tW scattering at the LHC, J. High Energy Phys. 01 (2016) 071.
[2] F. Maltoni, L. Mantani, and K. Mimasu, Top-quark electroweak interactions at high energy, J. High Energy Phys. 10 (2019) 004.
[3] ATLAS Collaboration, Measurement of the total and differential cross-sections of $t\bar{t}W$ production in pp collisions at $\sqrt{s} = 13$ TeV with the ATLAS detector, J. High Energy Phys. 05 (2024) 131,
[4] R. Frederix, D. Pagani, and M. Zaro, Large NLO corrections in $t\bar{t}W^{\pm}$ and $t\bar{t}t\bar{t}$ hadroproduction from supposedly subleading EW contributions, J. High Energy Phys. 02 (2018) 031.
[5] F. Febres Cordero, M. Kraus, and L. Reina, Top-quark pair production in association with a $W^{\pm}$ gauge boson in the POWHEG-BOX, Phys. Rev. D **103**, 094014 (2021).
[6] ATLAS Collaboration, Measurement of the $t\bar{t}W$ and $t\bar{t}Z$ production cross sections in pp collisions at $\sqrt{s} = 8$ TeV with the ATLAS detector, J. High Energy Phys. 11 (2015) 172.
[7] CMS Collaboration, Observation of top quark pairs produced in association with a vector boson in pp collisions at $\sqrt{s} = 8$ TeV, J. High Energy Phys. 01 (2016) 096.
[8] ATLAS Collaboration, Measurement of the $t\bar{t}Z$ and $t\bar{t}W$ production cross sections in multilepton final states using 3.2 fb^{-1} of pp collisions at $\sqrt{s} = 13$ TeV with the ATLAS detector, Eur. Phys. J. C **77**, 40 (2017).
[9] ATLAS Collaboration, Measurement of the $t\bar{t}Z$ and $t\bar{t}W$ cross sections in proton–proton collisions at $\sqrt{s} = 13$ TeV with the ATLAS detector, Phys. Rev. D **99**, 072009 (2019).
[10] CMS Collaboration, Measurement of the cross section for top quark pair production in association with a W or Z boson in proton–proton collisions at $\sqrt{s} = 13$ TeV, J. High Energy Phys. 08 (2018) 011,
[11] CMS Collaboration, Measurement of the cross section of top quark–antiquark pair production in association with a W boson in proton–proton collisions at $\sqrt{s} = 13$ TeV, J. High Energy Phys. 07 (2023) 219,
[12] R. Frederix and I. Tsinikos, On improving NLO merging for tt̄W production, J. High Energy Phys. 11 (2021) 029,
[13] L. Buonocore, S. Devoto, M. Grazzini, S. Kallweit, J. Mazzitelli, L. Rottoli, and C. Savoini, Precise predictions for the associated production of a W boson with a top-antitop quark pair at the LHC, Phys. Rev. Lett. **131**, 231901 (2023).
[14] ATLAS Collaboration, Evidence for the associated production of the Higgs boson and a top quark pair with the ATLAS detector, Phys. Rev. D **97**, 072003 (2018).
[15] CMS Collaboration, Measurement of the Higgs boson production rate in association with top quarks in final states with electrons, muons, and hadronically decaying tau leptons at $\sqrt{s} = 13$ TeV, Eur. Phys. J. C **81**, 378 (2021).
[16] ATLAS Collaboration, Observation of four-top-quark production in the multilepton final state with the ATLAS detector, Eur. Phys. J. C **83**, 496 (2023); **84**, 156(E) (2024).
[17] CMS Collaboration, Observation of four top quark production in proton–proton collisions at $\sqrt{s} = 13$ TeV, Phys. Lett. B **847**, 138290 (2023).
[18] J. A. Aguilar-Saavedra, Identifying top partners at LHC, J. High Energy Phys. 11 (2009) 030.
[19] J. A. Aguilar-Saavedra, R. Benbrik, S. Heinemeyer, and M. Pérez-Victoria, Handbook of vectorlike quarks: Mixing and single production, Phys. Rev. D **88**, 094010 (2013).
[20] M. Perelstein, Little Higgs models and their phenomenology, Prog. Part. Nucl. Phys. **58**, 247 (2007).
[21] R. S. Chivukula, S. B. Selipsky, and E. H. Simmons, Nonoblique effects in the $Zb\bar{b}$ vertex from ETC dynamics, Phys. Rev. Lett. **69**, 575 (1992).
[22] R. S. Chivukula, E. H. Simmons, and J. Terning, A heavy top quark and the $Zb\bar{b}$ vertex in noncommuting extended technicolor, Phys. Lett. B **331**, 383 (1994).
[23] K. Hagiwara and N. Kitazawa, Extended technicolor contribution to the Zbb vertex, Phys. Rev. D **52**, 5374 (1995).
[24] U. Mahanta, Noncommuting ETC corrections to $zt\bar{t}$ vertex, Phys. Rev. D **55**, 5848 (1997).
[25] U. Mahanta, Probing noncommuting extended technicolor effects by $e^+e^- \to t\bar{t}$ at the next linear collider, Phys. Rev. D **56**, 402 (1997).
[26] ATLAS Collaboration, IInterpretations of the ATLAS measurements of Higgs boson production and decay rates and differential cross-sections inpp collisions at $\sqrt{s} = 13$ TeV, J. High Energy Phys. 11 (2024) 097,
[27] D. Barducci *et al.*, Interpreting top-quark LHC measurements in the standard-model effective field theory, arXiv:1802.07237.

[28] A. Azatov, R. Contino, C. S. Machado, and F. Riva, Helicity selection rules and noninterference for BSM amplitudes, Phys. Rev. D **95**, 065014 (2017).

[29] ATLAS Collaboration, The ATLAS experiment at the CERN large hadron collider, J. Instrum. **3**, S08003 (2008).

[30] ATLAS Collaboration, ATLAS insertable B-layer: Technical design report, ATLAS-TDR-19; CERN-LHCC-2010-013, 2010, URL: https://cds.cern.ch/record/1291633, Addendum: ATLAS-TDR-19-ADD-1; CERN-LHCC-2012-009, 2012, URL: https://cds.cern.ch/record/1451888.

[31] B. Abbott *et al.*, Production and integration of the ATLAS Insertable B-Layer, J. Instrum. **13**, T05008 (2018).

[32] G. Avoni *et al.*, The new LUCID-2 detector for luminosity measurement and monitoring in ATLAS, J. Instrum. **13**, P07017 (2018).

[33] ATLAS Collaboration, Performance of the ATLAS trigger system in 2015, Eur. Phys. J. C **77**, 317 (2017).

[34] ATLAS Collaboration, Software and computing for Run 3 of the ATLAS experiment at the LHC, Eur. Phys. J. C **85**, 234 (2025); **85**, 907(E) (2025).

[35] ATLAS Collaboration, ATLAS data quality operations and performance for 2015–2018 data-taking, J. Instrum. **15**, P04003 (2020).

[36] ATLAS Collaboration, Performance of electron and photon triggers in ATLAS during LHC Run 2, Eur. Phys. J. C **80**, 47 (2020).

[37] ATLAS Collaboration, Performance of the ATLAS muon triggers in Run 2, J. Instrum. **15**, P09015 (2020).

[38] ATLAS Collaboration, 2015 start-up trigger menu and initial performance assessment of the ATLAS trigger using Run-2 data, ATL-DAQ-PUB-2016-001, 2016, URL: https://cds.cern.ch/record/2136007.

[39] ATLAS Collaboration, Trigger menu in 2016, ATL-DAQ-PUB-2017-001, 2017, URL: https://cds.cern.ch/record/2242069.

[40] ATLAS Collaboration, Trigger menu in 2017, ATL-DAQ-PUB-2018-002, 2018, URL: https://cds.cern.ch/record/2625986.

[41] ATLAS Collaboration, Trigger menu in 2018, ATL-DAQ-PUB-2019-001, 2019, URL: https://cds.cern.ch/record/2693402.

[42] S. Agostinelli *et al.*, Geant4—a simulation toolkit, Nucl. Instrum. Methods Phys. Res., Sect. A **506**, 250 (2003).

[43] T. Sjöstrand, S. Mrenna, and P. Skands, A brief introduction to PYTHIA 8.2, Comput. Phys. Commun. **178**, 852 (2008).

[44] R. D. Ball *et al.* (NNPDF Collaboration), Parton distributions with LHC data, Nucl. Phys. **B867**, 244 (2013).

[45] T. Sjöstrand *et al.*, An introduction to PYTHIA 8.2, Comput. Phys. Commun. **191**, 159 (2015).

[46] R. D. Ball *et al.* (NNPDF Collaboration), Parton distributions for the LHC run II, J. High Energy Phys. 04 (2015) 040.

[47] D. J. Lange, The EvtGen particle decay simulation package, Nucl. Instrum. Methods Phys. Res., Sect. A **462**, 152 (2001).

[48] E. Bothmann *et al.*, Event generation with Sherpa 2.2, SciPost Phys. **7**, 034 (2019).

[49] T. Gleisberg, S. Höche, F. Krauss, M. Schönherr, S. Schumann, F. Siegert, and J. Winter, Event generation with SHERPA 1.1, J. High Energy Phys. 02 (2009) 007.

[50] R. D. Ball *et al.* (NNPDF Collaboration), Parton distributions from high-precision collider data, Eur. Phys. J. C **77**, 663 (2017).

[51] T. Gleisberg and S. Höche, Comix, a new matrix element generator, J. High Energy Phys. 12 (2008) 039.

[52] F. Cascioli, P. Maierhöfer, and S. Pozzorini, Scattering amplitudes with open loops, Phys. Rev. Lett. **108**, 111601 (2012).

[53] A. Denner, S. Dittmaier, and L. Hofer, Collier: A fortran-based complex one-loop library in extended regularizations, Comput. Phys. Commun. **212**, 220 (2017).

[54] F. Buccioni, J.-N. Lang, J. M. Lindert, P. Maierhöfer, S. Pozzorini, H. Zhang, and M. F. Zoller, OpenLoops 2, Eur. Phys. J. C **79**, 866 (2019).

[55] S. Schumann and F. Krauss, A parton shower algorithm based on Catani–Seymour dipole factorisation, J. High Energy Phys. 03 (2008) 038.

[56] S. Höche, F. Krauss, M. Schönherr, and F. Siegert, QCD matrix elements + parton showers. The NLO case, J. High Energy Phys. 04 (2013) 027.

[57] S. Höche, F. Krauss, M. Schönherr, and F. Siegert, A critical appraisal of NLO + PS matching methods, J. High Energy Phys. 09 (2012) 049.

[58] S. Catani, F. Krauss, B. R. Webber, and R. Kuhn, QCD matrix elements + parton showers, J. High Energy Phys. 11 (2001) 063.

[59] S. Höche, F. Krauss, S. Schumann, and F. Siegert, QCD matrix elements and truncated showers, J. High Energy Phys. 05 (2009) 053.

[60] D. de Florian *et al.*, Handbook of LHC Higgs cross sections: 4. Deciphering the nature of the Higgs sector, CERN Yellow Rep. Monogr. **2**, 1 (2017).

[61] S. Alioli, P. Nason, C. Oleari, and E. Re, A general framework for implementing NLO calculations in shower Monte Carlo programs: the POWHEG BOX, J. High Energy Phys. 06 (2010) 043.

[62] I. Brivio, SMEFTsim 3.0—a practical guide, J. High Energy Phys. 04 (2021) 073.

[63] C. Degrande, C. Duhr, B. Fuks, D. Grellscheid, O. Mattelaer, and T. Reiter, UFO—The Universal FeynRules Output, Comput. Phys. Commun. **183**, 1201 (2012).

[64] I. Brivio *et al.*, Electroweak input parameters, arXiv:2111.12515.

[65] ATLAS Collaboration, The ATLAS simulation infrastructure, Eur. Phys. J. C **70**, 823 (2010).

[66] ATLAS Collaboration, Vertex reconstruction performance of the ATLAS detector at ($\sqrt{s} = 13$ TeV), ATL-PHYS-PUB-2015-026, 2015, URL: https://cds.cern.ch/record/2037717.

[67] ATLAS Collaboration, Electron and photon performance measurements with the ATLAS detector using the 2015–2017 LHC proton–proton collision data, J. Instrum. **14**, P12006 (2019).

[68] ATLAS Collaboration, Muon reconstruction and identification efficiency in ATLAS using the full Run 2 (pp) collision data set at ($\sqrt{s} = 13$ TeV), Eur. Phys. J. C **81**, 578 (2021).

[69] ATLAS Collaboration, Jet reconstruction and performance using particle flow with the ATLAS detector, Eur. Phys. J. C **77**, 466 (2017).

[70] M. Cacciari, G. P. Salam, and G. Soyez, The anti-k_t jet clustering algorithm, J. High Energy Phys. 04 (2008) 063.
[71] M. Cacciari, G. P. Salam, and G. Soyez, FastJet user manual, Eur. Phys. J. C **72**, 1896 (2012).
[72] ATLAS Collaboration, Jet energy scale and resolution measured in proton–proton collisions at ($\sqrt{s} = 13$ TeV) with the ATLAS detector, Eur. Phys. J. C **81**, 689 (2021).
[73] ATLAS Collaboration, Performance of pile-up mitigation techniques for jets in pp collisions at $\sqrt{s} = 8$ TeV using the ATLAS detector, Eur. Phys. J. C **76**, 581 (2016).
[74] ATLAS Collaboration, Selection of jets produced in 13 TeV proton–proton collisions with the ATLAS detector, ATLAS-CONF-2015-029, 2015, URL: https://cds.cern.ch/record/2037702.
[75] ATLAS Collaboration, ATLAS flavour-tagging algorithms for the LHC Run 2 (pp) collision dataset, Eur. Phys. J. C **83**, 681 (2023).
[76] ATLAS Collaboration, Identification of jets containing (b)-hadrons with recurrent neural networks at the ATLAS experiment, ATL-PHYS-PUB-2017-003, 2017, URL: https://cds.cern.ch/record/2255226.
[77] ATLAS Collaboration, ATLAS b-jet identification performance and efficiency measurement with $t\bar{t}$ events in pp collisions at $\sqrt{s} = 13$ TeV, Eur. Phys. J. C **79**, 970 (2019).
[78] ATLAS Collaboration, Measurement of the c-jet mistagging efficiency in $t\bar{t}$ events using pp collision data at ($\sqrt{s} = 13$ TeV) collected with the ATLAS detector, Eur. Phys. J. C **82**, 95 (2022).
[79] ATLAS Collaboration, Calibration of the light-flavour jet mistagging efficiency of the$b$-tagging algorithms with $Z+$ jets events using 139 fb^{-1} of ATLAS proton–proton collision data at $\sqrt{s} = 13$ TeV, Eur. Phys. J. C **83**, 728 (2023).
[80] ATLAS Collaboration, Performance of missing transverse momentum reconstruction with the ATLAS detector using proton–proton collisions at $\sqrt{s} = 13$ TeV, Eur. Phys. J. C **78**, 903 (2018).
[81] ATLAS Collaboration, Electron and photon efficiencies in LHC Run 2 with the ATLAS experiment, J. High Energy Phys. 05 (2024) 162.
[82] ATLAS Collaboration, Studies of the muon momentum calibration and performance of the ATLAS detector with pp collisions at $\sqrt{s} = 13$ TeV, Eur. Phys. J. C **83**, 686 (2023).
[83] ATLAS Collaboration, Measurement of the top quark-pair production cross section with ATLAS in pp collisions at $\sqrt{s} = 7$ TeV, Eur. Phys. J. C **71**, 1577 (2011).
[84] ATLAS Collaboration, Luminosity determination in pp collisions at $\sqrt{s} = 13$ TeV using the ATLAS detector at the LHC, Eur. Phys. J. C **83**, 982 (2023).
[85] ATLAS Collaboration, Electron and photon energy calibration with the ATLAS detector using LHC Run 2 data, J. Instrum. **19**, P02009 (2024).
[86] ATLAS Collaboration, Properties of jets and inputs to jet reconstruction and calibration with the ATLAS detector using proton–proton collisions at $\sqrt{s} = 13$ TeV, ATL-PHYS-PUB-2015-036, 2015, URL: https://cds.cern.ch/record/2044564.
[87] ATLAS Collaboration, Observation of Higgs boson production in association with a top quark pair at the LHC with the ATLAS detector, Phys. Lett. B **784**, 173 (2018).
[88] ATLAS and CMS Collaborations, Combination of the W boson polarization measurements in top quark decays using ATLAS and CMS data at $\sqrt{s} = 8$ TeV, J. High Energy Phys. 08 (2020) 051.
[89] J. Butterworth *et al.*, PDF4LHC recommendations for LHC Run II, J. Phys. G **43**, 023001 (2016).
[90] G. Cowan, K. Cranmer, E. Gross, and O. Vitells, Asymptotic formulae for likelihood-based tests of new physics, Eur. Phys. J. C **71**, 1554 (2011); **73**, 2501(E) (2013).
[91] M. Aly, T. Dado, A. Held, M. Pinamonti, and L. Valery, TRExFitter, version 1.2.0, 2025, URL: 10.5281/zenodo.15524537.
[92] R. Barlow and C. Beeston, Fitting using finite Monte Carlo samples, Comput. Phys. Commun. **77**, 219 (1993).
[93] A. L. Read, Presentation of search results: TheCL_s technique, J. Phys. G **28**, 2693 (2002).
[94] ATLAS Collaboration, Inclusive and differential cross-section measurements of $t\bar{t}Z$ production in pp collisions at $\sqrt{s} = 13$ TeV with the ATLAS detector, including EFT and spin-correlation interpretations, J. High Energy Phys. 07 (2024) 163.
[95] A. Kulesza, L. Motyka, D. Schwartländer, T. Stebel, and V. Theeuwes, Associated top quark pair production with a heavy boson: Differential cross sections at NLO + NNLL accuracy, Eur. Phys. J. C **80**, 428 (2020).
[96] S. S. Wilks, The large-sample distribution of the likelihood ratio for testing composite hypotheses, Annals Math. Statist. **9**, 60 (1938).
[97] F. U. Bernlochner, D. C. Fry, S. B. Menary, and E. Persson, Cover your bases: Asymptotic distributions of the profile likelihood ratio when constraining effective field theories in high-energy physics, SciPost Phys. Core **6**, 013 (2023).
[98] ATLAS Collaboration, ATLAS computing acknowledgements, ATL-SOFT-PUB-2026-001, 2026, https://cds.cern.ch/record/2952666.

G. Aad,[103] E. Aakvaag,[17] B. Abbott,[122] S. Abdelhameed,[118a] K. Abeling,[55] N. J. Abicht,[49] S. H. Abidi,[30] M. Aboelela,[45] A. Aboulhorma,[36e] H. Abramowicz,[156] Y. Abulaiti,[119] B. S. Acharya,[69a,69b,b] A. Ackermann,[63a] C. Adam Bourdarios,[4] L. Adamczyk,[86a] S. V. Addepalli,[148] M. J. Addison,[102] J. Adelman,[117] A. Adiguzel,[22c] T. Adye,[136] A. A. Affolder,[138] Y. Afik,[40] M. N. Agaras,[13] A. Aggarwal,[101] C. Agheorghiesei,[28c] F. Ahmadov,[39,c] S. Ahuja,[96] S. Ahuja,[168] X. Ai,[142b] G. Aielli,[76a,76b] A. Aikot,[168] M. Ait Tamlihat,[36e] B. Aitbenchikh,[36a] T. P. A. Åkesson,[99] A. V. Akimov,[150] D. Akiyama,[173] N. N. Akolkar,[25] S. Aktas,[171] G. L. Alberghi,[24b]

J. Albert,[170] U. Alberti,[20] P. Albicocco,[53] G. L. Albouy,[60] S. Alderweireldt,[52] Z. L. Alegria,[123] M. Aleksa,[37] I. N. Aleksandrov,[39] C. Alexa,[28b] T. Alexopoulos,[10] F. Alfonsi,[24b] M. Algren,[56] M. Alhroob,[172] B. Ali,[134] H. M. J. Ali,[92,d] S. Ali,[32] S. W. Alibocus,[93] M. Aliev,[34c] G. Alimonti,[71a] W. Alkakhi,[55] C. Allaire,[66] B. M. M. Allbrooke,[151] D. R. Allen,[123] J. S. Allen,[102] J. F. Allen,[52] P. P. Allport,[21] A. Aloisio,[72a,72b] F. Alonso,[91] C. Alpigiani,[141] Z. M. K. Alsolami,[92] A. Alvarez Fernandez,[101] M. Alves Cardoso,[56] M. G. Alviggi,[72a,72b] M. Aly,[102] Y. Amaral Coutinho,[82b] A. Ambler,[105] C. Amelung,[37] M. Amerl,[102] C. G. Ames,[110] T. Amezza,[129] D. Amidei,[107] B. Amini,[54] K. Amirie,[160] A. Amirkhanov,[39] S. P. Amor Dos Santos,[132a] K. R. Amos,[168] D. Amperiadou,[157] S. An,[83] C. Anastopoulos,[144] T. Andeen,[11] J. K. Anders,[93] A. C. Anderson,[59] A. Andreazza,[71a,71b] S. Angelidakis,[9] A. Angerami,[42] A. V. Anisenkov,[39] A. Annovi,[74a] C. Antel,[37] E. Antipov,[150] M. Antonelli,[53] F. Anulli,[75a] M. Aoki,[83] T. Aoki,[158] M. A. Aparo,[151] L. Aperio Bella,[48] M. Apicella,[31] C. Appelt,[156] A. Apyan,[27] M. Arampatzi,[10] S. J. Arbiol Val,[87] C. Arcangeletti,[53] A. T. H. Arce,[51] J-F. Arguin,[109] S. Argyropoulos,[157] J.-H. Arling,[48] O. Arnaez,[4] H. Arnold,[150] G. Artoni,[75a,75b] H. Asada,[112] K. Asai,[120] S. Asatryan,[178] N. A. Asbah,[37] R. A. Ashby Pickering,[172] A. M. Aslam,[96] K. Assamagan,[30] R. Astalos,[29a] K. S. V. Astrand,[99] S. Atashi,[164] R. J. Atkin,[34a] H. Atmani,[36f] P. A. Atmasiddha,[130] K. Augsten,[134] A. D. Auriol,[41] V. A. Austrup,[102] A. S. Avad,[95] G. Avolio,[37] K. Axiotis,[56] A. Azzam,[13] D. Babal,[29b] H. Bachacou,[137] K. Bachas,[157,e] A. Bachiu,[35] E. Bachmann,[50] M. J. Backes,[63a] A. Badea,[40] T. M. Baer,[107] P. Bagnaia,[75a,75b] M. Bahmani,[19] D. Bahner,[54] K. Bai,[125] J. T. Baines,[136] L. Baines,[95] O. K. Baker,[177] E. Bakos,[16] D. Bakshi Gupta,[8] L. E. Balabram Filho,[82b] V. Balakrishnan,[122] R. Balasubramanian,[4] E. M. Baldin,[38] P. Balek,[86a] E. Ballabene,[24b,24a] F. Balli,[137] L. M. Baltes,[63a] W. K. Balunas,[33] J. Balz,[101] I. Bamwidhi,[118b] E. Banas,[87] M. Bandieramonte,[131] A. Bandyopadhyay,[25] S. Bansal,[25] L. Barak,[156] M. Barakat,[48] E. L. Barberio,[106] D. Barberis,[18b] M. Barbero,[103] M. Z. Barel,[116] T. Barillari,[111] M-S. Barisits,[37] T. Barklow,[148] P. Baron,[135] D. A. Baron Moreno,[102] A. Baroncelli,[62] A. J. Barr,[128] J. D. Barr,[97] F. Barreiro,[100] J. Barreiro Guimarães da Costa,[14] M. G. Barros Teixeira,[132a] S. Barsov,[38] F. Bartels,[63a] R. Bartoldus,[148] A. E. Barton,[92] P. Bartos,[29a] M. Baselga,[49] S. Bashiri,[87] A. Bassalat,[66,f] M. J. Basso,[161a] S. Bataju,[45] R. Bate,[169] R. L. Bates,[59] S. Batlamous,[100] M. Battaglia,[138] D. Battulga,[19] M. Bauce,[75a,75b] M. Bauer,[79] P. Bauer,[25] L. T. Bayer,[48] L. T. Bazzano Hurrell,[31] J. B. Beacham,[111] T. Beau,[129] J. Y. Beaucamp,[91] P. H. Beauchemin,[163] P. Bechtle,[25] H. P. Beck,[20,g] K. Becker,[172] A. J. Beddall,[81] V. A. Bednyakov,[39] C. P. Bee,[150] L. J. Beemster,[16] M. Begalli,[82d] M. Begel,[30] J. K. Behr,[48] J. F. Beirer,[37] F. Beisiegel,[25] M. Belfkir,[118b] G. Bella,[156] L. Bellagamba,[24b] A. Bellerive,[35] C. D. Bellgraph,[68] P. Bellos,[21] K. Beloborodov,[38] I. Benaoumeur,[21] D. Benchekroun,[36a] F. Bendebba,[36a] Y. Benhammou,[156] K. C. Benkendorfer,[61] L. Beresford,[48] M. Beretta,[53] E. Bergeaas Kuutmann,[166] N. Berger,[4] B. Bergmann,[134] J. Beringer,[18a] G. Bernardi,[5] C. Bernius,[148] F. U. Bernlochner,[25] A. Berrocal Guardia,[13] T. Berry,[96] P. Berta,[135] A. Berti,[132a] R. Bertrand,[103] S. Bethke,[111] A. Betti,[75a,75b] A. J. Bevan,[95] L. Bezio,[56] N. K. Bhalla,[54] S. Bharthuar,[111] S. Bhatta,[150] P. Bhattarai,[148] Z. M. Bhatti,[119] K. D. Bhide,[54] V. S. Bhopatkar,[123] R. M. Bianchi,[131] G. Bianco,[24b,24a] O. Biebel,[110] M. Biglietti,[77a] C. S. Billingsley,[45] Y. Bimgdi,[36f] M. Bindi,[55] A. Bingham,[176] A. Bingul,[22b] C. Bini,[75a,75b] G. A. Bird,[33] M. Birman,[174] M. Biros,[135] S. Biryukov,[151] T. Bisanz,[49] E. Bisceglie,[24b,24a] J. P. Biswal,[136] D. Biswas,[146] I. Bloch,[48] A. Blue,[59] U. Blumenschein,[95] V. S. Bobrovnikov,[39] L. Boccardo,[57b,57a] M. Boehler,[54] B. Boehm,[171] D. Bogavac,[13] A. G. Bogdanchikov,[38] L. S. Boggia,[129] V. Boisvert,[96] P. Bokan,[37] T. Bold,[86a] M. Bomben,[5] M. Bona,[95] M. Boonekamp,[137] A. G. Borbély,[59] I. S. Bordulev,[38] G. Borissov,[92] D. Bortoletto,[128] D. Boscherini,[24b] M. Bosman,[13] K. Bouaouda,[36a] N. Bouchhar,[168] L. Boudet,[4] J. Boudreau,[131] E. V. Bouhova-Thacker,[92] D. Boumediene,[41] R. Bouquet,[57b,57a] A. Boveia,[121] J. Boyd,[37] D. Boye,[30] I. R. Boyko,[39] L. Bozianu,[56] J. Bracinik,[21] N. Brahimi,[4] G. Brandt,[176] O. Brandt,[33] B. Brau,[104] J. E. Brau,[125] R. Brener,[174] L. Brenner,[116] R. Brenner,[166] S. Bressler,[174] G. Brianti,[78a,78b] D. Britton,[59] D. Britzger,[111] I. Brock,[25] R. Brock,[108] G. Brooijmans,[42] A. J. Brooks,[68] E. M. Brooks,[161b] E. Brost,[30] L. M. Brown,[170,161a] L. E. Bruce,[61] T. L. Bruckler,[128] P. A. Bruckman de Renstrom,[87] B. Brüers,[48] A. Bruni,[24b] G. Bruni,[24b] D. Brunner,[47a,47b] M. Bruschi,[24b] N. Bruscino,[75a,75b] T. Buanes,[17] Q. Buat,[141] D. Buchin,[111] A. G. Buckley,[59] O. Bulekov,[81] B. A. Bullard,[148] S. Burdin,[93] C. D. Burgard,[49] A. M. Burger,[90] B. Burghgrave,[8] O. Burlayenko,[54] J. Burleson,[167] J. C. Burzynski,[147] E. L. Busch,[42] V. Büscher,[101] P. J. Bussey,[59] O. But,[25] J. M. Butler,[26] C. M. Buttar,[59] J. M. Butterworth,[97] W. Buttinger,[136] C. J. Buxo Vazquez,[108] A. R. Buzykaev,[39]

S. Cabrera Urbán,[168] L. Cadamuro,[66] H. Cai,[37] Y. Cai,[24b,113c,24a] Y. Cai,[113a] V. M. M. Cairo,[37] O. Cakir,[3a] N. Calace,[37] P. Calafiura,[18a] G. Calderini,[129] P. Calfayan,[35] L. Calic,[99] G. Callea,[59] L. P. Caloba,[82b] D. Calvet,[41] S. Calvet,[41] R. Camacho Toro,[129] S. Camarda,[37] D. Camarero Munoz,[27] P. Camarri,[76a,76b] C. Camincher,[170] M. Campanelli,[97] A. Camplani,[43] V. Canale,[72a,72b] A. C. Canbay,[3a] E. Canonero,[96] J. Cantero,[168] Y. Cao,[167] F. Capocasa,[27] M. Capua,[44b,44a] A. Carbone,[71a,71b] R. Cardarelli,[76a] J. C. J. Cardenas,[8] M. P. Cardiff,[27] G. Carducci,[44b,44a] T. Carli,[37] G. Carlino,[72a] J. I. Carlotto,[13] B. T. Carlson,[131,h] E. M. Carlson,[170] J. Carmignani,[93] L. Carminati,[71a,71b] A. Carnelli,[4] M. Carnesale,[37] S. Caron,[115] E. Carquin,[139g] I. B. Carr,[106] S. Carrá,[73a,73b] G. Carratta,[24b,24a] C. Carrion Martinez,[168] A. M. Carroll,[125] M. P. Casado,[13,i] P. Casolaro,[72a,72b] M. Caspar,[48] W. R. Castiglioni,[40] F. L. Castillo,[4] L. Castillo Garcia,[13] V. Castillo Gimenez,[168] N. F. Castro,[132a,132e] A. Catinaccio,[37] J. R. Catmore,[127] T. Cavaliere,[4] V. Cavaliere,[30] L. J. Caviedes Betancourt,[23b] E. Celebi,[81] S. Cella,[37] V. Cepaitis,[56] K. Cerny,[124] A. S. Cerqueira,[82a] A. Cerri,[74a,j] L. Cerrito,[76a,76b] F. Cerutti,[18a] B. Cervato,[71a,71b] A. Cervelli,[24b] G. Cesarini,[53] S. A. Cetin,[81] P. M. Chabrillat,[129] R. Chakkappai,[66] S. Chakraborty,[172] A. Chambers,[61] J. Chan,[18a] W. Y. Chan,[158] J. D. Chapman,[33] E. Chapon,[137] B. Chargeishvili,[154b] D. G. Charlton,[21] C. Chauhan,[135] Y. Che,[113a] S. Chekanov,[6] G. A. Chelkov,[39,k] B. Chen,[156] B. Chen,[170] H. Chen,[30] J. Chen,[143a] J. Chen,[147] M. Chen,[128] S. Chen,[88] S. J. Chen,[113a] X. Chen,[143a] X. Chen,[15,l] Z. Chen,[62] C. L. Cheng,[175] H. C. Cheng,[64a] S. Cheong,[148] A. Cheplakov,[39] E. Cherepanova,[116] R. Cherkaoui El Moursli,[36e] E. Cheu,[7] K. Cheung,[65] L. Chevalier,[137] V. Chiarella,[53] G. Chiarelli,[74a] G. Chiodini,[70a] A. S. Chisholm,[21] A. Chitan,[28b] M. Chitishvili,[168] M. V. Chizhov,[39,m] K. Choi,[11] Y. Chou,[141] E. Y. S. Chow,[115] K. L. Chu,[174] M. C. Chu,[64a] X. Chu,[14,113c] Z. Chubinidze,[53] J. Chudoba,[133] J. J. Chwastowski,[87] D. Cieri,[111] K. M. Ciesla,[86a] V. Cindro,[94] A. Ciocio,[18a] F. Cirotto,[72a,72b] Z. H. Citron,[174] M. Citterio,[71a] D. A. Ciubotaru,[28b] A. Clark,[56] P. J. Clark,[52] N. Clarke Hall,[97] C. Clarry,[160] S. E. Clawson,[48] C. Clement,[47a,47b] L. Clissa,[24b,24a] Y. Coadou,[103] M. Cobal,[69a,69c] A. Coccaro,[57b] R. F. Coelho Barrue,[132a] R. Coelho Lopes De Sa,[104] S. Coelli,[71a] M. M. Cohen,[130] L. S. Colangeli,[160] B. Cole,[42] P. Collado Soto,[100] J. Collot,[60] M. R. Coluccia,[70a] P. Conde Muiño,[132a,132g] M. P. Connell,[34c] S. H. Connell,[34c] E. I. Conroy,[128] M. Contreras Cossio,[11] F. Conventi,[72a,n] A. M. Cooper-Sarkar,[128] L. Corazzina,[75a,75b] F. A. Corchia,[24b,24a] A. Cordeiro Oudot Choi,[141] L. D. Corpe,[41] M. Corradi,[75a,75b] F. Corriveau,[105,o] A. Cortes-Gonzalez,[158] M. J. Costa,[168] F. Costanza,[4] D. Costanzo,[144] J. Couthures,[4] G. Cowan,[96] K. Cranmer,[175] L. Cremer,[49] D. Cremonini,[24b,24a] S. Crépé-Renaudin,[60] F. Crescioli,[129] T. Cresta,[73a,73b] M. Cristinziani,[146] M. Cristoforetti,[78a,78b] E. Critelli,[97] V. Croft,[116] G. Crosetti,[44b,44a] A. Cueto,[100] H. Cui,[97] Z. Cui,[7] B. M. Cunnett,[151] W. R. Cunningham,[59] F. Curcio,[168] J. R. Curran,[52] M. J. Da Cunha Sargedas De Sousa,[57b,57a] J. V. Da Fonseca Pinto,[82b] C. Da Via,[102] W. Dabrowski,[86a] T. Dado,[37] S. Dahbi,[153] T. Dai,[107] D. Dal Santo,[20] C. Dallapiccola,[104] M. Dam,[43] G. D'amen,[30] V. D'Amico,[110] J. R. Dandoy,[35] M. D'Andrea,[57b,57a] D. Dannheim,[37] G. D'anniballe,[74a,74b] M. Danninger,[147] V. Dao,[150] G. Darbo,[57b] S. J. Das,[30] F. Dattola,[48] S. D'Auria,[71a,71b] A. D'Avanzo,[72a,72b] T. Davidek,[135] J. Davidson,[172] I. Dawson,[95] K. De,[8] C. De Almeida Rossi,[160] R. De Asmundis,[72a] N. De Biase,[48] S. De Castro,[24b,24a] N. De Groot,[115] P. de Jong,[116] H. De la Torre,[117] A. De Maria,[113a] A. De Salvo,[75a] U. De Sanctis,[76a,76b] F. De Santis,[70a,70b] A. De Santo,[151] J. B. De Vivie De Regie,[60] J. Debevc,[94] D. V. Dedovich,[39] J. Degens,[93] A. M. Deiana,[45] J. Del Peso,[100] L. Delagrange,[129] F. Deliot,[137] C. M. Delitzsch,[49] M. Della Pietra,[72a,72b] D. Della Volpe,[56] A. Dell'Acqua,[37] L. Dell'Asta,[71a,71b] M. Delmastro,[4] C. C. Delogu,[57b,57a] P. A. Delsart,[60] S. Demers,[177] M. Demichev,[39] S. P. Denisov,[38] H. Denizli,[22a,p] M. G. Depala,[93] L. D'Eramo,[41] D. Derendarz,[87] F. Derue,[129] P. Dervan,[93,a] A. M. Desai,[1] K. Desch,[25] F. A. Di Bello,[74a,74b] A. Di Ciaccio,[76a,76b] L. Di Ciaccio,[4] A. Di Domenico,[75a,75b] C. Di Donato,[72a,72b] A. Di Girolamo,[37] G. Di Gregorio,[66] A. Di Luca,[78a,78b] B. Di Micco,[77a,77b] R. Di Nardo,[77a,77b] K. F. Di Petrillo,[40] M. Diamantopoulou,[35] F. A. Dias,[116] M. A. Diaz,[139a,139b] A. R. Didenko,[39] M. Didenko,[168] S. D. Diefenbacher,[18a] E. B. Diehl,[107] S. Díez Cornell,[48] C. Diez Pardos,[146] C. Dimitriadi,[149] A. Dimitrievska,[21] A. Dimri,[150] Y. Ding,[62] J. Dingfelder,[25] T. Dingley,[128] I-M. Dinu,[28b] S. J. Dittmeier,[63b] F. Dittus,[37] M. Divisek,[135] B. Dixit,[93] F. Djama,[103] T. Djobava,[154b] C. Doglioni,[102,99] A. Dohnalova,[29a] Z. Dolezal,[135] K. Domijan,[86a] K. M. Dona,[40] M. Donadelli,[82d] B. Dong,[108] J. Donini,[41] A. D'Onofrio,[72a,72b] M. D'Onofrio,[93] J. Dopke,[136] A. Doria,[72a] N. Dos Santos Fernandes,[132a] I. A. Dos Santos Luz,[82e] P. Dougan,[102] M. T. Dova,[91] A. T. Doyle,[59] M. P. Drescher,[55] E. Dreyer,[174] I. Drivas-koulouris,[10] M. Drnevich,[119] D. Du,[62] T. A. du Pree,[116]

Z. Duan,[113a] M. Dubau,[4] F. Dubinin,[39] M. Dubovsky,[29a] E. Duchovni,[174] G. Duckeck,[110] P. K. Duckett,[97] O. A. Ducu,[28b] D. Duda,[52] A. Dudarev,[37] M. M. Dudek,[87] E. R. Duden,[27] M. D'uffizi,[102] L. Duflot,[66] M. Dührssen,[37] I. Duminica,[28g] A. E. Dumitriu,[28b] M. Dunford,[63a] K. Dunne,[47a,47b] A. Duperrin,[103] H. Duran Yildiz,[3a] A. Durglishvili,[154b] G. I. Dyckes,[18a] M. Dyndal,[86a] B. S. Dziedzic,[37] Z. O. Earnshaw,[151] G. H. Eberwein,[128] B. Eckerova,[29a] S. Eggebrecht,[55] E. Egidio Purcino De Souza,[82e] G. Eigen,[17] K. Einsweiler,[18a] T. Ekelof,[166] P. A. Ekman,[99] S. El Farkh,[36b] Y. El Ghazali,[62] H. El Jarrari,[105] A. El Moussaouy,[36a] D. Elitez,[37] M. Ellert,[166] F. Ellinghaus,[176] T. A. Elliot,[96] N. Ellis,[37] J. Elmsheuser,[30] M. Elsawy,[118a] M. Elsing,[37] D. Emeliyanov,[136] Y. Enari,[83] S. Epari,[109] D. Ernani Martins Neto,[87] F. Ernst,[37] M. Escalier,[66] C. Escobar,[168] E. Etzion,[156] G. Evans,[132a,132b] H. Evans,[68] L. S. Evans,[48] A. Ezhilov,[38] S. Ezzarqtouni,[36a] F. Fabbri,[24b,24a] L. Fabbri,[24b,24a] G. Facini,[97] V. Fadeyev,[138] R. M. Fakhrutdinov,[38] D. Fakoudis,[101] S. Falciano,[75a] L. F. Falda Ulhoa Coelho,[27] F. Fallavollita,[111] G. Falsetti,[44b,44a] J. Faltova,[135] C. Fan,[167] K. Y. Fan,[64b] Y. Fan,[14] Y. Fang,[14,113c] M. Fanti,[71a,71b] M. Faraj,[69a,69b] Z. Farazpay,[98] A. Farbin,[8] A. Farilla,[77a] K. Farman,[153] T. Farooque,[108] J. N. Farr,[177] M. S. Farrington,[61] S. M. Farrington,[136,52] F. Fassi,[36e] D. Fassouliotis,[9] L. Fayard,[66] P. Federic,[135] P. Federicova,[133] O. L. Fedin,[38,k] M. Feickert,[175] L. Feligioni,[103] D. E. Fellers,[18a] C. Feng,[142a] Y. Feng,[14] Z. Feng,[116] M. J. Fenton,[164] L. Ferencz,[48] B. Fernandez Barbadillo,[92] P. Fernandez Martinez,[67] M. J. V. Fernoux,[103] J. Ferrando,[92] A. Ferrari,[166] P. Ferrari,[116,115] R. Ferrari,[73a] D. Ferrere,[56] C. Ferretti,[107] M. P. Fewell,[1] D. Fiacco,[75a,75b] F. Fiedler,[101] P. Fiedler,[134] S. Filimonov,[39] M. S. Filip,[28b,q] A. Filipčič,[94] E. K. Filmer,[161a] F. Filthaut,[115] M. C. N. Fiolhais,[132a,132c,r] L. Fiorini,[168] W. C. Fisher,[108] T. Fitschen,[102] P. M. Fitzhugh,[137] I. Fleck,[146] P. Fleischmann,[107] T. Flick,[176] M. Flores,[34d,s] L. R. Flores Castillo,[64a] F. M. Follega,[78a,78b] N. Fomin,[33] J. H. Foo,[160] A. Formica,[137] A. C. Forti,[102] E. Fortin,[37] A. W. Fortman,[18a] L. Foster,[18a] L. Fountas,[9,t] D. Fournier,[66] H. Fox,[92] P. Francavilla,[74a,74b] S. Francescato,[61] S. Franchellucci,[56] M. Franchini,[24b,24a] S. Franchino,[63a] D. Francis,[37] L. Franco,[48] L. Franconi,[48] M. Franklin,[61] G. Frattari,[27] Y. Y. Frid,[156] J. Friend,[59] N. Fritzsche,[37] A. Froch,[56] D. Froidevaux,[37] J. A. Frost,[136] Y. Fu,[108] S. Fuenzalida Garrido,[139g] M. Fujimoto,[150] K. Y. Fung,[64a] E. Furtado De Simas Filho,[82e] M. Furukawa,[158] M. Fuste Costa,[48] J. Fuster,[168] A. Gaa,[55] A. Gabrielli,[24b,24a] A. Gabrielli,[160] P. Gadow,[37] G. Gagliardi,[57b,57a] L. G. Gagnon,[18a] S. Gaid,[84b] S. Galantzan,[156] J. Gallagher,[1] E. J. Gallas,[128] A. L. Gallen,[166] B. J. Gallop,[136] K. K. Gan,[121] S. Ganguly,[158] Y. Gao,[52] A. Garabaglu,[141] F. M. Garay Walls,[139a,139b] C. García,[168] A. Garcia Alonso,[116] A. G. Garcia Caffaro,[177] J. E. García Navarro,[168] M. A. Garcia Ruiz,[23b] M. Garcia-Sciveres,[18a] G. L. Gardner,[130] R. W. Gardner,[40] N. Garelli,[163] R. B. Garg,[148] J. M. Gargan,[33] C. A. Garner,[160] C. M. Garvey,[34a] V. K. Gassmann,[163] G. Gaudio,[73a] V. Gautam,[13] P. Gauzzi,[75a,75b] J. Gavranovic,[94] I. L. Gavrilenko,[132a] A. Gavrilyuk,[38] C. Gay,[169] G. Gaycken,[125] E. N. Gazis,[10] A. Gekow,[121] C. Gemme,[57b] M. H. Genest,[60] A. D. Gentry,[114] S. George,[96] T. Geralis,[46] A. A. Gerwin,[122] P. Gessinger-Befurt,[37] M. Ghani,[172] K. Ghorbanian,[95] A. Ghosal,[146] A. Ghosh,[164] A. Ghosh,[7] B. Giacobbe,[24b] S. Giagu,[75a,75b] T. Giani,[116] A. Giannini,[62] S. M. Gibson,[96] M. Gignac,[138] D. T. Gil,[86b] A. K. Gilbert,[86a] B. J. Gilbert,[42] D. Gillberg,[35] G. Gilles,[116] D. M. Gingrich,[2,u] M. P. Giordani,[69a,69c] P. F. Giraud,[137] G. Giugliarelli,[69a,69c] D. Giugni,[71a] F. Giuli,[76a,76b] I. Gkialas,[9,t] L. K. Gladilin,[38] C. Glasman,[100] M. Glazewska,[20] R. M. Gleason,[164] G. Glemža,[48] M. Glisic,[125] I. Gnesi,[44b] Y. Go,[30] M. Goblirsch-Kolb,[37] B. Gocke,[49] D. Godin,[109] B. Gokturk,[22a] S. Goldfarb,[106] T. Golling,[56] M. G. D. Gololo,[34c] A. Golub,[141] D. Golubkov,[38] J. P. Gombas,[108] A. Gomes,[132a,132b] G. Gomes Da Silva,[146] A. J. Gomez Delegido,[37] R. Gonçalo,[132a] L. Gonella,[21] A. Gongadze,[154c] F. Gonnella,[21] J. L. Gonski,[148] R. Y. González Andana,[52] S. González de la Hoz,[168] M. V. Gonzalez Rodrigues,[48] R. Gonzalez Suarez,[166] S. Gonzalez-Sevilla,[56] L. Goossens,[37] B. Gorini,[37] E. Gorini,[70a,70b] A. Gorišek,[94] T. C. Gosart,[130] A. T. Goshaw,[51] M. I. Gostkin,[39] S. Goswami,[123] C. A. Gottardo,[37] S. A. Gotz,[110] M. Gouighri,[36b] A. G. Goussiou,[141] N. Govender,[34c] R. P. Grabarczyk,[128] I. Grabowska-Bold,[86a] K. Graham,[35] E. Gramstad,[127] S. Grancagnolo,[70a,70b] C. M. Grant,[1] P. M. Gravila,[28f] F. G. Gravili,[70a,70b] H. M. Gray,[18a] M. Greco,[111] M. J. Green,[1] C. Grefe,[25] A. S. Grefsrud,[17] I. M. Gregor,[48] K. T. Greif,[164] P. Grenier,[148] S. G. Grewe,[111] A. A. Grillo,[138] K. Grimm,[32] S. Grinstein,[13,v] J.-F. Grivaz,[66] E. Gross,[174] J. Grosse-Knetter,[55] L. Guan,[107] G. Guerrieri,[37] R. Guevara,[127] R. Gugel,[101] J. A. M. Guhit,[107] A. Guida,[19] E. Guilloton,[172] S. Guindon,[37] F. Guo,[14,113c] J. Guo,[143a] L. Guo,[48] L. Guo,[113b,w] Y. Guo,[107] Y. Guo,[42] A. Gupta,[49] R. Gupta,[131] S. Gupta,[27] S. Gurbuz,[25] S. S. Gurdasani,[48] G. Gustavino,[75a,75b] P. Gutierrez,[122]

L. F. Gutierrez Zagazeta,[130] M. Gutsche,[50] C. Gutschow,[97] C. Gwenlan,[128] C. B. Gwilliam,[93] E. S. Haaland,[127] A. Haas,[119] M. Habedank,[59] C. Haber,[18a] H. K. Hadavand,[8] A. Haddad,[41] A. Hadef,[50] A. I. Hagan,[92] J. J. Hahn,[146] E. H. Haines,[97] M. Haleem,[171] J. Haley,[123] G. D. Hallewell,[103] J. A. Hallford,[48] K. Hamano,[170] H. Hamdaoui,[166] M. Hamer,[25] S. E. D. Hammoud,[66] E. J. Hampshire,[96] J. Han,[142a] L. Han,[113a] L. Han,[62] S. Han,[14] K. Hanagaki,[83] M. Hance,[138] D. A. Hangal,[42] H. Hanif,[147] M. D. Hank,[130] J. B. Hansen,[43] P. H. Hansen,[43] T. Harenberg,[176] S. Harkusha,[178] M. L. Harris,[104] Y. T. Harris,[25] J. Harrison,[13] P. F. Harrison,[172] M. L. E. Hart,[97] N. M. Hartman,[111] N. M. Hartmann,[110] R. Z. Hasan,[96,136] Y. Hasegawa,[145] F. Haslbeck,[128] S. Hassan,[17] R. Hauser,[108] M. Haviernik,[135] C. M. Hawkes,[21] R. J. Hawkings,[37] Y. Hayashi,[158] D. Hayden,[108] C. Hayes,[107] R. L. Hayes,[116] C. P. Hays,[128] J. M. Hays,[95] H. S. Hayward,[93] M. He,[14,113c] Y. He,[48] Y. He,[97] N. B. Heatley,[95] V. Hedberg,[99] J. Heilman,[35] S. Heim,[48] T. Heim,[18a] J. J. Heinrich,[125] L. Heinrich,[111] J. Hejbal,[133] M. Helbig,[50] A. Held,[175] S. Hellesund,[17] C. M. Helling,[169] S. Hellman,[47a,47b] A. M. Henriques Correia,[37] H. Herde,[99] Y. Hernández Jiménez,[150] L. M. Herrmann,[25] T. Herrmann,[50] G. Herten,[54] R. Hertenberger,[110] L. Hervas,[37] M. E. Hesping,[101] N. P. Hessey,[161a] J. Hessler,[111] M. Hidaoui,[36b] N. Hidic,[135] E. Hill,[160] T. S. Hillersoy,[17] S. J. Hillier,[21] J. R. Hinds,[108] F. Hinterkeuser,[25] M. Hirose,[126] S. Hirose,[162] D. Hirschbuehl,[176] T. G. Hitchings,[102] B. Hiti,[94] J. Hobbs,[150] R. Hobincu,[28e] N. Hod,[174] A. M. Hodges,[167] M. C. Hodgkinson,[144] B. H. Hodkinson,[128] A. Hoecker,[37] D. D. Hofer,[107] J. Hofer,[168] J. Hofner,[101] M. Holzbock,[37] L. B. A. H. Hommels,[33] V. Homsak,[128] J. J. Hong,[68] T. M. Hong,[131] B. H. Hooberman,[167] W. H. Hopkins,[6] M. C. Hoppesch,[167] Y. Horii,[112] M. E. Horstmann,[111] S. Hou,[153] M. R. Housenga,[167] J. Howarth,[59] J. Hoya,[6] M. Hrabovsky,[124] T. Hryn'ova,[4] P. J. Hsu,[65] S.-C. Hsu,[141] T. Hsu,[66] M. Hu,[18a] Q. Hu,[62] S. Huang,[33] X. Huang,[14,113c] Y. Huang,[135] Y. Huang,[113b] Y. Huang,[14] Z. Huang,[66] Z. Hubacek,[134] F. Huegging,[25] T. B. Huffman,[128] M. Hufnagel Maranha De Faria,[82a] C. A. Hugli,[48] M. Huhtinen,[37] S. K. Huiberts,[127] R. Hulsken,[105] C. E. Hultquist,[18a] D. L. Humphreys,[104] N. Huseynov,[12] J. Huston,[108] B. Huth,[37] J. Huth,[61] L. Huth,[48] R. Hyneman,[7] G. Iacobucci,[56] G. Iakovidis,[30] L. Iconomidou-Fayard,[66] J. P. Iddon,[37] P. Iengo,[72a,72b] Y. Iiyama,[158] T. Iizawa,[158] Y. Ikegami,[83] D. Iliadis,[157] N. Ilic,[160] H. Imam,[36a] G. Inacio Goncalves,[82d] S. A. Infante Cabanas,[139c] T. Ingebretsen Carlson,[47a,47b] J. M. Inglis,[95] G. Introzzi,[73a,73b] M. Iodice,[77a] V. Ippolito,[75a,75b] R. K. Irwin,[93] M. Ishino,[158] W. Islam,[175] C. Issever,[19] S. Istin,[22a,x] K. Itabashi,[126] H. Ito,[173] R. Iuppa,[78a,78b] A. Ivina,[174] S. Izumiyama,[112] V. Izzo,[72a] P. Jacka,[134] P. Jackson,[1] P. Jain,[48] K. Jakobs,[54] T. Jakoubek,[174] J. Jamieson,[59] W. Jang,[158] S. Jankovych,[135] M. Javurkova,[104] P. Jawahar,[102] L. Jeanty,[125] J. Jejelava,[154a,y] P. Jenni,[54,z] C. E. Jessiman,[35] C. Jia,[142a] H. Jia,[169] J. Jia,[150] X. Jia,[111,113c] Z. Jia,[113a] C. Jiang,[52] Q. Jiang,[64b] S. Jiggins,[48] M. Jimenez Ortega,[168] J. Jimenez Pena,[13] S. Jin,[113a] A. Jinaru,[28b] O. Jinnouchi,[140] P. Johansson,[144] K. A. Johns,[7] J. W. Johnson,[138] F. A. Jolly,[48] D. M. Jones,[151] E. Jones,[48] K. S. Jones,[8] P. Jones,[33] R. W. L. Jones,[92] T. J. Jones,[93] H. L. Joos,[55] R. Joshi,[121] J. Jovicevic,[16] X. Ju,[18a] J. J. Junggeburth,[37] T. Junkermann,[63a] A. Juste Rozas,[13,v] M. K. Juzek,[87] S. Kabana,[139f] A. Kaczmarska,[87] S. A. Kadir,[148] M. Kado,[111] H. Kagan,[121] M. Kagan,[148] A. Kahn,[130] C. Kahra,[101] T. Kaji,[158] E. Kajomovitz,[155] N. Kakati,[174] N. Kakoty,[13] I. Kalaitzidou,[54] S. Kandel,[8] N. Kanellos,[10] N. J. Kang,[138] D. Kar,[34j,a] E. Karentzos,[25] K. Karki,[8] O. Karkout,[116] S. N. Karpov,[39] Z. M. Karpova,[39] V. Kartvelishvili,[92,154b] A. N. Karyukhin,[38] E. Kasimi,[157] J. Katzy,[48] S. Kaur,[35] K. Kawade,[145] M. P. Kawale,[122] C. Kawamoto,[88] T. Kawamoto,[62] E. F. Kay,[37] S. Kazakos,[108] V. F. Kazanin,[38] J. M. Keaveney,[34a] R. Keeler,[170] G. V. Kehris,[61] J. S. Keller,[35] J. M. Kelly,[170] J. J. Kempster,[151] O. Kepka,[133] J. Kerr,[161b] B. P. Kerridge,[136] B. P. Kerševan,[94] L. Keszeghova,[29a] R. A. Khan,[131] A. Khanov,[123] A. G. Kharlamov,[38] T. Kharlamova,[38] E. E. Khoda,[141] M. Kholodenko,[132a] T. J. Khoo,[19] G. Khoriauli,[171] Y. Khoulaki,[36a] Y. A. R. Khwaira,[129] B. Kibirige,[34j] D. Kim,[6] D. W. Kim,[18b] Y. K. Kim,[40] N. Kimura,[97] M. K. Kingston,[55] A. Kirchhoff,[55] C. Kirfel,[25] F. Kirfel,[25] J. Kirk,[136] A. E. Kiryunin,[111] S. Kita,[162] O. Kivernyk,[25] M. Klassen,[163] C. Klein,[35] L. Klein,[171] M. H. Klein,[45] S. B. Klein,[56] U. Klein,[93] A. Klimentov,[30] T. Klioutchnikova,[37] P. Kluit,[116] S. Kluth,[111] E. Kneringer,[79] T. M. Knight,[160] A. Knue,[49] M. Kobel,[50] D. Kobylianskii,[174] S. F. Koch,[128] M. Kocian,[148] P. Kodyš,[135] D. M. Koeck,[125] T. Koffas,[35] O. Kolay,[50] I. Koletsou,[4] T. Komarek,[87] K. Köneke,[55] A. X. Y. Kong,[1] T. Kono,[120] N. Konstantinidis,[97] P. Kontaxakis,[56] B. Konya,[99] R. Kopeliansky,[42] S. Koperny,[86a] R. Koppenhofer,[54] K. Korcyl,[87] K. Kordas,[157,aa] A. Korn,[97] S. Korn,[55] I. Korolkov,[13] N. Korotkova,[38] B. Kortman,[116] O. Kortner,[111] S. Kortner,[111] W. H. Kostecka,[117] M. Kostov,[29a] V. V. Kostyukhin,[146]

A. Kotsokechagia,[37] A. Kotwal,[51] A. Koulouris,[37] A. Kourkoumeli-Charalampidi,[73a,73b] C. Kourkoumelis,[9] E. Kourlitis,[111] O. Kovanda,[125] R. Kowalewski,[170] W. Kozanecki,[125] A. S. Kozhin,[38] V. A. Kramarenko,[38] G. Kramberger,[94] P. Kramer,[25] M. W. Krasny,[129] A. Krasznahorkay,[104] A. C. Kraus,[117] J. W. Kraus,[176] J. A. Kremer,[48] N. B. Krengel,[146] T. Kresse,[50] L. Kretschmann,[176] J. Kretzschmar,[93] P. Krieger,[160] K. Krizka,[21] K. Kroeninger,[49] H. Kroha,[111] J. Kroll,[133] J. Kroll,[130] K. S. Krowpman,[108] U. Kruchonak,[39] H. Krüger,[25] N. Krumnack,[80] M. C. Kruse,[51] O. Kuchinskaia,[39] S. Kuday,[3a] S. Kuehn,[37] R. Kuesters,[54] T. Kuhl,[48] V. Kukhtin,[39] Y. Kulchitsky,[39] S. Kuleshov,[139d,139b] J. Kull,[1] E. V. Kumar,[110] M. Kumar,[34j] N. Kumari,[48] P. Kumari,[161b] A. Kupco,[133] A. Kupich,[38] O. Kuprash,[54] H. Kurashige,[85] L. L. Kurchaninov,[161a] O. Kurdysh,[4] A. Kurova,[38] M. Kuze,[140] A. K. Kvam,[104] J. Kvita,[124] N. G. Kyriacou,[141] M. Laassiri,[30] C. Lacasta,[168] F. Lacava,[75a,75b] H. Lacker,[19] D. Lacour,[129] N. N. Lad,[97] E. Ladygin,[39] A. Lafarge,[41] B. Laforge,[129] T. Lagouri,[177] F. Z. Lahbabi,[36a] S. Lai,[55,37] W. S. Lai,[97] I. K. Lakomiec,[55] J. E. Lambert,[170] S. Lammers,[68] W. Lampl,[7] C. Lampoudis,[157,aa] G. Lamprinoudis,[171] A. N. Lancaster,[117] E. Lançon,[30] U. Landgraf,[54] M. P. J. Landon,[95] V. S. Lang,[54] A. J. Lankford,[164] F. Lanni,[37] K. Lantzsch,[25] A. Lanza,[73a] M. Lanzac Berrocal,[168] J. F. Laporte,[137] T. Lari,[71a] D. Larsen,[17] L. Larson,[11] F. Lasagni Manghi,[24b] M. Lassnig,[37] S. D. Lawlor,[144] R. Lazaridou,[164] M. Lazzaroni,[71a,71b] E. T. T. Le,[164] H. D. M. Le,[108] E. M. Le Boulicaut,[177] L. T. Le Pottier,[18a] B. Leban,[24b,24a] F. Ledroit-Guillon,[60] T. F. Lee,[161b] L. L. Leeuw,[34c] M. Lefebvre,[170] C. Leggett,[18a] G. Lehmann Miotto,[37] M. Leigh,[56] W. A. Leight,[104] W. Leinonen,[115] A. Leisos,[157,bb] M. A. L. Leite,[82c] C. E. Leitgeb,[19] R. Leitner,[135] K. J. C. Leney,[45] T. Lenz,[25] S. Leone,[74a] C. Leonidopoulos,[52] A. Leopold,[149] J. LePage-Bourbonnais,[35] R. Les,[108] C. G. Lester,[33] M. Levchenko,[38] J. Levêque,[4] L. J. Levinson,[174] G. Levrini,[24b,24a] M. P. Lewicki,[87] C. Lewis,[141] D. J. Lewis,[4] L. Lewitt,[144] A. Li,[30] B. Li,[142a] C. Li,[107] C-Q. Li,[111] H. Li,[142a] H. Li,[102] H. Li,[15] H. Li,[62] H. Li,[142a] J. Li,[143a] K. Li,[14] L. Li,[143a] R. Li,[177] S. Li,[14,113c] S. Li,[143b,143a] T. Li,[5] X. Li,[105] Y. Li,[14] Z. Li,[158] Z. Li,[14,113c] Z. Li,[62] S. Liang,[14,113c] Z. Liang,[14] M. Liberatore,[137] B. Liberti,[76a] G. B. Libotte,[82d] K. Lie,[64c] J. Lieber Marin,[82e] H. Lien,[68] H. Lin,[107] S. F. Lin,[150] L. Linden,[110] R. E. Lindley,[7] J. H. Lindon,[37] J. Ling,[61] E. Lipeles,[130] A. Lipniacka,[17] A. Lister,[169] J. D. Little,[68] B. Liu,[14] B. X. Liu,[113b] D. Liu,[155] D. Liu,[138] E. H. L. Liu,[21] J. K. K. Liu,[119] K. Liu,[143b] K. Liu,[143b,143a] M. Liu,[62] M. Y. Liu,[62] P. Liu,[14] Q. Liu,[148] S. Liu,[150] X. Liu,[142a] Y. Liu,[113b,113c] Y. Liu,[167] Y. L. Liu,[142a] Y. W. Liu,[62] Z. Liu,[66,cc] S. L. Lloyd,[95] E. M. Lobodzinska,[48] P. Loch,[7] E. Lodhi,[160] K. Lohwasser,[144] E. Loiacono,[48] J. D. Lomas,[21] J. D. Long,[42] I. Longarini,[164] R. Longo,[167] A. Lopez Solis,[13] N. A. Lopez-canelas,[7] N. Lorenzo Martinez,[4] A. M. Lory,[110] M. Losada,[118a] G. Löschcke Centeno,[4] X. Lou,[47a,47b] X. Lou,[14,113c] A. Lounis,[66] P. A. Love,[92] M. Lu,[66] S. Lu,[130] Y. J. Lu,[153] H. J. Lubatti,[141] C. Luci,[75a,75b] F. L. Lucio Alves,[113a] F. Luehring,[68] B. S. Lunday,[130] O. Lundberg,[149] J. Lunde,[37] N. A. Luongo,[6] M. S. Lutz,[37] A. B. Lux,[26] D. Lynn,[30] R. Lysak,[133] V. Lysenko,[134] E. Lytken,[99] V. Lyubushkin,[39] T. Lyubushkina,[39] M. M. Lyukova,[150] H. Ma,[30] K. Ma,[62] L. L. Ma,[142a] W. Ma,[62] Y. Ma,[123] J. C. MacDonald,[101] P. C. Machado De Abreu Farias,[82e] D. Macina,[37] R. Madar,[41] T. Madula,[97] J. Maeda,[85] T. Maeno,[30] P. T. Mafa,[34c,dd] H. Maguire,[144] M. Maheshwari,[33] V. Maiboroda,[66] A. Maio,[132a,132b,132d] K. Maj,[86a] O. Majersky,[48] S. Majewski,[125] R. Makhmanazarov,[38] N. Makovec,[66] V. Maksimovic,[16] B. Malaescu,[129] J. Malamant,[127] Pa. Malecki,[87] V. P. Maleev,[38] F. Malek,[60,ee] M. Mali,[94] D. Malito,[96] A. Maloizel,[5] S. Maltezos,[10] A. Malvezzi Lopes,[82d] S. Malyukov,[39] J. Mamuzic,[94] G. Mancini,[53] M. N. Mancini,[27] G. Manco,[73a,73b] J. P. Mandalia,[95] S. S. Mandarry,[151] I. Mandić,[94] L. Manhaes de Andrade Filho,[82a] I. M. Maniatis,[174] J. Manjarres Ramos,[90] D. C. Mankad,[174] A. Mann,[110] T. Manoussos,[37] M. N. Mantinan,[40] S. Manzoni,[37] L. Mao,[143a] X. Mapekula,[34c] A. Marantis,[157] R. R. Marcelo Gregorio,[95] G. Marchiori,[5] C. Marcon,[71a] E. Maricic,[16] M. Marinescu,[48] S. Marium,[48] M. Marjanovic,[122] A. Markhoos,[54] M. Markovitch,[66] M. K. Maroun,[104] M. C. Marr,[147] G. T. Marsden,[102] E. J. Marshall,[92] Z. Marshall,[18a] S. Marti-Garcia,[168] J. Martin,[97] T. A. Martin,[136] V. J. Martin,[52] B. Martin dit Latour,[17] L. Martinelli,[75a,75b] M. Martinez,[13,v] P. Martinez Agullo,[168] V. I. Martinez Outschoorn,[104] P. Martinez Suarez,[37] S. Martin-Haugh,[136] G. Martinovicova,[135] V. S. Martoiu,[28b] A. C. Martyniuk,[97] A. Marzin,[37] D. Mascione,[78a,78b] L. Masetti,[101] J. Masik,[102] A. L. Maslennikov,[39] S. L. Mason,[42] P. Massarotti,[72a,72b] P. Mastrandrea,[74a,74b] A. Mastroberardino,[44b,44a] T. Masubuchi,[126] T. T. Mathew,[125] J. Matousek,[135] D. M. Mattern,[49] K. Mauer,[48] J. Maurer,[28b] T. Maurin,[59] A. J. Maury,[66] B. Maček,[94] C. Mavungu Tsava,[103] D. A. Maximov,[38] A. E. May,[102]

E. Mayer,[41] R. Mazini,[34j] I. Maznas,[117] S. M. Mazza,[138] E. Mazzeo,[37] J. P. Mc Gowan,[170] S. P. Mc Kee,[107] C. A. Mc Lean,[6] C. C. McCracken,[169] E. F. McDonald,[106] A. E. McDougall,[116] L. F. Mcelhinney,[92] J. A. Mcfayden,[151] R. P. McGovern,[130] R. P. Mckenzie,[34j] T. C. Mclachlan,[48] D. J. Mclaughlin,[97] S. J. McMahon,[136] C. M. Mcpartland,[93] R. A. McPherson,[170,o] S. Mehlhase,[110] A. Mehta,[93] D. Melini,[168] B. R. Mellado Garcia,[34j] A. H. Melo,[55] F. Meloni,[48] A. M. Mendes Jacques Da Costa,[102] L. Meng,[92] S. Menke,[111] M. Mentink,[37] E. Meoni,[44b,44a] G. Mercado,[117] S. Merianos,[157] C. Merlassino,[69a,69c] C. Meroni,[71a,71b] J. Metcalfe,[6] A. S. Mete,[6] E. Meuser,[101] C. Meyer,[68] J-P. Meyer,[137] Y. Miao,[113a] R. P. Middleton,[136] M. Mihovilovic,[66] L. Mijović,[52] G. Mikenberg,[174] M. Mikestikova,[133] M. Mikuž,[94] H. Mildner,[101] A. Milic,[37] D. W. Miller,[40] E. H. Miller,[148] A. Milov,[174] D. A. Milstead,[47a,47b] T. Min,[113a] A. A. Minaenko,[38] I. A. Minashvili,[154b] A. I. Mincer,[119] B. Mindur,[86a] M. Mineev,[39] Y. Mino,[88] L. M. Mir,[13] M. Miralles Lopez,[59] M. Mironova,[18a] M. Missio,[41] A. Mitra,[172] V. A. Mitsou,[168] Y. Mitsumori,[112] O. Miu,[160] P. S. Miyagawa,[95] T. Mkrtchyan,[37] M. Mlinarevic,[97] T. Mlinarevic,[97] M. Mlynarikova,[135] L. Mlynarska,[86a] C. Mo,[143a] S. Mobius,[20] M. H. Mohamed Farook,[114] S. Mohapatra,[42] M. F. Mohd Soberi,[52] S. Mohiuddin,[123] G. Mokgatitswane,[34j] L. Moleri,[174] U. Molinatti,[128] L. G. Mollier,[20] B. Mondal,[133] S. Mondal,[134] K. Mönig,[48] E. Monnier,[103] L. Monsonis Romero,[168] J. Montejo Berlingen,[13] A. Montella,[47a,47b] M. Montella,[121] F. Montereali,[77a,77b] F. Monticelli,[91] S. Monzani,[69a,69c] A. Morancho Tarda,[43] N. Morange,[66] A. L. Moreira De Carvalho,[48] M. Moreno Llácer,[168] C. Moreno Martinez,[56] J. M. Moreno Perez,[23b] P. Morettini,[57b] S. Morgenstern,[37] M. Morii,[61] M. Morinaga,[158] M. Moritsu,[89] F. Morodei,[75a,75b] P. Moschovakos,[37] B. Moser,[54] M. Mosidze,[154b] T. Moskalets,[45] P. Moskvitina,[115] J. Moss,[32] P. Moszkowicz,[86a] T. Motta Quirino,[82d] A. Moussa,[36d] Y. Moyal,[174] H. Moyano Gomez,[13] E. J. W. Moyse,[104] T. G. Mroz,[87] S. Muanza,[103] M. Mucha,[25] J. Mueller,[131] G. A. Mullier,[166] A. J. Mullin,[33] J. J. Mullin,[51] A. C. Mullins,[45] A. E. Mulski,[61] D. P. Mungo,[160] D. Munoz Perez,[168] F. J. Munoz Sanchez,[102] W. J. Murray,[172,136] M. Muškinja,[94] C. Mwewa,[48] A. G. Myagkov,[38,k] A. J. Myers,[8] G. Myers,[107] M. Myska,[134] B. P. Nachman,[148] K. Nagai,[128] K. Nagano,[83] R. Nagasaka,[158] J. L. Nagle,[30,ff] E. Nagy,[103] A. M. Nairz,[37] Y. Nakahama,[83] K. Nakamura,[83] K. Nakkalil,[5] A. Nandi,[63b] H. Nanjo,[126] E. A. Narayanan,[45] Y. Narukawa,[158] I. Naryshkin,[38] L. Nasella,[71a,71b] S. Nasri,[118b] C. Nass,[25] G. Navarro,[23a] A. Nayaz,[19] P. Y. Nechaeva,[38] S. Nechaeva,[24b,24a] F. Nechansky,[133] L. Nedic,[128] T. J. Neep,[21] A. Negri,[73a,73b] M. Negrini,[24b] C. Nellist,[116] C. Nelson,[105] K. Nelson,[107] S. Nemecek,[133] M. Nessi,[37,gg] M. S. Neubauer,[167] J. Newell,[93] P. R. Newman,[21] Y. W. Y. Ng,[167] B. Ngair,[118a] H. D. N. Nguyen,[109] J. D. Nichols,[122] R. B. Nickerson,[128] R. Nicolaidou,[137] J. Nielsen,[138] M. Niemeyer,[55] J. Niermann,[37] N. Nikiforou,[37] V. Nikolaenko,[38,k] I. Nikolic-Audit,[129] P. Nilsson,[30] I. Ninca,[48] G. Ninio,[156] A. Nisati,[75a] R. Nisius,[111] N. Nitika,[174] E. K. Nkadimeng,[34b] T. Nobe,[158] D. Noll,[148] T. Nommensen,[152] M. B. Norfolk,[144] B. J. Norman,[35] L. C. Nosler,[18a] M. Noury,[36a] J. Novak,[94] T. Novak,[94] R. Novotny,[134] L. Nozka,[124] K. Ntekas,[164] D. Ntounis,[148] N. M. J. Nunes De Moura Junior,[82b] J. Ocariz,[129] I. Ochoa,[132a] A. Odella Rodriguez,[13] S. Oerdek,[48] J. T. Offermann,[40] A. Ogrodnik,[87] A. Oh,[102] C. C. Ohm,[149] H. Oide,[83] M. L. Ojeda,[37] Y. Okumura,[158] L. F. Oleiro Seabra,[132a] I. Oleksiyuk,[56] G. Oliveira Correa,[13] D. Oliveira Damazio,[30] J. L. Oliver,[1] R. Omar,[68] Ö. O. Öncel,[54] A. P. O'Neill,[20] Y. Onoda,[140] A. Onofre,[132a,132e,hh] P. U. E. Onyisi,[11] M. J. Oreglia,[40] D. Orestano,[77a,77b] R. Orlandini,[77a,77b] R. S. Orr,[160] L. M. Osojnak,[42] Y. Osumi,[112] G. Otero y Garzón,[31] H. Otono,[89] M. Ouchrif,[36d] F. Ould-Saada,[127] T. Ovsiannikova,[141] M. Owen,[59] R. E. Owen,[136] V. E. Ozcan,[22a] F. Ozturk,[87] N. Ozturk,[8] S. Ozturk,[81] H. A. Pacey,[128] K. Pachal,[161a] A. Pacheco Pages,[13] C. Padilla Aranda,[13] G. Padovano,[75a,75b] S. Pagan Griso,[18a] J. Pampel,[25] J. Pan,[177] D. K. Panchal,[11] C. E. Pandini,[60] J. G. Panduro Vazquez,[136] H. D. Pandya,[1] H. Pang,[137] P. Pani,[48] G. Panizzo,[69a,69c] L. Panwar,[129] L. Paolozzi,[56] S. Parajuli,[167] A. Paramonov,[6] C. Paraskevopoulos,[53] D. Paredes Hernandez,[64b] S. R. Paredes Saenz,[52] A. Pareti,[73a,73b] K. R. Park,[42] T. H. Park,[111] F. Parodi,[57b,57a] J. A. Parsons,[42] U. Parzefall,[54] B. Pascual Dias,[41] L. Pascual Dominguez,[100] E. Pasqualucci,[75a] S. Passaggio,[57b] F. Pastore,[96] P. Patel,[87] U. M. Patel,[51] J. R. Pater,[102] T. Pauly,[37] F. Pauwels,[135] C. I. Pazos,[163] M. Pedersen,[127] R. Pedro,[132a] S. V. Peleganchuk,[38] O. Penc,[133] S. Peng,[15] G. D. Penn,[177] K. E. Penski,[110] M. Penzin,[38] B. S. Peralva,[82d] A. P. Pereira Peixoto,[141] L. Pereira Sanchez,[148] D. V. Perepelitsa,[30,ff] G. Perera,[104] E. Perez Codina,[37] M. Perganti,[10] H. Pernegger,[37] S. Perrella,[75a,75b] K. Peters,[48] R. F. Y. Peters,[102] B. A. Petersen,[37] T. C. Petersen,[43] E. Petit,[103] V. Petousis,[134] A. R. Petri,[71a,71b] C. Petridou,[157,aa] T. Petru,[135]

M. Pettee,[18a] A. Petukhov,[81] K. Petukhova,[37] R. Pezoa,[139g] L. Pezzotti,[24b,24a] G. Pezzullo,[177] L. Pfaffenbichler,[37] A. J. Pfleger,[79] T. M. Pham,[175] T. Pham,[106] P. W. Phillips,[136] G. Piacquadio,[150] E. Pianori,[18a] F. Piazza,[125] R. Piegaia,[31] D. Pietreanu,[28b] A. D. Pilkington,[102] M. Pinamonti,[69a,69c] J. L. Pinfold,[2] G. Pinheiro Matos,[42] B. C. Pinheiro Pereira,[132a] J. Pinol Bel,[13] A. E. Pinto Pinoargote,[129] L. Pintucci,[69a,69c] K. M. Piper,[151] A. Pirttikoski,[56] D. A. Pizzi,[35] L. Pizzimento,[64b] A. Plebani,[33] M.-A. Pleier,[30] V. Pleskot,[135] E. Plotnikova,[39] G. Poddar,[95] R. Poettgen,[99] L. Poggioli,[129] S. Polacek,[135] G. Polesello,[73a] A. Poley,[147] A. Polini,[24b] C. S. Pollard,[172] Z. B. Pollock,[121] E. Pompa Pacchi,[122] N. I. Pond,[97] D. Ponomarenko,[68] L. Pontecorvo,[37] S. Popa,[28a] G. A. Popeneciu,[28d] A. Poreba,[37] D. M. Portillo Quintero,[161a] S. Pospisil,[134] M. A. Postill,[144] P. Postolache,[28c] K. Potamianos,[172] P. A. Potepa,[86a] I. N. Potrap,[39] C. J. Potter,[33] H. Potti,[152] J. Poveda,[168] M. E. Pozo Astigarraga,[37] R. Pozzi,[37] A. Prades Ibanez,[76a,76b] S. R. Pradhan,[144] J. Pretel,[170] D. Price,[102] M. Primavera,[70a] L. Primomo,[69a,69c] M. A. Principe Martin,[100] R. Privara,[124] T. Procter,[86b] M. L. Proffitt,[141] N. Proklova,[130] K. Prokofiev,[64c] G. Proto,[111] J. Proudfoot,[6] M. Przybycien,[86a] W. W. Przygoda,[86b] A. Psallidas,[46] J. E. Puddefoot,[144] D. Pudzha,[53] H. I. Purnell,[1] D. Pyatiizbyantseva,[115] J. Qian,[107] R. Qian,[108] D. Qichen,[128] Y. Qin,[13] T. Qiu,[52] A. Quadt,[55] M. Queitsch-Maitland,[102] G. Quetant,[56] R. P. Quinn,[169] G. Rabanal Bolanos,[61] D. Rafanoharana,[111] F. Raffaeli,[76a,76b] F. Ragusa,[71a,71b] J. L. Rainbolt,[40] S. Rajagopalan,[30] E. Ramakoti,[39] L. Rambelli,[57b,57a] I. A. Ramirez-Berend,[35] K. Ran,[107,113c] D. S. Rankin,[130] N. P. Rapheeha,[34j] H. Rasheed,[28b] A. Rastogi,[18a] S. Rave,[101] S. Ravera,[57b,57a] B. Ravina,[37] I. Ravinovich,[174] M. Raymond,[37] A. L. Read,[127] N. P. Readioff,[144] D. M. Rebuzzi,[73a,73b] A. S. Reed,[59] K. Reeves,[27] D. Reikher,[37] A. Rej,[49] C. Rembser,[37] H. Ren,[62] M. Renda,[28b] F. Renner,[48] A. G. Rennie,[59] M. Repik,[56] A. L. Rescia,[57b,57a] S. Resconi,[71a] M. Ressegotti,[57b] S. Rettie,[116] W. F. Rettie,[35] M. M. Revering,[33] E. Reynolds,[18a] O. L. Rezanova,[39] P. Reznicek,[135] H. Riani,[36d] N. Ribaric,[51] B. Ricci,[69a,69c] E. Ricci,[78a,78b] R. Richter,[111] S. Richter,[47a,47b] E. Richter-Was,[86b] M. Ridel,[129] S. Ridouani,[36d] P. Rieck,[119] P. Riedler,[37] E. M. Riefel,[47a,47b] J. O. Rieger,[116] M. Rijssenbeek,[150] M. Rimoldi,[34c] L. Rinaldi,[24b,24a] P. Rincke,[166,55] G. Ripellino,[166] I. Riu,[13] J. C. Rivera Vergara,[170] F. Rizatdinova,[123] E. Rizvi,[95] B. R. Roberts,[40] S. S. Roberts,[138] D. Robinson,[33] A. Robson,[59] A. Rocchi,[76a,76b] C. Roda,[74a,74b] F. A. Rodriguez,[117] S. Rodriguez Bosca,[37] Y. Rodriguez Garcia,[23a] A. M. Rodríguez Vera,[117] S. Roe,[37] J. T. Roemer,[37] O. Røhne,[127] R. A. Rojas,[37] C. P. A. Roland,[129] A. Romaniouk,[79] E. Romano,[73a,73b] M. Romano,[24b] A. C. Romero Hernandez,[167] N. Rompotis,[93] L. Roos,[129] S. Rosati,[75a] B. J. Rosser,[40] E. Rossi,[128] E. Rossi,[72a,72b] L. P. Rossi,[61] L. Rossini,[54] R. Rosten,[121] M. Rotaru,[28b] R. Roth,[37] D. Rousseau,[66] D. Rousso,[48] S. Roy-Garand,[160] A. Rozanov,[103] Z. M. A. Rozario,[59] Y. Rozen,[155] A. Rubio Jimenez,[168] V. H. Ruelas Rivera,[19] T. A. Ruggeri,[1] A. Ruggiero,[128] A. Ruiz-Martinez,[168] A. Rummler,[37] G. B. Rupnik Boero,[37] Z. Rurikova,[54] N. A. Rusakovich,[39] S. Ruscelli,[49] H. L. Russell,[170] G. Russo,[75a,75b] J. P. Rutherfoord,[7] S. Rutherford Colmenares,[33] M. Rybar,[135] P. Rybczynski,[86a] A. Ryzhov,[45] H. F-W. Sadrozinski,[138] F. Safai Tehrani,[75a] S. Saha,[1] M. Sahinsoy,[81] B. Sahoo,[174] A. Saibel,[168] B. T. Saifuddin,[122] M. Saimpert,[137] G. T. Saito,[82c] M. Saito,[158] T. Saito,[158] A. Sala,[71a,71b] A. Salnikov,[148] J. Salt,[168] A. Salvador Salas,[156] F. Salvatore,[151] A. Salzburger,[37] D. Sammel,[54] E. Sampson,[92] D. Sampsonidis,[157,aa] D. Sampsonidou,[125] M. A. A. Samy,[59] J. Sánchez,[168] V. Sanchez Sebastian,[168] H. Sandaker,[127] C. O. Sander,[48] J. A. Sandesara,[175] M. Sandhoff,[176] C. Sandoval,[23b] L. Sanfilippo,[63a] D. P. C. Sankey,[136] T. Sano,[88] A. Sansoni,[53] M. Santana Queiroz,[18b] L. Santi,[37] C. Santoni,[41] H. Santos,[132a,132b] A. Santra,[174] E. Sanzani,[24b,24a] K. A. Saoucha,[84b] J. G. Saraiva,[132a,132d] J. Sardain,[7] O. Sasaki,[83] K. Sato,[162] C. Sauer,[37] E. Sauvan,[4] P. Savard,[160,u] R. Sawada,[158] C. Sawyer,[136] L. Sawyer,[98] A. M. Sayed,[27] C. Sbarra,[24b] A. Sbrizzi,[24b,24a] T. Scanlon,[97] J. Schaarschmidt,[141] U. Schäfer,[101] A. C. Schaffer,[66,45] D. Schaile,[110] R. D. Schamberger,[150] C. Scharf,[19] M. M. Schefer,[20] V. A. Schegelsky,[38] D. Scheirich,[135] M. Schernau,[139f] C. Scheulen,[56] C. Schiavi,[57b,57a] M. Schioppa,[44b,44a] B. Schlag,[148] S. Schlenker,[37] J. Schmeing,[176] E. Schmidt,[111] M. A. Schmidt,[176] K. Schmieden,[25] C. Schmitt,[101] N. Schmitt,[101] S. Schmitt,[48] N. A. Schneider,[110] L. Schoeffel,[137] A. Schoening,[63b] P. G. Scholer,[35] E. Schopf,[146] M. Schott,[25] S. Schramm,[56] T. Schroer,[56] H-C. Schultz-Coulon,[63a] M. Schumacher,[54] B. A. Schumm,[138] Ph. Schune,[137] H. R. Schwartz,[7] A. Schwartzman,[148] T. A. Schwarz,[107] Ph. Schwemling,[137] R. Schwienhorst,[108] F. G. Sciacca,[20] A. Sciandra,[30] G. Sciolla,[27] F. Scuri,[74a] C. D. Sebastiani,[37] K. Sedlaczek,[117] S. C. Seidel,[114] A. Seiden,[138] B. D. Seidlitz,[42] C. Seitz,[48] J. M. Seixas,[82b] G. Sekhniaidze,[72a] L. Selem,[60] N. Semprini-Cesari,[24b,24a] A. Semushin,[178]

D. Sengupta,[56] V. Senthilkumar,[168] L. Serin,[66] M. Sessa,[72a,72b] H. Severini,[122] F. Sforza,[57b,57a] A. Sfyrla,[56] Q. Sha,[14] H. Shaddix,[117] A. H. Shah,[33] R. Shaheen,[149] J. D. Shahinian,[130] M. Shamim,[37] L. Y. Shan,[14] M. Shapiro,[18a] A. Sharma,[37] A. S. Sharma,[169] P. Sharma,[30] P. B. Shatalov,[38] K. Shaw,[151] S. M. Shaw,[102] Q. Shen,[14] D. J. Sheppard,[147] P. Sherwood,[97] L. Shi,[97] X. Shi,[14] S. Shimizu,[83] I. P. J. Shipsey,[128,a] S. Shirabe,[89] M. Shiyakova,[39,ii] M. J. Shochet,[40] D. R. Shope,[127] B. Shrestha,[122] S. Shrestha,[121,jj] I. Shreyber,[39] M. J. Shroff,[170] P. Sicho,[133] A. M. Sickles,[167] E. Sideras Haddad,[34j,165] A. C. Sidley,[116] A. Sidoti,[24b] F. Siegert,[50] Dj. Sijacki,[16] F. Sili,[62] J. M. Silva,[52] I. Silva Ferreira,[82b] M. V. Silva Oliveira,[30] S. B. Silverstein,[47a] S. Simion,[66] R. Simoniello,[37] E. L. Simpson,[102] H. Simpson,[151] L. R. Simpson,[6] S. Simsek,[81] S. Sindhu,[55] P. Sinervo,[160] S. N. Singh,[27] S. Singh,[30] S. Sinha,[48] S. Sinha,[102] M. Sioli,[24b,24a] K. Sioulas,[9] I. Siral,[37] E. Sitnikova,[48] J. Sjölin,[47a,47b] A. Skaf,[55] E. Skorda,[21] P. Skubic,[122] M. Slawinska,[87] I. Slazyk,[17] I. Sliusar,[127] V. Smakhtin,[174] B. H. Smart,[136] S. Yu. Smirnov,[139b] Y. Smirnov,[81] L. N. Smirnova,[38,k] O. Smirnova,[99] A. C. Smith,[42] D. R. Smith,[164] J. L. Smith,[102] M. B. Smith,[35] R. Smith,[148] H. Smitmanns,[101] M. Smizanska,[92] K. Smolek,[134] P. Smolyanskiy,[134] A. A. Snesarev,[39] H. L. Snoek,[116] R. M. Snyder,[51] S. Snyder,[30] R. Sobie,[170,o] A. Soffer,[156] C. A. Solans Sanchez,[37] E. Yu. Soldatov,[39] U. Soldevila,[168] A. A. Solodkov,[34j] S. Solomon,[27] A. Soloshenko,[39] K. Solovieva,[54] O. V. Solovyanov,[41] P. Sommer,[50] A. Sonay,[13] A. Sopczak,[134] A. L. Sopio,[52] F. Sopkova,[29b] J. D. Sorenson,[114] I. R. Sotarriva Alvarez,[140] V. Sothilingam,[63a] O. J. Soto Sandoval,[139c,139b] S. Sottocornola,[68] R. Soualah,[84a] Z. Soumaimi,[36e] D. South,[48] N. Soybelman,[174] S. Spagnolo,[70a,70b] D. Sperlich,[54] B. Spisso,[72a,72b] D. P. Spiteri,[59] L. Splendori,[103] M. Spousta,[135] E. J. Staats,[35] R. Stamen,[63a] E. Stanecka,[87] W. Stanek-Maslouska,[48] M. V. Stange,[50] B. Stanislaus,[18a] M. M. Stanitzki,[48] E. A. Starchenko,[38] G. H. Stark,[138] J. Stark,[90] P. Staroba,[133] P. Starovoitov,[84b] R. Staszewski,[87] C. Stauch,[110] G. Stavropoulos,[46] A. Stefl,[37] A. Stein,[101] P. Steinberg,[30] B. Stelzer,[147,161a] H. J. Stelzer,[131] O. Stelzer,[161a] H. Stenzel,[58] T. J. Stevenson,[151] G. A. Stewart,[37] J. R. Stewart,[123] G. Stoicea,[28b] M. Stolarski,[132a] S. Stonjek,[111] A. Straessner,[50] J. Strandberg,[149] S. Strandberg,[47a,47b] M. Stratmann,[176] M. Strauss,[122] T. Strebler,[103] P. Strizenec,[29b] R. Ströhmer,[171] D. M. Strom,[125] R. Stroynowski,[45] A. Strubig,[47a,47b] S. A. Stucci,[30] B. Stugu,[17] J. Stupak,[122] N. A. Styles,[48] D. Su,[148] S. Su,[62] X. Su,[62] D. Suchy,[29a] A. D. Sudhakar Ponnu,[55] K. Sugizaki,[130] V. V. Sulin,[38] D. M. S. Sultan,[128] L. Sultanaliyeva,[25] S. Sultansoy,[3b] S. Sun,[175] W. Sun,[14] N. Sur,[99] M. R. Sutton,[151] M. Svatos,[133] P. N. Swallow,[33] M. Swiatlowski,[161a] A. Swoboda,[37] I. Sykora,[29a] M. Sykora,[135] T. Sykora,[135] D. Ta,[101] K. Tackmann,[48,kk] A. Taffard,[164] R. Tafirout,[161a] Y. Takubo,[83] M. Talby,[103] A. A. Talyshev,[38] K. C. Tam,[64b] N. M. Tamir,[156] A. Tanaka,[158] J. Tanaka,[158] R. Tanaka,[66] M. Tanasini,[150] Z. Tao,[169] S. Tapia Araya,[139g] S. Tapprogge,[101] A. Tarek Abouelfadl Mohamed,[37] S. Tarem,[155] K. Tariq,[14] G. Tarna,[37] G. F. Tartarelli,[71a] M. J. Tartarin,[90] P. Tas,[135] M. Tasevsky,[133] E. Tassi,[44b,44a] A. C. Tate,[167] Y. Tayalati,[36e,ll] G. N. Taylor,[106] W. Taylor,[161b] R. J. Taylor Vara,[168] A. S. Tegetmeier,[90] P. Teixeira-Dias,[96] J. J. Teoh,[160] K. Terashi,[158] J. Terron,[100] S. Terzo,[13] M. Testa,[53] R. J. Teuscher,[160,o] A. Thaler,[79] O. Theiner,[56] T. Theveneaux-Pelzer,[103] D. W. Thomas,[96] J. P. Thomas,[21] E. A. Thompson,[18a] P. D. Thompson,[21] E. Thomson,[130] R. E. Thornberry,[45] C. Tian,[62] Y. Tian,[56] V. Tikhomirov,[81] Yu. A. Tikhonov,[39] S. Timoshenko,[38] D. Timoshyn,[135] E. X. L. Ting,[1] P. Tipton,[177] A. Tishelman-Charny,[30] K. Todome,[140] S. Todorova-Nova,[135] L. Toffolin,[69a,69c] M. Togawa,[83] J. Tojo,[89] S. Tokár,[29a] O. Toldaiev,[68] G. Tolkachev,[103] M. Tomoto,[83] L. Tompkins,[148,mm] E. Torrence,[125] H. Torres,[90] D. I. Torres Arza,[139g] E. Torró Pastor,[168] M. Toscani,[31] C. Tosciri,[40] M. Tost,[11] D. R. Tovey,[144] T. Trefzger,[171] P. M. Tricarico,[13] A. Tricoli,[30] I. M. Trigger,[161a] S. Trincaz-Duvoid,[129] D. A. Trischuk,[170] A. Tropina,[39] D. Truncali,[76a,76b] L. Truong,[34c] M. Trzebinski,[87] A. Trzupek,[87] F. Tsai,[150] M. Tsai,[107] A. Tsiamis,[157] P. V. Tsiareshka,[39] S. Tsigaridas,[161a] A. Tsirigotis,[157,bb] V. Tsiskaridze,[154a] E. G. Tskhadadze,[154a] Y. Tsujikawa,[88] I. I. Tsukerman,[38] V. Tsulaia,[18a] S. Tsuno,[83] K. Tsuri,[120] D. Tsybychev,[150] Y. Tu,[64b] A. Tudorache,[28b] V. Tudorache,[28b] S. B. Tuncay,[128] S. Turchikhin,[57b,57a] I. Turk Cakir,[3a] R. Turra,[71a] T. Turtuvshin,[39,nn] P. M. Tuts,[42] S. Tzamarias,[157,aa] Y. Uematsu,[83] F. Ukegawa,[162] P. A. Ulloa Poblete,[139c,139b] E. N. Umaka,[30] G. Unal,[37] A. Undrus,[30] G. Unel,[164] J. Urban,[29b] P. Urrejola,[139e] G. Usai,[8] R. Ushioda,[159] M. Usman,[109] F. Ustuner,[52] Z. Uysal,[81] V. Vacek,[134] B. Vachon,[105] T. Vafeiadis,[37] A. Vaitkus,[97] C. Valderanis,[110] E. Valdes Santurio,[47a,47b] M. Valente,[37] S. Valentinetti,[24b,24a] A. Valero,[168] E. Valiente Moreno,[168] A. Vallier,[90] J. A. Valls Ferrer,[168] D. R. Van Arneman,[116] A. Van Der Graaf,[49] H. Z. Van Der Schyf,[34j] P. Van Gemmeren,[6] M. Van Rijnbach,[37] S. Van Stroud,[97] I. Van Vulpen,[116] P. Vana,[135]

M. Vanadia,[76a,76b] U. M. Vande Voorde,[149] W. Vandelli,[37] E. R. Vandewall,[148] D. Vannicola,[156] L. Vannoli,[53] R. Vari,[75a] M. Varma,[177] E. W. Varnes,[7] C. Varni,[79] D. Varouchas,[66] L. Varriale,[168] K. E. Varvell,[152] M. E. Vasile,[28b] L. Vaslin,[83] M. D. Vassilev,[148] A. Vasyukov,[39] L. M. Vaughan,[123] R. Vavricka,[135] T. Vazquez Schroeder,[13] J. Veatch,[32] V. Vecchio,[102] M. J. Veen,[104] I. Veliscek,[30] I. Velkovska,[94] L. M. Veloce,[160] F. Veloso,[132a,132c] A. G. Veltman,[52] S. H. Venetianer,[163] S. Veneziano,[75a] A. Ventura,[70a,70b] A. Verbytskyi,[111] M. Verducci,[74a,74b] C. Vergis,[95] M. Verissimo De Araujo,[82b] W. Verkerke,[116] J. C. Vermeulen,[116] C. Vernieri,[148] M. Vessella,[164] M. C. Vetterli,[147,u] A. Vgenopoulos,[101] N. Viaux Maira,[139g,oo] T. Vickey,[144] O. E. Vickey Boeriu,[144] G. H. A. Viehhauser,[128] L. Vigani,[63b] M. Vigl,[111] M. Villa,[24b,24a] M. Villaplana Perez,[168] E. M. Villhauer,[40] E. Vilucchi,[53] M. Vincent,[168] M. G. Vincter,[35] A. Visibile,[116] A. Visive,[116] C. Vittori,[37] I. Vivarelli,[24b,24a] M. I. Vivas Albornoz,[48] E. Voevodina,[111] F. Vogel,[110] J. C. Voigt,[50] P. Vokac,[134] Yu. Volkotrub,[86b] L. Vomberg,[25] E. Von Toerne,[25] B. Vormwald,[37] K. Vorobev,[51] M. Vos,[168] K. Voss,[146] M. Vozak,[37] L. Vozdecky,[122] N. Vranjes,[16] M. Vranjes Milosavljevic,[16] M. Vreeswijk,[116] N. K. Vu,[143b,143a] R. Vuillermet,[37] O. Vujinovic,[101] I. Vukotic,[40] I. K. Vyas,[35] J. F. Wack,[33] S. Wada,[162] C. Wagner,[148] J. M. Wagner,[18a] W. Wagner,[176] S. Wahdan,[176] H. Wahlberg,[91] C. H. Waits,[122] J. Walder,[136] R. Walker,[110] K. Walkingshaw Pass,[59] W. Walkowiak,[146] A. Wall,[130] E. J. Wallin,[99] T. Wamorkar,[18a] K. Wandall-Christensen,[168] A. Wang,[62] A. Z. Wang,[138] C. Wang,[48] C. Wang,[11] H. Wang,[18a] J. Wang,[64c] P. Wang,[102] P. Wang,[97] R. Wang,[61] R. Wang,[6] S. M. Wang,[153] S. Wang,[14] T. Wang,[115] T. Wang,[62] W. T. Wang,[128] W. Wang,[14] X. Wang,[167] X. Wang,[143a] X. Wang,[48] Y. Wang,[150] Y. Wang,[62] Z. Wang,[107] Z. Wang,[143b] Z. Wang,[107] C. Wanotayaroj,[83] A. Warburton,[105] A. L. Warnerbring,[146] S. Waterhouse,[96] A. T. Watson,[21] H. Watson,[52] M. F. Watson,[21] E. Watton,[37] G. Watts,[141] B. M. Waugh,[97] J. M. Webb,[54] C. Weber,[30] M. S. Weber,[20] S. M. Weber,[63a] C. Wei,[62] Y. Wei,[54] A. R. Weidberg,[128] E. J. Weik,[119] J. Weingarten,[49] C. Weiser,[54] C. J. Wells,[48] T. Wenaus,[30] T. Wengler,[37] N. S. Wenke,[111] N. Wermes,[25] M. Wessels,[63a] A. M. Wharton,[92] A. S. White,[61] A. White,[8] M. J. White,[1] D. Whiteson,[164] L. Wickremasinghe,[126] W. Wiedenmann,[175] M. Wielers,[136] R. Wierda,[149] C. Wiglesworth,[43] H. G. Wilkens,[37] J. J. H. Wilkinson,[33] D. M. Williams,[42] H. H. Williams,[130] S. Williams,[33] S. Willocq,[104] B. J. Wilson,[102] D. J. Wilson,[102] P. J. Windischhofer,[40] F. I. Winkel,[31] F. Winklmeier,[125] B. T. Winter,[54] M. Wittgen,[148] M. Wobisch,[98] T. Wojtkowski,[60] Z. Wolffs,[116] J. Wollrath,[37] M. W. Wolter,[87] H. Wolters,[132a,132c] M. C. Wong,[138] E. L. Woodward,[42] S. D. Worm,[48] B. K. Wosiek,[87] K. W. Woźniak,[87] S. Wozniewski,[55] K. Wraight,[59] C. Wu,[160] C. Wu,[21] J. Wu,[158] M. Wu,[113b] M. Wu,[115] S. L. Wu,[175] S. Wu,[14,pp] X. Wu,[62] Y. Q. Wu,[160] Y. Wu,[62] Z. Wu,[4] Z. Wu,[113a] J. Wuerzinger,[111] T. R. Wyatt,[102] B. M. Wynne,[52] S. Xella,[43] L. Xia,[113a] M. Xie,[62] A. Xiong,[125] D. Xu,[14] H. Xu,[62] L. Xu,[62] R. Xu,[130] T. Xu,[107] W. Xu,[113a] Y. Xu,[141] Z. Xu,[52] R. Xue,[131] B. Yabsley,[152] S. Yacoob,[34a] Y. Yamaguchi,[83] E. Yamashita,[158] H. Yamauchi,[162] T. Yamazaki,[18a] Y. Yamazaki,[85] S. Yan,[59] Z. Yan,[104] H. J. Yang,[143a,143b] H. T. Yang,[62] S. Yang,[62] T. Yang,[64c] X. Yang,[37] X. Yang,[14] Y. Yang,[158] Y. Yang,[62] W-M. Yao,[18a] C. L. Yardley,[151] J. Ye,[14] S. Ye,[30] X. Ye,[62] Y. Yeh,[97] I. Yeletskikh,[39] B. Yeo,[18b] M. R. Yexley,[97] T. P. Yildirim,[128] K. Yorita,[173] C. J. S. Young,[37] C. Young,[148] I. N. L. Young,[59] N. D. Young,[125] Y. Yu,[62] J. Yuan,[14,113c,pp] M. Yuan,[107] R. Yuan,[143b] L. Yue,[97] M. Zaazoua,[62] B. Zabinski,[87] I. Zahir,[36a] A. Zaio,[57b,57a] Z. K. Zak,[87] T. Zakareishvili,[168] S. Zambito,[56] J. A. Zamora Saa,[139d] J. Zang,[158] R. Zanzottera,[71a,71b] O. Zaplatilek,[134] C. Zeitnitz,[176] H. Zeng,[14] D. T. Zenger Jr.,[27] O. Zenin,[38] T. Ženiš,[29a] S. Zenz,[95] D. Zerwas,[66] D. F. Zhang,[144] G. Zhang,[14,pp] J. Zhang,[142a] J. Zhang,[6] L. Zhang,[62] L. Zhang,[113a] P. Zhang,[14,113c] R. Zhang,[113a] S. Zhang,[90] T. Zhang,[158] Y. Zhang,[141] Y. Zhang,[97] Y. Zhang,[62] Y. Zhang,[113a] Z. Zhang,[18a] Z. Zhang,[142a] Z. Zhang,[66] H. Zhao,[141] T. Zhao,[142a] Y. Zhao,[35] Z. Zhao,[62] Z. Zhao,[62] A. Zhemchugov,[39] J. Zheng,[113a] K. Zheng,[167] X. Zheng,[62] Z. Zheng,[148] D. Zhong,[167] B. Zhou,[107] B. Zhou,[143b,143a] H. Zhou,[7] N. Zhou,[143a] Y. Zhou,[15] Y. Zhou,[113a] Y. Zhou,[7] J. Zhu,[107] X. Zhu,[143b] Y. Zhu,[143a] Y. Zhu,[62] X. Zhuang,[14] K. Zhukov,[68] N. I. Zimine,[39] J. Zinsser,[63b] M. Ziolkowski,[146] L. Živković,[16] A. Zoccoli,[24b,24a] K. Zoch,[61] A. Zografos,[37] T. G. Zorbas,[144] O. Zormpa,[46] and L. Zwalinski[37]

(ATLAS Collaboration)

[1]Department of Physics, University of Adelaide, Adelaide, Australia
[2]Department of Physics, University of Alberta, Edmonton AB, Canada
[3a]Department of Physics, Ankara University, Ankara, Türkiye
[3b]Division of Physics, TOBB University of Economics and Technology, Ankara, Türkiye
[4]LAPP, Université Savoie Mont Blanc, CNRS/IN2P3, Annecy, France
[5]APC, Université Paris Cité, CNRS/IN2P3, Paris, France
[6]High Energy Physics Division, Argonne National Laboratory, Argonne Illinois, USA
[7]Department of Physics, University of Arizona, Tucson Arizona, USA
[8]Department of Physics, University of Texas at Arlington, Arlington Texas, USA
[9]Physics Department, National and Kapodistrian University of Athens, Athens, Greece
[10]Physics Department, National Technical University of Athens, Zografou, Greece
[11]Department of Physics, University of Texas at Austin, Austin Texas, USA
[12]Institute of Physics, Azerbaijan Academy of Sciences, Baku, Azerbaijan
[13]Institut de Física d'Altes Energies (IFAE), Barcelona Institute of Science and Technology, Barcelona, Spain
[14]Institute of High Energy Physics, Chinese Academy of Sciences, Beijing, China
[15]Physics Department, Tsinghua University, Beijing, China
[16]Institute of Physics, University of Belgrade, Belgrade, Serbia
[17]Department for Physics and Technology, University of Bergen, Bergen, Norway
[18a]Physics Division, Lawrence Berkeley National Laboratory, Berkeley California, USA
[18b]University of California, Berkeley California, USA
[19]Institut für Physik, Humboldt Universität zu Berlin, Berlin, Germany
[20]Albert Einstein Center for Fundamental Physics and Laboratory for High Energy Physics, University of Bern, Bern, Switzerland
[21]School of Physics and Astronomy, University of Birmingham, Birmingham, United Kingdom
[22a]Department of Physics, Bogazici University, Istanbul, Türkiye
[22b]Department of Physics Engineering, Gaziantep University, Gaziantep, Türkiye
[22c]Department of Physics, Istanbul University, Istanbul, Türkiye
[23a]Facultad de Ciencias y Centro de Investigaciónes, Universidad Antonio Nariño, Bogotá, Colombia
[23b]Departamento de Física, Universidad Nacional de Colombia, Bogotá, Colombia
[24a]Dipartimento di Fisica e Astronomia A. Righi, Università di Bologna, Bologna, Italy
[24b]INFN Sezione di Bologna, Italy
[25]Physikalisches Institut, Universität Bonn, Bonn, Germany
[26]Department of Physics, Boston University, Boston Massachusetts, USA
[27]Department of Physics, Brandeis University, Waltham Massachusetts, USA
[28a]Transilvania University of Brasov, Brasov, Romania
[28b]Horia Hulubei National Institute of Physics and Nuclear Engineering, Bucharest, Romania
[28c]Department of Physics, Alexandru Ioan Cuza University of Iasi, Iasi, Romania
[28d]National Institute for Research and Development of Isotopic and Molecular Technologies, Physics Department, Cluj-Napoca, Romania
[28e]National University of Science and Technology Politechnica, Bucharest, Romania
[28f]West University in Timisoara, Timisoara, Romania
[28g]Faculty of Physics, University of Bucharest, Bucharest, Romania
[29a]Faculty of Mathematics, Physics and Informatics, Comenius University, Bratislava, Slovak Republic
[29b]Department of Subnuclear Physics, Institute of Experimental Physics of the Slovak Academy of Sciences, Kosice, Slovak Republic
[30]Physics Department, Brookhaven National Laboratory, Upton NewYork, USA
[31]Universidad de Buenos Aires, Facultad de Ciencias Exactas y Naturales, Departamento de Física, y CONICET, Instituto de Física de Buenos Aires (IFIBA), Buenos Aires, Argentina
[32]California State University, California, USA
[33]Cavendish Laboratory, University of Cambridge, Cambridge, United Kingdom
[34a]Department of Physics, University of Cape Town, Cape Town, South Africa
[34b]iThemba Labs, Western Cape, South Africa
[34c]Department of Mechanical Engineering Science, University of Johannesburg, Johannesburg, South Africa
[34d]National Institute of Physics, University of the Philippines Diliman (Philippines), Philippines
[34e]Department of Physics, Stellenbosch University, Matieland, South Africa
[34f]University of KwaZulu-Natal, School of Agriculture and Science, Mathematics, Westville, South Africa
[34g]University of South Africa, Department of Physics, Pretoria, South Africa

[34h]*University of Pretoria, Department of Mechanical and Aeronautical Engineering, Pretoria, South Africa*
[34i]*University of Zululand, KwaDlangezwa, South Africa*
[34j]*School of Physics, University of the Witwatersrand, Johannesburg, South Africa*
[35]*Department of Physics, Carleton University, Ottawa ON, Canada*
[36a]*Faculté des Sciences Ain Chock, Université Hassan II de Casablanca, Morocco*
[36b]*Faculté des Sciences, Université Ibn-Tofail, Kénitra, Morocco*
[36c]*Faculté des Sciences Semlalia, Université Cadi Ayyad, LPHEA-Marrakech, Morocco*
[36d]*LPMR, Faculté des Sciences, Université Mohamed Premier, Oujda, Morocco*
[36e]*Faculté des sciences, Université Mohammed V, Rabat, Morocco*
[36f]*Institute of Applied Physics, Mohammed VI Polytechnic University, Ben Guerir, Morocco*
[37]*CERN, Geneva, Switzerland*
[38]*Affiliated with an institute formerly covered by a cooperation agreement with CERN*
[39]*Affiliated with an international laboratory covered by a cooperation agreement with CERN*
[40]*Enrico Fermi Institute, University of Chicago, Chicago Illinois, USA*
[41]*LPC, Université Clermont Auvergne, CNRS/IN2P3, Clermont-Ferrand, France*
[42]*Nevis Laboratory, Columbia University, Irvington NewYork, USA*
[43]*Niels Bohr Institute, University of Copenhagen, Copenhagen, Denmark*
[44a]*Dipartimento di Fisica, Università della Calabria, Rende, Italy*
[44b]*INFN Gruppo Collegato di Cosenza, Laboratori Nazionali di Frascati, Italy*
[45]*Physics Department, Southern Methodist University, Dallas Texas, USA*
[46]*National Centre for Scientific Research "Demokritos", Agia Paraskevi, Greece*
[47a]*Department of Physics, Stockholm University, Sweden*
[47b]*Oskar Klein Centre, Stockholm, Sweden*
[48]*Deutsches Elektronen-Synchrotron DESY, Hamburg and Zeuthen, Germany*
[49]*Fakultät Physik, Technische Universität Dortmund, Dortmund, Germany*
[50]*Institut für Kern- und Teilchenphysik, Technische Universität Dresden, Dresden, Germany*
[51]*Department of Physics, Duke University, Durham North Carolina, USA*
[52]*SUPA—School of Physics and Astronomy, University of Edinburgh, Edinburgh, United Kingdom*
[53]*INFN e Laboratori Nazionali di Frascati, Frascati, Italy*
[54]*Physikalisches Institut, Albert-Ludwigs-Universität Freiburg, Freiburg, Germany*
[55]*II. Physikalisches Institut, Georg-August-Universität Göttingen, Göttingen, Germany*
[56]*Département de Physique Nucléaire et Corpusculaire, Université de Genève, Genève, Switzerland*
[57a]*Dipartimento di Fisica, Università di Genova, Genova, Italy*
[57b]*INFN Sezione di Genova, Italy*
[58]*II. Physikalisches Institut, Justus-Liebig-Universität Giessen, Giessen, Germany*
[59]*SUPA—School of Physics and Astronomy, University of Glasgow, Glasgow, United Kingdom*
[60]*LPSC, Université Grenoble Alpes, CNRS/IN2P3, Grenoble INP, Grenoble, France*
[61]*Laboratory for Particle Physics and Cosmology, Harvard University, Cambridge Massachusetts, USA*
[62]*Department of Modern Physics and State Key Laboratory of Particle Detection and Electronics, University of Science and Technology of China, Hefei, China*
[63a]*Kirchhoff-Institut für Physik, Ruprecht-Karls-Universität Heidelberg, Heidelberg, Germany*
[63b]*Physikalisches Institut, Ruprecht-Karls-Universität Heidelberg, Heidelberg, Germany*
[64a]*Department of Physics, Chinese University of Hong Kong, Shatin, New Territories, Hong Kong, China*
[64b]*Department of Physics, University of Hong Kong, Hong Kong, China*
[64c]*Department of Physics and Institute for Advanced Study, Hong Kong University of Science and Technology, Clear Water Bay, Kowloon, Hong Kong, China*
[65]*Department of Physics, National Tsing Hua University, Hsinchu, Taiwan*
[66]*IJCLab, Université Paris-Saclay, CNRS/IN2P3, 91405, Orsay, France*
[67]*Centro Nacional de Microelectrónica (IMB-CNM-CSIC), Barcelona, Spain*
[68]*Department of Physics, Indiana University, Bloomington Indiana, USA*
[69a]*INFN Gruppo Collegato di Udine, Sezione di Trieste, Udine, Italy*
[69b]*ICTP, Trieste, Italy*
[69c]*Dipartimento Politecnico di Ingegneria e Architettura, Università di Udine, Udine, Italy*
[70a]*INFN Sezione di Lecce, Italy*
[70b]*Dipartimento di Matematica e Fisica, Università del Salento, Lecce, Italy*
[71a]*INFN Sezione di Milano, Italy*
[71b]*Dipartimento di Fisica, Università di Milano, Milano, Italy*
[72a]*INFN Sezione di Napoli, Italy*
[72b]*Dipartimento di Fisica, Università di Napoli, Napoli, Italy*

[73a]INFN Sezione di Pavia, Italy
[73b]Dipartimento di Fisica, Università di Pavia, Pavia, Italy
[74a]INFN Sezione di Pisa, Italy
[74b]Dipartimento di Fisica E. Fermi, Università di Pisa, Pisa, Italy
[75a]INFN Sezione di Roma, Italy
[75b]Dipartimento di Fisica, Sapienza Università di Roma, Roma, Italy
[76a]INFN Sezione di Roma Tor Vergata, Italy
[76b]Dipartimento di Fisica, Università di Roma Tor Vergata, Roma, Italy
[77a]INFN Sezione di Roma Tre, Italy
[77b]Dipartimento di Matematica e Fisica, Università Roma Tre, Roma, Italy
[78a]INFN-TIFPA, Italy
[78b]Università degli Studi di Trento, Trento, Italy
[79]Universität Innsbruck, Department of Astro and Particle Physics, Innsbruck, Austria
[80]Department of Physics and Astronomy, Iowa State University, Ames Iowa, USA
[81]Istinye University, Sariyer, Istanbul, Türkiye
[82a]Departamento de Engenharia Elétrica, Universidade Federal de Juiz de Fora (UFJF), Juiz de Fora, Brazil
[82b]Universidade Federal do Rio De Janeiro COPPE/EE/IF, Rio de Janeiro, Brazil
[82c]Instituto de Física, Universidade de São Paulo, São Paulo, Brazil
[82d]Rio de Janeiro State University, Rio de Janeiro, Brazil
[82e]Federal University of Bahia, Bahia, Brazil
[83]KEK, High Energy Accelerator Research Organization, Tsukuba, Japan
[84a]Khalifa University of Science and Technology, Abu Dhabi, United Arab Emirates
[84b]University of Sharjah, Sharjah, United Arab Emirates
[85]Graduate School of Science, Kobe University, Kobe, Japan
[86a]AGH University of Krakow, Faculty of Physics and Applied Computer Science, Krakow, Poland
[86b]Marian Smoluchowski Institute of Physics, Jagiellonian University, Krakow, Poland
[87]Institute of Nuclear Physics Polish Academy of Sciences, Krakow, Poland
[88]Faculty of Science, Kyoto University, Kyoto, Japan
[89]Research Center for Advanced Particle Physics and Department of Physics, Kyushu University, Fukuoka, Japan
[90]L2IT, Université de Toulouse, CNRS/IN2P3, UPS, Toulouse, France
[91]Instituto de Física La Plata, Universidad Nacional de La Plata and CONICET, La Plata, Argentina
[92]Physics Department, Lancaster University, Lancaster, United Kingdom
[93]Oliver Lodge Laboratory, University of Liverpool, Liverpool, United Kingdom
[94]Department of Experimental Particle Physics, Jožef Stefan Institute and Department of Physics, University of Ljubljana, Ljubljana, Slovenia
[95]Department of Physics and Astronomy, Queen Mary University of London, London, United Kingdom
[96]Department of Physics, Royal Holloway University of London, Egham, United Kingdom
[97]Department of Physics and Astronomy, University College London, London, United Kingdom
[98]Louisiana Tech University, Ruston Louisiana, USA
[99]Fysiska institutionen, Lunds universitet, Lund, Sweden
[100]Departamento de Física Teorica C-15 and CIAFF, Universidad Autónoma de Madrid, Madrid, Spain
[101]Institut für Physik, Universität Mainz, Mainz, Germany
[102]School of Physics and Astronomy, University of Manchester, Manchester, United Kingdom
[103]CPPM, Aix-Marseille Université, CNRS/IN2P3, Marseille, France
[104]Department of Physics, University of Massachusetts, Amherst Massachusetts, USA
[105]Department of Physics, McGill University, Montreal QC, Canada
[106]School of Physics, University of Melbourne, Victoria, Australia
[107]Department of Physics, University of Michigan, Ann Arbor Michigan, USA
[108]Department of Physics and Astronomy, Michigan State University, East Lansing Michigan, USA
[109]Group of Particle Physics, University of Montreal, Montreal QC, Canada
[110]Fakultät für Physik, Ludwig-Maximilians-Universität München, München, Germany
[111]Max-Planck-Institut für Physik (Werner-Heisenberg-Institut), München, Germany
[112]Graduate School of Science and Kobayashi-Maskawa Institute, Nagoya University, Nagoya, Japan
[113a]Department of Physics, Nanjing University, Nanjing, China
[113b]School of Science, Shenzhen Campus of Sun Yat-sen University, China
[113c]University of Chinese Academy of Science (UCAS), Beijing, China
[114]Department of Physics and Astronomy, University of New Mexico, Albuquerque New Mexico, USA

[115]*Institute for Mathematics, Astrophysics and Particle Physics, Radboud University/Nikhef, Nijmegen, Netherlands*
[116]*Nikhef National Institute for Subatomic Physics and University of Amsterdam, Amsterdam, Netherlands*
[117]*Department of Physics, Northern Illinois University, DeKalb Illinois, USA*
[118a]*New York University Abu Dhabi, Abu Dhabi, United Arab Emirates*
[118b]*United Arab Emirates University, Al Ain, United Arab Emirates*
[119]*Department of Physics, New York University, New York New York, USA*
[120]*Ochanomizu University, Otsuka, Bunkyo-ku, Tokyo, Japan*
[121]*Ohio State University, Columbus Ohio, USA*
[122]*Homer L. Dodge Department of Physics and Astronomy, University of Oklahoma, Norman Oklahoma, USA*
[123]*Department of Physics, Oklahoma State University, Stillwater Oklahoma, USA*
[124]*Palacký University, Joint Laboratory of Optics, Olomouc, Czech Republic*
[125]*Institute for Fundamental Science, University of Oregon, Eugene Oregon, USA*
[126]*Graduate School of Science, University of Osaka, Osaka, Japan*
[127]*Department of Physics, University of Oslo, Oslo, Norway*
[128]*Department of Physics, Oxford University, Oxford, United Kingdom*
[129]*LPNHE, Sorbonne Université, Université Paris Cité, CNRS/IN2P3, Paris, France*
[130]*Department of Physics, University of Pennsylvania, Philadelphia Pennsylvania, USA*
[131]*Department of Physics and Astronomy, University of Pittsburgh, Pittsburgh Pennsylvania, USA*
[132a]*Laboratório de Instrumentação e Física Experimental de Partículas—LIP, Lisboa, Portugal*
[132b]*Departamento de Física, Faculdade de Ciências, Universidade de Lisboa, Lisboa, Portugal*
[132c]*Departamento de Física, Universidade de Coimbra, Coimbra, Portugal*
[132d]*Centro de Física Nuclear da Universidade de Lisboa, Lisboa, Portugal*
[132e]*Departamento de Física, Escola de Ciências, Universidade do Minho, Braga, Portugal*
[132f]*Departamento de Física Teórica y del Cosmos, Universidad de Granada, Granada (Spain), Spain*
[132g]*Departamento de Física, Instituto Superior Técnico, Universidade de Lisboa, Lisboa, Portugal*
[133]*Institute of Physics of the Czech Academy of Sciences, Prague, Czech Republic*
[134]*Czech Technical University in Prague, Prague, Czech Republic*
[135]*Charles University, Faculty of Mathematics and Physics, Prague, Czech Republic*
[136]*Particle Physics Department, Rutherford Appleton Laboratory, Didcot, United Kingdom*
[137]*IRFU, CEA, Université Paris-Saclay, Gif-sur-Yvette, France*
[138]*Santa Cruz Institute for Particle Physics, University of California Santa Cruz, Santa Cruz California, USA*
[139a]*Departamento de Física, Pontificia Universidad Católica de Chile, Santiago, Chile*
[139b]*Millennium Institute for Subatomic physics at high energy frontier (SAPHIR), Santiago, Chile*
[139c]*Instituto de Investigación Multidisciplinario en Ciencia y Tecnología, y Departamento de Física, Universidad de La Serena, Chile*
[139d]*Universidad Andres Bello, Department of Physics, Santiago, Chile*
[139e]*Universidad San Sebastian, Recoleta, Chile*
[139f]*Instituto de Alta Investigación, Universidad de Tarapacá, Arica, Chile*
[139g]*Departamento de Física, Universidad Técnica Federico Santa María, Valparaíso, Chile*
[140]*Department of Physics, Institute of Science, Tokyo, Japan*
[141]*Department of Physics, University of Washington, Seattle Washington, USA*
[142a]*Institute of Frontier and Interdisciplinary Science and Key Laboratory of Particle Physics and Particle Irradiation (MOE), Shandong University, Qingdao, China*
[142b]*School of Physics, Zhengzhou University, China*
[143a]*State Key Laboratory of Dark Matter Physics, School of Physics and Astronomy, Shanghai Jiao Tong University, Key Laboratory for Particle Astrophysics and Cosmology (MOE), SKLPPC, Shanghai, China*
[143b]*State Key Laboratory of Dark Matter Physics, Tsung-Dao Lee Institute, Shanghai Jiao Tong University, Shanghai, China*
[144]*Department of Physics and Astronomy, University of Sheffield, Sheffield, United Kingdom*
[145]*Department of Physics, Shinshu University, Nagano, Japan*
[146]*Department Physik, Universität Siegen, Siegen, Germany*
[147]*Department of Physics, Simon Fraser University, Burnaby BC, Canada*
[148]*SLAC National Accelerator Laboratory, Stanford California, USA*
[149]*Department of Physics, Royal Institute of Technology, Stockholm, Sweden*
[150]*Departments of Physics and Astronomy, Stony Brook University, Stony Brook NewYork, USA*
[151]*Department of Physics and Astronomy, University of Sussex, Brighton, United Kingdom*

[152]School of Physics, University of Sydney, Sydney, Australia
[153]Institute of Physics, Academia Sinica, Taipei, Taiwan
[154a]E. Andronikashvili Institute of Physics, Iv. Javakhishvili Tbilisi State University, Tbilisi, Georgia
[154b]High Energy Physics Institute, Tbilisi State University, Tbilisi, Georgia
[154c]University of Georgia, Tbilisi, Georgia
[155]Department of Physics, Technion, Israel Institute of Technology, Haifa, Israel
[156]Raymond and Beverly Sackler School of Physics and Astronomy, Tel Aviv University, Tel Aviv, Israel
[157]Department of Physics, Aristotle University of Thessaloniki, Thessaloniki, Greece
[158]International Center for Elementary Particle Physics and Department of Physics, University of Tokyo, Tokyo, Japan
[159]Graduate School of Science and Technology, Tokyo Metropolitan University, Tokyo, Japan
[160]Department of Physics, University of Toronto, Toronto ON, Canada
[161a]TRIUMF, Vancouver BC, Canada
[161b]Department of Physics and Astronomy, York University, Toronto ON, Canada
[162]Division of Physics and Tomonaga Center for the History of the Universe, Faculty of Pure and Applied Sciences, University of Tsukuba, Tsukuba, Japan
[163]Department of Physics and Astronomy, Tufts University, Medford Massachusetts, USA
[164]Department of Physics and Astronomy, University of California Irvine, Irvine California, USA
[165]University of West Attica, Athens, Greece
[166]Department of Physics and Astronomy, University of Uppsala, Uppsala, Sweden
[167]Department of Physics, University of Illinois, Urbana Illinois, USA
[168]Instituto de Física Corpuscular (IFIC), Centro Mixto Universidad de Valencia—CSIC, Valencia, Spain
[169]Department of Physics, University of British Columbia, Vancouver BC, Canada
[170]Department of Physics and Astronomy, University of Victoria, Victoria BC, Canada
[171]Fakultät für Physik und Astronomie, Julius-Maximilians-Universität Würzburg, Würzburg, Germany
[172]Department of Physics, University of Warwick, Coventry, United Kingdom
[173]Waseda University, Tokyo, Japan
[174]Department of Particle Physics and Astrophysics, Weizmann Institute of Science, Rehovot, Israel
[175]Department of Physics, University of Wisconsin, Madison Wisconsin, USA
[176]Fakultät für Mathematik und Naturwissenschaften, Fachgruppe Physik, Bergische Universität Wuppertal, Wuppertal, Germany
[177]Department of Physics, Yale University, New Haven Connecticut, USA
[178]Yerevan Physics Institute, Yerevan, Armenia

[a]Deceased.
[b]Also at Department of Physics, King's College London, London, United Kingdom.
[c]Also at Institute of Physics, Azerbaijan Academy of Sciences, Baku, Azerbaijan.
[d]Also at Imam Mohammad Ibn Saud Islamic University, Saudi Arabia.
[e]Also at Department of Physics, University of Thessaly, Greece.
[f]Also at An-Najah National University, Nablus, Palestine.
[g]Also at Department of Physics, University of Fribourg, Fribourg, Switzerland.
[h]Also at Department of Physics, Westmont College, Santa Barbara, USA.
[i]Also at Departament de Fisica de la Universitat Autonoma de Barcelona, Barcelona, Spain.
[j]Also at University of Siena, Italy.
[k]Also at Affiliated with an institute formerly covered by a cooperation agreement with CERN.
[l]Also at The Collaborative Innovation Center of Quantum Matter (CICQM), Beijing, China.
[m]Also at Faculty of Physics, Sofia University, 'St. Kliment Ohridski', Sofia, Bulgaria.
[n]Also at Università di Napoli Parthenope, Napoli, Italy.
[o]Also at Institute of Particle Physics (IPP), Canada.
[p]Also at Department of Physics, Bolu Abant Izzet Baysal University, Bolu, Türkiye.
[q]Also at Faculty of Physics, University of Bucharest, Romania.
[r]Also at Borough of Manhattan Community College, City University of New York, New York New York, USA.
[s]Also at National Institute of Physics, University of the Philippines Diliman (Philippines), Philippines.
[t]Also at Department of Financial and Management Engineering, University of the Aegean, Chios, Greece.
[u]Also at TRIUMF, Vancouver BC, Canada.
[v]Also at Institucio Catalana de Recerca i Estudis Avancats, ICREA, Barcelona, Spain.
[w]Also at Henan University, China.
[x]Also at Yeditepe University, Physics Department, Istanbul, Türkiye.
[y]Also at Institute of Theoretical Physics, Ilia State University, Tbilisi, Georgia.
[z]Also at CERN, Geneva, Switzerland.

[aa]Also at Center for Interdisciplinary Research and Innovation (CIRI-AUTH), Thessaloniki, Greece.
[bb]Also at Hellenic Open University, Patras, Greece.
[cc]Also at Department of Modern Physics and State Key Laboratory of Particle Detection and Electronics, University of Science and Technology of China, Hefei, China.
[dd]Also at Department of Mathematical Sciences, University of South Africa, Johannesburg, South Africa.
[ee]Also at Department of Physics, Stellenbosch University, South Africa.
[ff]Also at University of Colorado Boulder, Department of Physics, Colorado, USA.
[gg]Also at Département de Physique Nucléaire et Corpusculaire, Université de Genève, Genève, Switzerland.
[hh]Also at Centre of Physics of the Universities of Minho and Porto (CF-UM-UP), Portugal.
[ii]Also at Institute for Nuclear Research and Nuclear Energy (INRNE) of the Bulgarian Academy of Sciences, Sofia, Bulgaria.
[jj]Also at Washington College, Chestertown, MD, USA.
[kk]Also at Institut für Experimentalphysik, Universität Hamburg, Hamburg, Germany.
[ll]Also at Institute of Applied Physics, Mohammed VI Polytechnic University, Ben Guerir, Morocco.
[mm]Also at Department of Physics, Stanford University, Stanford California, USA.
[nn]Also at Institute of Physics and Technology, Mongolian Academy of Sciences, Ulaanbaatar, Mongolia.
[oo]Also at Millennium Institute for Subatomic physics at high energy frontier (SAPHIR), Santiago, Chile.
[pp]Also at University of Chinese Academy of Sciences (UCAS), Beijing, China.